Homotopy-Based Methods for Fractional Differential Equations

İnan Ateş

Utrecht University

Thesis committee:
Prof. dr. R.P. Stevenson, University of Amsterdam, the Netherlands
Prof. dr. A. Doelman, Leiden University, the Netherlands
Prof. dr. S. Pop, Hasselt University, Belgium
Prof. dr. S.M. Verduyn Lunel, Utrecht University, the Netherlands
Dr. T. van Leeuwen, Utrecht University, the Netherlands

ISBN: 978-90-393-6812-1
Printed by Ridderprint BV

Homotopy-Based Methods for Fractional Differential Equations

Op homotopie gebaseerde methoden voor fractionele differentiaalvergelijkingen

(met een samenvatting in het Nederlands)

Proefschrift

ter verkrijging van de graad van doctor aan de Universiteit Utrecht op gezag van de rector magnificus, prof.dr. G.J. van der Zwaan, ingevolge het besluit van het college voor promoties in het openbaar te verdedigen op woensdag 30 augustus 2017 des middags te 2.30 uur

door

İnan Ateş

geboren op 22 augustus 1984 te Antalya, Turkije

Promotor: Prof.dr. R.H. Bisseling
Co-promotor: Dr. P.A. Zegeling

This thesis was accomplished with financial support from the Turkish Ministry of National Education.

Contents

Chapter 1

Introduction

1.1 Motivation of the work

The intention of this thesis is two-fold. The first aim is to describe and apply, series-based, numerical methods to fractional differential equation models. For this, it is needed to distinguish between space-fractional and time-fractional derivatives. The set-up of the work is done in three chapters with increasing numerical complexity and effectiveness. The second goal of this thesis is to give a clear and fair numerical analysis to show that these methods, mainly based on so-called homotopy principles, may, in certain cases, provide accurate results for nonlinear models. However, it will also be stressed that, in contrast with many articles on this topic, there may be many disadvantages when applying such methods in general. Tuning of numerical parameters still plays an important role to obtain convergent series solutions. Therefore, the main focus of this work is the numerical performance of series-based methods for space- and time-fractional differential equations.

1.2 A brief history of fractional derivatives

Most authors on this topic cite a particular date as the birthday of so called "Fractional Calculus" [84, 111]. In a letter dated September 30th 1695, L'Hôpital wrote to Leibniz asking him about a particular notation he had used in his publications for the nth-derivative of the linear function $f(x) = x : \frac{\mathcal{D}^n x}{\mathcal{D}x^n}$. L'Hôpital posed the following question to Leibniz: "what would the result be if $n = 1/2$?". Leibniz's response was: "An apparent paradox, from which one day useful consequences will be drawn." These words were, in fact, the origin of fractional calculus. Following L'Hôpital's and Leibniz's first notion, fractional calculus was primarily a study reserved for the brightest minds in mathematics. Fourier [114], Euler [88] and Laplace [71] are among the many who got interested in fractional calculus and its mathematical consequences.

Many mathematicians found, using their own notation and methodology, definitions that fit the concept of a non-integer order integral or derivative. Well-known definitions of fractional derivatives, perhaps not yet completely accepted in the calculus community, are the Riemann-Liouville [101, 109, 97], Caputo [22] and Grünwald-Letnikov [101, 109, 97] definitions.

In 1819, the first serious approach to mathematically understand a derivative of an arbitrary order was made by the French mathematician S. F. Lacroix [107]. In his publication, he devoted a few pages to this subject among the total of more than 700 pages. Lacroix started with the monomial $y = x^n$, where n is a positive integer, and worked out the mth derivative for this function:

$$\frac{d^m y}{dx^m} = \frac{n!}{(n-m)!} x^{n-m}. \tag{1.1}$$

Then, he found, realizing the connection between the factorial "!" and the Gamma-function, for the function $y = x^a$ with $a \in \mathbb{R}^+$:

$$\frac{d^{1/2}y}{dx^{1/2}} = \frac{\Gamma(a+1)}{\Gamma(a+1/2)} x^{a-1/2}. \tag{1.2}$$

Note that the function denoted by Γ will be defined in section 1.3.1. Lacroix expressed the arbitrary order derivative of the function x^a with $a \in \mathbb{R}$. The special case $a = 1$ reads then:

$$\frac{d^{1/2}}{dx^{1/2}} x = \frac{2\sqrt{x}}{\sqrt{\pi}}, \tag{1.3}$$

since $\Gamma(3/2) = \frac{1}{2}\Gamma(1/2) = \frac{1}{2}\sqrt{\pi}$ and $\Gamma(2) = 1$ (see also section 1.3.1).

The concept of fractional derivative has taken almost three hundred years to be formally proposed in a text, since L'Hôpital [111] first described it. The first application in the literature was given by Niels Henrik Abel [12] in 1823. He applied fractional calculus in the solution of an integral equation related with the tautochrone problem [46]. Abel worked out an elegant solution to this problem. It took the attention of Liouville who first gave the formal definition of a fractional derivative. He published a number of memoirs between 1832 and 1855. His starting point was the equality:

$$D^m \mathrm{e}^{\lambda x} = \lambda^m \mathrm{e}^{\lambda x}. \tag{1.4}$$

After some algebraic calculations, he finally defined the fractional *integral* as follows:

$$D_x^{-\alpha} f(x) = \frac{1}{\Gamma(\alpha)} \int_a^x f(u)(x-u)^{\alpha-1}\,\mathrm{d}u, \;\; a \in (-\infty, 0). \tag{1.5}$$

Liouville succeeded to apply his definitions in potential theory. But some of his colleagues believed that these definitions were too narrow.

During the period from 1835 until 1850, there was some controversy between Lacroix's generalization, favored by George Peacock [107], and Liouville's definition. Augustus De Morgan claimed that these two definitions could provide a more general definition. In 1850, William Center [107] found a discrepancy between Lacroix and Liouville. While Lacroix claimed that a fractional derivative of a constant must be unequal to zero, Liouville stated that it is zero because of the property $\Gamma(0) = \infty$.

In 1847, when Riemann was still a student, he published a paper on fractional integrals. He followed Liouville's idea and defined:

$$I^{\alpha} f(x) = \frac{1}{\Gamma(\alpha)} \int_a^x f(u)(x-u)^{\alpha-1}\,\mathrm{d}u + \Psi(x), \tag{1.6}$$

where he added a complementary function $\Psi(x)$ (see also [106]).

Most of the mathematical studies regarding fractional calculus were developed prior to the turn of the 20th century. For example, Caputo [101, 109, 97] reformulated the more 'classic' definition of the Riemann-Liouville fractional derivative in order to use integer order initial conditions to solve his fractional order differential equations. Erdélyi and Kober [41] introduced the properties of a generalization of the Riemann-Liouville and Weyl definitions. The topic of fractional calculus wasn't deeply surveyed between the early 1940s and the 1960s of the last century. From that moment, a number of papers were published by Erdélyi, Mikolás [91], Higgins [63], Al-Bassam [4] and others in the 1960's and 1970's. Recently, in the mid 1990's, Kolowankar, as mentioned in [84, 111], again reformulated the Riemann-Liouville fractional derivative in order to differentiate non-differentiable fractal functions.

It is interesting to note that most applications in engineering and sciences have been developed in the past hundred years. Especially, in the last twenty years, numerous applications

and physical interpretations of fractional calculus have been described in literature. Among others, we find nowadays fractional derivatives in hydrology (non-Fickian laws), finance (Lévy-flights and non-Markovian models), non-Brownian motions, super- and sub-diffusion (anomalous transport), visco-elasticity, rheology, and electro-physiology of the heart. A few of those will be discussed in section 1.6.

1.3 Special functions in fractional calculus

In this section we discuss two important special functions, that are widely used in fractional calculus.

1.3.1 The Gamma function

The Gamma function $\Gamma(z)$ (see [101, 109, 97]), sometimes denoted by the Euler-Gamma function, plays an important role not only in ordinary calculus and physics, but also in fractional calculus, which allows us to generalize the factorial $n!$ to non-integer values. The Gamma function is often used in probability, statistics and combinatorics. It is defined as follows:

$$\Gamma(z) = \int_0^\infty e^{-t} t^{z-1} \, \mathrm{d}t, \tag{1.7}$$

or, alternatively, by

$$\int_0^1 [-\ln(t)]^{z-1} dt,$$

which is known to converge in the complex plane for $\Re(z) > 0$ (see [101]).

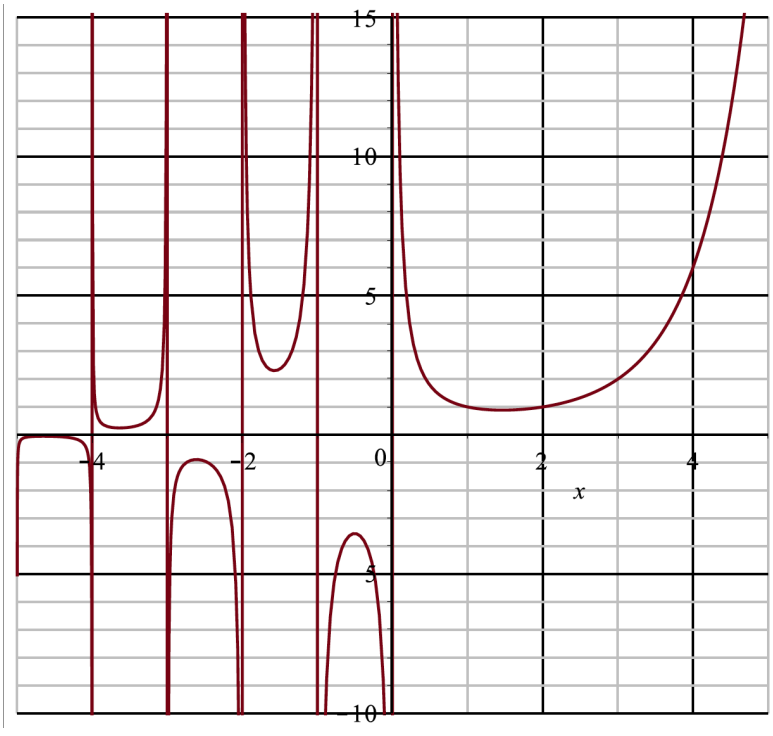

FIGURE 1.1: The Gamma function on the real axis.

An important and widely-used property of the Gamma function is given by the functional equation:

$$\Gamma(z+1) = z\,\Gamma(z), \tag{1.8}$$

which can be easily checked as follows:

$$\Gamma(z+1) = \int_0^\infty e^{-t}t^z\,\mathrm{d}t = [-e^{-t}t^z]_{t=0}^{t=\infty} + z\int_0^\infty e^{-t}t^{z-1}\,\mathrm{d}t = z\,\Gamma(z). \tag{1.9}$$

It is obvious that $\Gamma(1) = 1$. We can conclude from (1.8):

$$\begin{cases} \Gamma(2) = 1! = 1, \\ \Gamma(3) = 2! = 2, \\ \Gamma(4) = 3! = 6, \\ ... \\ \Gamma(n+1) = n\,\Gamma(n) = n\,(n-1)! = n!. \end{cases} \tag{1.10}$$

The Gamma function has simple poles at the points $z = -n$ for $n = 0,\ 1,\ 2,\ ....$ Another interesting formula in which the Gamma function appears is the following limit representation:

$$\Gamma(z) = \lim_{n\to\infty} \frac{n!n^z}{z(z+1)\cdots(z+n)}, \quad \Re(z) > 0. \tag{1.11}$$

Further, it can also be shown that $\Gamma(z)$ defines an analytical function on $z \in \mathbb{C} :\ \Re(z) > 0$ (see [101]). There exist also several alternative definitions for the Gamma function:

$$\Gamma(z) = \frac{1}{z}\prod_{n=1}^{\infty} \frac{(1+\frac{1}{n})^z}{1+\frac{z}{n}}, \tag{1.12}$$

$$\Gamma(z) = \frac{\mathrm{e}^{-\gamma z}}{z}\prod_{n=1}^{\infty}(1+\frac{z}{n})^{-1}\mathrm{e}^{\frac{z}{n}}, \tag{1.13}$$

where γ is the Euler-Mascheroni constant, approximately equal to $0.577216....$ Another useful property of the Gamma function is the one given by Euler's reflection formula:

$$\Gamma(1-z)\Gamma(z) = \frac{\pi}{\sin(\pi z)}, \quad z \notin \mathbb{Z}. \tag{1.14}$$

From this follows, for example, easily that $\Gamma(\frac{1}{2}) = \sqrt{\pi}$. This property helps us to calculate fractional order derivatives and integrals more easily. Some other Gamma function values are [101]:

$$\begin{cases} \Gamma(-2) = \infty \\ \Gamma(-\frac{3}{2}) = \frac{4}{3}\sqrt{\pi} \approx 2.363271 \\ \Gamma(-1) = \infty \\ \Gamma(\frac{3}{2}) = \frac{1}{2}\sqrt{\pi} \approx 0.886226 \\ \Gamma(\frac{5}{2}) = \frac{3}{4}\sqrt{\pi} \approx 1.329340 \\ \Gamma(\frac{7}{2}) = \frac{15}{8}\sqrt{\pi} \approx 3.323350,\ \ etcetera. \end{cases} \tag{1.15}$$

The Gamma function is also strongly related to the so-called Beta function:

$$B(x,y) = \frac{\Gamma(x)\Gamma(y)}{\Gamma(x+y)}. \tag{1.16}$$

Note that the function $\Gamma(x)$ is not a unique solution of (1.8) (for positive values of $x = \Re(z)$). Other solutions of this functional equation are, e.g.:

$$\cos(2m\pi x)\Gamma(x),\ m \in \mathbb{N},$$
or
$$\frac{1}{\Gamma(1-x)}\frac{d}{dx}\ln\left(\frac{\Gamma(\frac{1}{2}-\frac{1}{2}x)}{\Gamma(1-\frac{1}{2}x)}\right).$$

With an extra condition on the function that must satisfy (1.8), Bohr and Mollerup in 1922 [20], proved that the Gamma function $\Gamma(x)$ *is* the unique solution of the functional equation. They added the extra constraint on $f(x)$, that it must be *logarithmically convex*. Their theorem is known as the Bohr-Mollerup theorem.

1.3.2 The Mittag-Leffler function

Another important formula in fractional calculus is the Mittag-Leffler (ML) function [93]. The Mittag-Leffler function shows its importantance in physics, biology, engineering and applied sciences. The Mittag-Leffler function is a fundamental solution of fractional differential equations and fractional order integral equations. The most noticeable general property of the Mittag-Leffler function is dealing with the Laplace transform and asymptotic expansions of these functions. The Mittag-Leffler function has two definitions in the literature:

$$E_\alpha(z) = \sum_{k=0}^{\infty} \frac{z^k}{\Gamma(\alpha k + 1)},\ \ \alpha \in \mathbb{C},\ \Re(\alpha) > 0, \tag{1.17}$$

and

$$E_{\alpha,\beta}(z) = \sum_{k=0}^{\infty} \frac{z^k}{\Gamma(\alpha k + \beta)},\ \ \alpha, \beta \in \mathbb{C},\ \Re(\alpha) > 0,\ \Re(\beta) > 0. \tag{1.18}$$

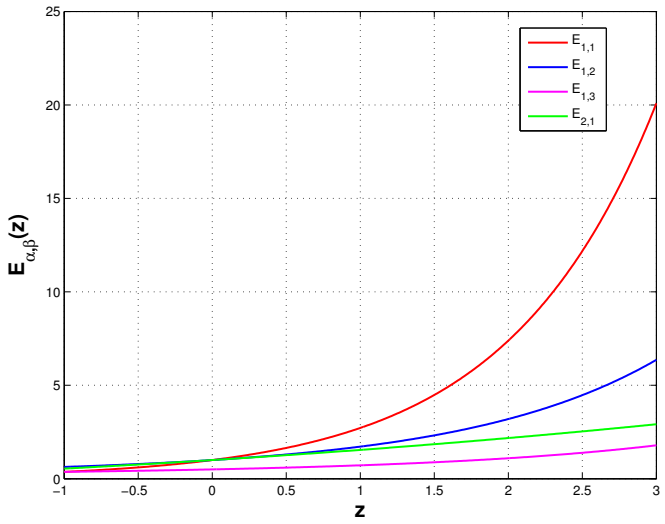

FIGURE 1.2: The Mittag-Leffler function (1.18) for different α and β values. The exponential function can be recognized, if we choose $\alpha = 1$ and $\beta = 1$: $\mathrm{E}_{1,1} = \mathrm{e}^x$.

Its graph is displayed in Figure 1.2 for different α and β values. Definition (1.17), which can be seen as a generalization of the exponential function, was studied by Mittag-Leffler in 1903.

This formula gives the Taylor series of the exponential function in the case $\alpha = 1$. The ML-function can be found in the exact solution of the following time-fractional fractional differential equation:

$$D_t^\alpha u(t) = -\lambda u(t),\ u(0) = u_0. \tag{1.19}$$

Its solution reads (using elements from section 1.4):

$$u(t) = E_\alpha(-\lambda t^\alpha). \tag{1.20}$$

In Figure 1.3 these solutions are displayed for several values of the parameter α. Definition

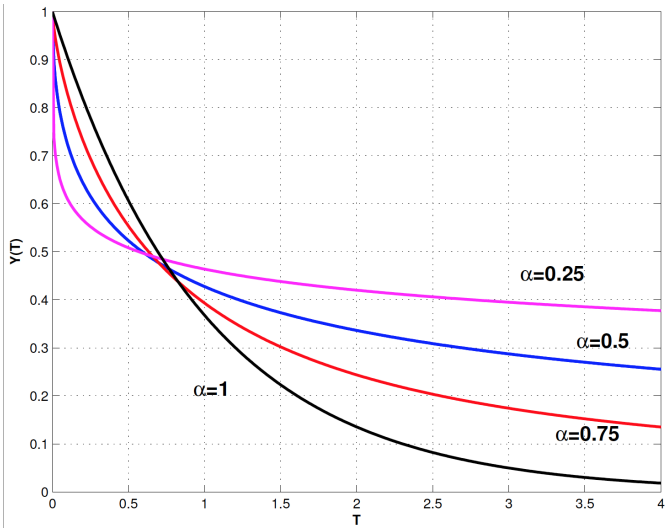

FIGURE 1.3: The solution (1.3) of the fractional differential equation (1.19) for several α values, $\lambda = 1$ and $u_0 = 1$. We see again, that for $\alpha = 1$, we obtain the solution $u(t) = \mathrm{e}^{-t}$

(1.18) is another, more general, version of (1.17). It was studied by Wiman [124] in 1905 and Agarwal [3] in 1953.

Here, we mention only a few basic properties of the Mittag-Leffler functions:

$$\begin{cases} E_{\alpha,\beta}(z) = zE_{\alpha,\beta+\alpha}(z) + \frac{1}{\Gamma(\beta)}, \\ E_{\alpha,\beta}(z) = \beta E_{\alpha,\beta+1}(z) + \alpha z \frac{d}{dz} E_{\alpha,\beta+1}(z), \\ \frac{d^m}{dz^m}\left[z^{\beta-1}E_{\alpha,\beta}(z^\alpha)\right] = z^{\beta-m-1}E_{\alpha,\beta-m}(z^\alpha), \quad \Re(\beta - m) > 0, \quad m = 0, 1, ... \\ \frac{d}{dz}E_{\alpha,\beta}(z) = \frac{E_{\alpha,\beta-1}(z) - (\beta-1)E_{\alpha,\beta}(z)}{\alpha z}. \end{cases}$$

More details and properties concerning these functions can be found in [56].

1.4 Definitions of fractional derivatives

In fractional calculus, many definitions of fractional derivatives exist, depending on the starting point of the theory, on the underlying function space and on the type of application, respectively. A complete overview will not be given (for this we refer to [101, 109, 12, 35]), but we would like to mention the four most relevant definitions connected to the underlying thesis.

We start with a well-known, seemingly, contradictory example that can be explained later on with two different points of view in defining fractional derivatives. We call it a "mysterious contradiction" and it can be worked out easily by applying, in a straightforward way, the Taylor

series of the exponential function in two ways. For this, consider the monomial $y(x) = x^k$ and calculate its nth derivative. Following the rule that connects the factorial and the Gamma-function from section 1.3.1, we recognize immediately:

$$\frac{d^n y}{dx^n} = \frac{k!}{(k-n)!}x^{k-n} = \frac{\Gamma(k+1)}{\Gamma(k-n+1)}x^{k-n} \quad , k \geq n. \tag{1.21}$$

There seems to be no objection to replace the integer n by the real number $\alpha > 0$:

$$\frac{d^\alpha y}{dx^\alpha} = \frac{\Gamma(k+1)}{\Gamma(k-\alpha+1)}x^{k-\alpha} \quad , k \geq \alpha \in \mathbb{R}^+. \tag{1.22}$$

Furthermore, working out the Taylor series of the exponential function, we find:

$$y(x) = \mathrm{e}^x \Rightarrow \frac{d^n y}{dx^n} = \mathrm{e}^x, \tag{1.23}$$

which suggests that we can take:

$$\frac{d^\alpha y}{dx^\alpha} = \mathrm{e}^x = \sum_{k=0}^{\infty}\frac{x^k}{k!} = \sum_{k=0}^{\infty}\frac{x^k}{\Gamma(k+1)}, \ \alpha \in \mathbb{R}^+. \tag{1.24}$$

On the other hand, using similar properties and calculations, we obtain the following:

$$y(x) = \mathrm{e}^x = \sum_{k=0}^{\infty}\frac{x^k}{k!} \tag{1.25}$$

$$\Rightarrow \ \frac{d^n y}{dx^n} = \sum_{k=0}^{\infty}\frac{1}{k!}\frac{k!}{(k-n)!}x^{k-n} = \sum_{k=0}^{\infty}\frac{x^{k-n}}{(k-n)!} = \sum_{k=0}^{\infty}\frac{x^{k-n}}{\Gamma(k-n+1)}. \tag{1.26}$$

From this would directly follow:

$$\frac{d^\alpha y}{dx^\alpha} = \sum_{k=0}^{\infty}\frac{x^{k-\alpha}}{\Gamma(k-\alpha+1)}. \tag{1.27}$$

Comparing equations (1.24) and (1.27), we might conclude that defining a fractional derivative would not be possible in a consistent way. In the following sections we will see that it is possible to explain the confusing difference in these two expressions. For this, we first need to define how we can calculate a fractional integral.

1.4.1 Fractional order integrals

Fractional order integrals can be defined using the well-known concept of repeated integration. This is done by using Cauchy's iterated integral formula. Next, we define the half-Schwartz space[1]

$$\tilde{S}(\mathbb{R}) := \{f \in C^\infty(\mathbb{R}^-) : ||f||_{k,l} < \infty, \ \forall\, k, l \in \mathbb{Z}^+\}, \tag{1.28}$$

where

$$||f||_{k,l} = \sup_{x\in\mathbb{R}^-}|x^k\frac{d^l f}{dx^l}|.$$

[1]This means, in fact, that functions f must satisfy the following property: $P(x)\frac{d^l f}{dx^l} \to 0,$ for $x \to -\infty$ for all polynomials $P(x)$ and all integer lth order derivatives.

For functions in $\tilde{S}(\mathbb{R})$, we define the sequence of integral operators $\mathcal{J}^0, \mathcal{J}^1, \mathcal{J}^2, ...$ in the following way:

$$\begin{aligned}
&\mathcal{J}^0 f(x) = f(x),\\
&\mathcal{J}^1 f(x) = \textstyle\int_{-\infty}^{x} f(s)\, ds,\\
&\mathcal{J}^2 f(x) = \textstyle\int_{-\infty}^{x} \mathcal{J}^1 f(s)\, ds,\\
&.....\\
&\mathcal{J}^n f(x) = \textstyle\int_{-\infty}^{x} \mathcal{J}^{n-1} f(s)\, ds.
\end{aligned} \tag{1.29}$$

When applying Cauchy's iterated integral formula to a function f on the interval $(-\infty, x]$, we obtain the nth order integral:

$$I^n f(x) := \frac{1}{(n-1)!} \int_{-\infty}^{x} (x-s)^{n-1} f(s)\, ds. \tag{1.30}$$

Note that, it can be checked easily, that $\mathcal{J}^n f = I^n f,\ n \in \mathbb{N}$. With this result, it is straightforward to define the fractional integral of order $\alpha \in \mathbb{R}^-$, making use of the fact that $n! = \Gamma(n+1)$ for $n \in \mathbb{N}$:

$$\mathcal{J}^\alpha f(x) := \frac{1}{\Gamma(\alpha)} \int_{-\infty}^{x} \frac{f(s)}{(x-s)^{1-\alpha}}\, ds. \tag{1.31}$$

An important property of this integral is related to a basic property in semi-group theory:

$$\begin{cases} \mathcal{J}^\alpha \mathcal{J}^\beta = \mathcal{J}^\beta \mathcal{J}^\alpha = \mathcal{J}^{\alpha+\beta}, \ \ \forall \alpha, \beta \geq 0 \\ \mathcal{J}^0 = \mathcal{I} \end{cases}. \tag{1.32}$$

This result states that one can interchange the order of fractional integration arbitrarily. The property does not hold, however, in general, for fractional derivatives (see the next sections).

1.4.2 The Riesz derivative

Using formula (1.31) for the fractional integral, we are now able to define, for functions $f \in \tilde{S}(\mathbb{R})$, the so-called Riesz fractional derivative:

$$\mathcal{D}_R^\alpha f(x) := \mathcal{J}^{m-\alpha}\left(\frac{d^m}{dx^m} f(x)\right), \ \ m = \lceil \alpha \rceil, \ \ f \in \tilde{S}(\mathbb{R}).$$

This derivative can be written as a convolution with a weakly singular kernel:

$$\begin{aligned}
\mathcal{J}^{m-\alpha} f(x) &= \tfrac{1}{\Gamma(m-\alpha)} \textstyle\int_{-\infty}^{x} \frac{f(s)}{(x-s)^{1+\alpha-m}}\, ds, \ \ m = \lceil \alpha \rceil, \ \ f \in \tilde{S}(\mathbb{R})\\
&= \chi_+^{m-\alpha} * f(x), \ \ \text{where } \chi_+^{m-\alpha}(x) := \tfrac{1}{\Gamma(m-\alpha)} x^{m-\alpha-1} H(x).
\end{aligned} \tag{1.33}$$

It can be checked that the Riesz derivative is consistent with the non-fractional (ordinary) derivative. For this, we can use the following basic steps:

$$\begin{aligned}\mathcal{D}_R^k f &= \mathcal{J}^{m-k}(\tfrac{d^m}{dx^m} f),\ m > k \\ &= \chi_+^{m-k} * (\tfrac{d^m}{dx^m} f) \\ &= \tfrac{d^k}{dx^k}[(\tfrac{d^{m-k}}{dx^{m-k}} \chi_+^{m-k}) * f] \\ &= \tfrac{d^k}{dx^k}[\delta * f] \\ &= \tfrac{d^k}{dx^k} f.\end{aligned} \tag{1.34}$$

Here, δ, χ and H are the Dirac-delta function, the indicator function and the Heaviside step function, respectively.

1.4.3 The Riemann-Liouville and Caputo derivative

Two other related types of fractional derivatives, named Caputo and Riemann-Liouville derivative, respectively, are defined by:

$$\mathcal{D}_C^\alpha f(x) := \mathcal{J}_0^{m-\alpha}(\frac{d^m}{dx^m} f(x)),\ \ x > 0,\ \ m = \lceil \alpha \rceil, \tag{1.35}$$

$$\mathcal{D}_{RL}^\alpha f(x) := \frac{d^m}{dx^m}(\mathcal{J}_0^{m-\alpha}(f(x))),\ \ x > 0,\ \ m = \lceil \alpha \rceil. \tag{1.36}$$

Note that we changed the lower limit in the fractional order integral (1.31) from $-\infty$ to 0. The underlying integral operator now reads:

$$\mathcal{J}_0^\alpha f(x) := \frac{1}{\Gamma(\alpha)} \int_0^x \frac{f(s)}{(x-s)^{1-\alpha}}\, ds,\ \ x > 0. \tag{1.37}$$

An interesting difference between the two derivatives (1.35) and (1.36) can be directly observed by applying them to a constant function:

$$\mathcal{D}_C^\alpha(constant) = 0, \tag{1.38}$$

whereas

$$\mathcal{D}_{RL}^\alpha(constant) \sim x^{-\alpha} \neq 0. \tag{1.39}$$

It is obvious then that the fractional derivative of a function depends on which definition is being used. However, there exist also correspondences between the Caputo and Riemann-Liouville derivatives. An important result connecting these two derivatives is given by the following result:

Theorem [101]

Let $f \in L^1([0,\infty)) \cap C^m([0,\infty))$ and $m-1 < \alpha \leq m$ for given $m \in \mathbb{N}$. Then:

$$\mathcal{D}_{RL}^\alpha f(x) = \mathcal{D}_C^\alpha f(x) + \sum_{k=0}^{m-1} \frac{f^{(k)}(0^+)}{\Gamma(1+k-\alpha)} x^{k-\alpha}\ \ , x > 0, \tag{1.40}$$

where the notation $f^{(k)}(0^+) = \lim_{x \downarrow 0} f^{(k)}(x)$ is being used.

As a corollary to this theorem we find then:

$$\text{if } f^{(k)}(0^+) = 0,\ k = 0, 1, ..., m-1, \text{ then } \mathcal{D}_{RL}^\alpha = \mathcal{D}_C^\alpha, \tag{1.41}$$

which connects the Caputo and Riemann-Liouville derivative, for special types of functions. The consistency of Caputo's definition will be discussed in Chapter 2.

1.4.4 The Grünwald-Letnikov derivative

The Grünwald-Letnikov definition of a fractional derivative can be viewed as a derivative which finds its roots in the definition of a first derivative in terms of a limit:

$$f'(x) = \lim_{h_1 \to 0} \frac{f(x) - f(x-h_1)}{h_1} \approx \frac{f(x) - f(x-h_1)}{h_1}, \text{ if } 0 < h_1 \ll 1. \tag{1.42}$$

In a similar way, we can define the second derivative of a function:

$$f''(x) = \lim_{h_2 \to 0} \frac{\lim_{h_1 \to 0} \frac{f(x) - f(x-h_1)}{h_1} - \lim_{h_1 \to 0} \frac{f(x-h_2) - f(x-h_1-h_2)}{h_1}}{h_2}. \tag{1.43}$$

It is clear that one can extend this derivation to third, fourth and higher integer derivatives as well. These formulas in ordinary calculus may be used in the construction of approximations, i.e., numerical discretizations of derivatives in terms of finite differences. If we take $h = h_1 = h_2$ in (1.43), we see that we obtain for the ordinary second derivative:

$$f''(x) = \lim_{h \to 0} \frac{f(x) - 2f(x-h) + f(x-2h)}{h^2} \approx \frac{f(x) - 2f(x-h) + f(x-2h)}{h^2}, \tag{1.44}$$

if $0 < h \ll 1$. Using the principle of mathematical induction one can extend this idea to the nth derivative in the following way:

$$f^{(n)}(x) = \lim_{h \to 0} \frac{1}{h^n} \sum_{m=0}^{n} (-1)^m \left(\begin{array}{c} n \\ m \end{array} \right) f(x - mh), \; n \in \mathbb{N}, \tag{1.45}$$

where $\left(\begin{array}{c} n \\ m \end{array} \right) = \frac{n!}{m!(n-m)!}$. We have set the upper limit of the sum to n in (1.45), but there is no harm in setting it to ∞, because the binomial coefficients will be zero for m larger than n. Next, replacing the "!"-terms with values in terms of the Gamma function, we define the Grünwald-Letnikov fractional derivative:

$$\mathcal{D}^{\alpha}_{GL} f(x) := \lim_{h \to 0} \frac{1}{h^{\alpha}} \sum_{m=0}^{\infty} (-1)^m \frac{\Gamma(\alpha + 1)}{m! \Gamma(\alpha - m + 1)} f(x - mh). \tag{1.46}$$

Note that the derivative of integer order n is obtained if $\alpha = n$ and the n-fold integral if $\alpha = -n$. This observation naturally leads to the idea of a generalization of the notions of differentiation and integration by allowing α to be an arbitrary real of even complex number. We have encountered four different definitions of fractional derivatives. An important result from [101] connects these definitions and states that they are *equivalent* for a special class of functions. This result is summarized as follows:

$$\text{For } \; f \in C^{m+1}_{0-}(\mathbb{R}^{\geq 0}) := \{ f \in C^{m+1}([0, \infty)) \; \& \; f(x) = 0 \text{ for } x \leq 0 \}, \tag{1.47}$$

the Riesz (section 1.4.2), Riemann-Liouville, Caputo (both in section 1.4.3) and Grünwald-Letnikov fractional derivatives are equivalent:

$$\mathcal{D}^{\alpha}_{RL} f(x) = \mathcal{D}^{\alpha}_{C} f(x) = \mathcal{D}^{\alpha}_{R} f(x) = \mathcal{D}^{\alpha}_{GL} f(x). \tag{1.48}$$

It is interesting to note that the mentioned "mysterious contradiction" at the beginning of this section can now be explained. In fact, the difference between equations (1.24) and (1.27) is due to the fact that in the calculations, almost unnoticeably, two different definitions have been used, which do not coincide for the exponential function. This difference is similar to the fact that the Caputo derivative of a constant function is zero, while it is a non-zero function in terms of the Riemann-Liouville sense. In the next section some other properties of fractional derivatives are given to show differences with ordinary calculus.

1.4.5 Properties of fractional derivatives

In this section, some additional properties of fractional derivatives are discussed (see also [74]).

Basic properties:

1. For $\alpha > 0$ and any $n \in \mathbb{Z}^+$: $\frac{d^n}{dx^n}[D^{\alpha}_{RL} f(x)] = D^{n+\alpha}_{RL} f(x)$
   and: $\frac{d^n}{dx^n}[D^{-\alpha}_{RL} f(x)] = D^{n-\alpha}_{RL} f(x)$.
2. For $\alpha,\ \beta > 0$: $D^{\alpha}_{RL}[D^{-\beta}_{RL} f(x)] = D^{\alpha-\beta}_{RL} f(x)$.
3. $D^{\alpha}_{C}[D^{-\beta}_{C} f(x)] = D^{\alpha-\beta}_{C} f(x)$ does <u>not</u> hold for all $\alpha,\ \beta > 0$.
4. $D^{-\alpha}_{RL}[D^{\alpha}_{RL} f(x)] = f(x) - \sum_{k=1}^{n} \big(x^{\alpha-k} \frac{[D^{\alpha-k}_{RL} f(x)]_{x=0}}{\Gamma(\alpha-k+1)}\big)$, where $\alpha \in (n-1, n)$, $n \in \mathbb{Z}^+$.
5. $D^{-n}_{RL}[D^{n}_{RL} f(x)] = f(x) - \sum_{k=0}^{n-1} \frac{x^k}{k!} f^{(k)}(0)$.
6. $D^{n}_{RL} c = \frac{x^{-\alpha} c}{\Gamma(1-\alpha)}$, where $\alpha > 0$ and c is an arbitrary constant.
7. $D^{\alpha}_{C} f(x) = D^{\alpha}_{RL} f(x) - \sum_{k=0}^{n-1} \frac{x^k}{k!} f^{(k)}(0)$, where $\alpha \in (n-1, n)$, $n \in \mathbb{Z}^+$.

Linearity of the operator:
As for integer-order differentiation, fractional differentiation defines a linear operator as well:

$$D^{\alpha}\Big(\lambda f(x) + \mu g(x)\Big) = \lambda D^{\alpha} f(x) + \mu D^{\alpha} g(x), \tag{1.49}$$

where D^{α} denotes the fractional operator.

This can easily be checked. For example, for the Grünwald-Letnikov fractional operator while $nh = x$:

$$\begin{aligned} D^{\alpha}_{GL}\Big(\lambda f(x) + \mu g(x)\Big) &= \lim_{h\to 0} h^{-\alpha} \sum_{r=0}^{n} (-1)^r \binom{\alpha}{r} \big(\lambda f(x-rh) + \mu g(x-rh)\big), \\ &= \lambda \lim_{h\to 0} h^{-\alpha} \sum_{r=0}^{n} (-1)^r \binom{\alpha}{r} f(x-rh) + \\ &\qquad + \mu \lim_{h\to 0} h^{-\alpha} \sum_{r=0}^{n} (-1)^r \binom{\alpha}{r} g(x-rh) \\ &= \lambda D^{\alpha}_{GL} f(x) + \mu D^{\alpha}_{G:} g(x). \end{aligned}$$

Note that we have used the fractional version of the binomial coefficient:

$$\binom{\alpha}{r} := \frac{\Gamma(\alpha+1)}{r!\,\Gamma(\alpha+1-r)}. \tag{1.50}$$

Similarly, we can show the linearity property for the Riemann-Liouville fractional derivative of order α $(1 \le \alpha < m)$:

$$D^{\alpha}_{RL}\Big(\lambda f(x) + \mu g(x)\Big) = \frac{1}{\Gamma(m-\alpha)} \frac{d^m}{dx^m} \int_0^x (x-\tau)^{m-\alpha-1} \big(\lambda f(\tau) + \mu g(\tau)\big) d\tau,$$

$$
\begin{aligned}
&= \frac{\lambda}{\Gamma(m-\alpha)} \frac{d^m}{dx^m} \int_0^x (x-\tau)^{m-\alpha-1} f(\tau) d\tau \\
&\quad + \frac{\mu}{\Gamma(m-\alpha)} \frac{d^m}{dx^m} \int_0^x (x-\tau)^{m-\alpha-1} g(\tau) d\tau \\
&= \lambda D^{\alpha}_{RL} f(x) + \mu D^{\alpha}_{RL} g(x).
\end{aligned}
$$

It may be obvious that one can show this property for the Caputo and Riesz derivative as well.

The Leibniz rule:
For two functions, $\varphi(x)$ and $\psi(x)$, the Leibniz rule for the n-th order derivative of the product $\varphi(x)\psi(x)$ reads:

$$
\frac{d^n}{dx^n}\big(\varphi(x)\psi(x)\big) = \sum_{k=0}^{n} \binom{n}{k} \varphi^{(k)}(x) \psi^{(n-k)}(x). \tag{1.51}
$$

Replacing the integer n in (1.51) by the real-valued parameter α, means that the integer order derivative $\psi^{(n-k)}(x)$ in the formula is replaced by, for example, the Grünwald-Letnikov fractional order derivative $D^{\alpha-k}_{GL}\psi(x)$. Then equation (1.51) becomes:

$$
D^{\alpha}_{GL}\big(\varphi(x)\psi(x)\big) = \sum_{k=0}^{\lceil \alpha \rceil} \binom{\alpha}{k} \varphi^{(k)}(x) D^{\alpha-k}_{GL} \psi(x), \tag{1.52}
$$

where formula (1.50) has been used.

The chain rule:
Unfortunately, the chain rule, $[f \circ g(x)]' = f'(g(x))g'(x)$ for ordinary derivatives, can *not* be applied to fractional derivatives. In general,

$$
D^{\alpha}[f \circ g(x)] \neq f'(g(x)) D^{\alpha} g(x) \neq D^{\alpha} f(g(x)) g'(x) \neq D^{\alpha} f(g(x)) D^{\alpha} g(x). \tag{1.53}
$$

Counter examples can be found in references [101, 109, 97].

To conclude this section: one way of understanding fractional derivatives is to see them as a *nonlinear* interpolation of ordinary derivatives in terms of a convolution with a weakly-singular kernel. For more detailed information about other properties of fractional derivatives, we refer to [69].

1.5 Why fractional derivatives?

We can also pose this question as "why don't we use the classical derivative?". Actually, this question is a modern counterpart of similar fundamental questions throughout the history of mathematics. For example, nowadays, nobody would ask: why do we need rational numbers or even real numbers, let alone, complex numbers? Or: why can't we work merely with the integers? Moreover, taking "1/2" powers (square roots) of numbers is no point of discussion anymore at all. During the last centuries, the use of the "fractional" versions of numbers and powers of numbers was understood, justified and clarified. Such a justification could also be made for fractional integrals and fractional derivatives. For example, fractional space derivatives and fractional Laplacian operators may be used to describe so-called Lévy processes of particles, whereas Brownian motions can be connected to the traditional Laplace operator. These aspects are illustrated in Figures 1.4, 1.5 and 1.6 and are also explained in much more detail in [30,

105, 67, 24] (for fractional derivatives and Lévy flights)) and in [130, 45, 96, 95] (for fractional Laplacians).

In Lévy flight processes the particles may, now and then, jump irregularly to other positions (see Figure 1.4). The effect of changing the order of the fractional space derivative, from values between one and two up to the traditional value of two, is depicted in Figure 1.5. Furthermore, Lévy flights (Figure 1.6, bottom) are of interest in epidemic modeling. They could model the diffusion process extended with an extra feature for the sudden travel of individuals by real flights from one city to another. The spreading of diseases in ancient times (Figure 1.6, top) does not need fractional derivatives: a traditional reaction-diffusion model suffices for such cases. To clarify the situation a little bit more: in Figure 1.7 the picture in the left panel shows solutions of the heat equation (normal diffusion) compared to those of a fractional heat equation, based on Caputo's definition (see previous sections), in the right panel. The differences in the decaying behavior of the solution are obvious from the figures, but, note that they may also depend on the particular choice of fractional derivative.

The use of fractional operators in the time direction (fractional time and time-fractional derivatives), is, due to the fundamental differences between space and time, high-lighted from an even more theoretical perspective in physics: what does 'time' mean and could time be even fractional? This fundamental question is still unsolved, and has been discussed in literature extensively (see, e.g., [66, 64, 65, 14, 51]). It must be remarked that the integer order derivative is a local operator which is, with regard to the above discussion, inappropriate for many interesting applications. In such cases, the effect of a larger neighborhood or larger time span can not be modeled easily without fractional order derivatives. In the next section, a series of interesting applications will be given to illustrate this.

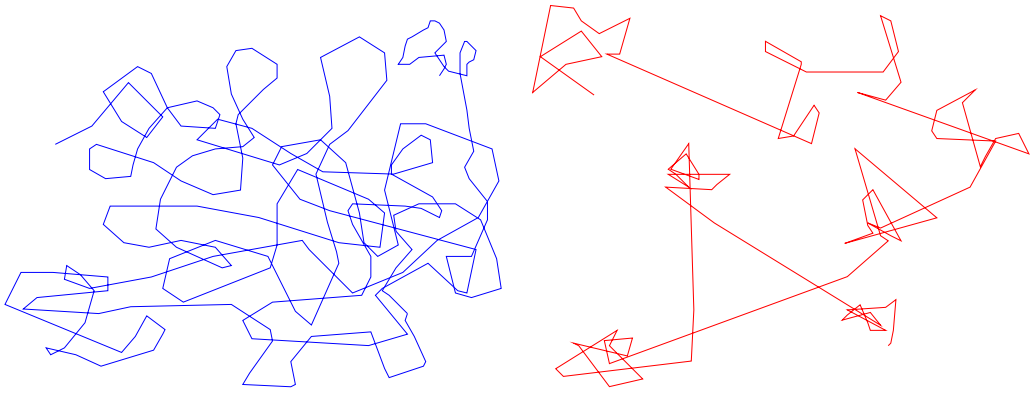

FIGURE 1.4: Brownian motions (left panel) vs Lévy flights (right panel).

1.6 Application areas

In this section, several applications of fractional calculus and fractional differential equations will be discussed. We will do this in a kaleidoscopic way: neither in chronological order, nor in order of increasing importance or impact. It shows the richdom of application areas of fractional order models, which mainly have been developed in the last three decennia.

The Tautochrone problem

The Tautochrone problem [46] was studied first by Abel in 1823. This problem is also important from a historical point of view, because it was one of the first applications of fractional calculus to a 'real-life' model. The question here is to find the curve for which the time taken

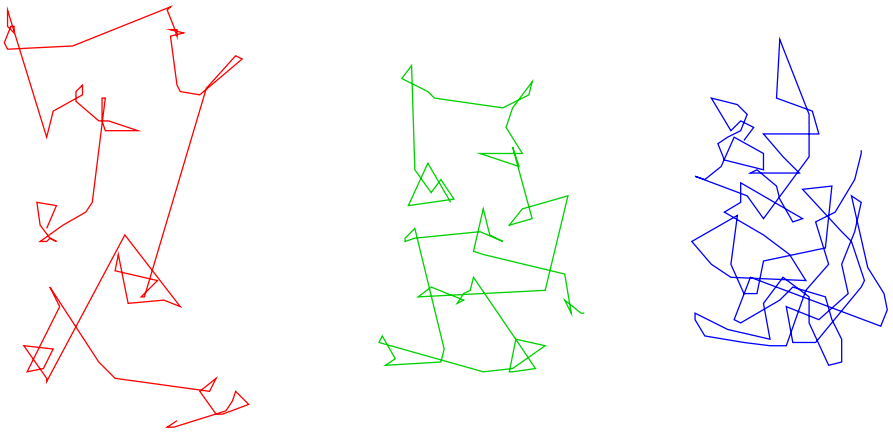

FIGURE 1.5: The variation of the fractional order α to illustrate the effect on the motion of particles: fractional diffusion with $\alpha = 1.5$ (left), $\alpha = 1.75$ (middle) and regular diffusion with $\alpha = 2$ (right).

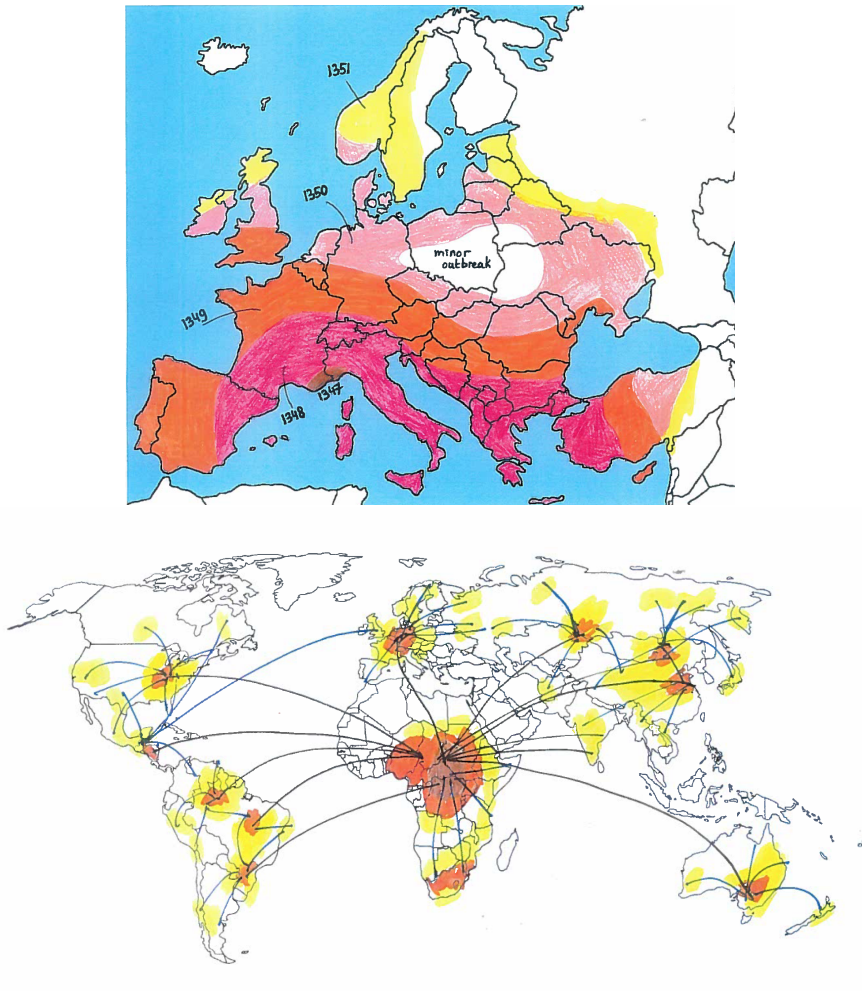

FIGURE 1.6: Diffusion processes in ancient epidemic modeling based on Brownian motions (top) versus Lévy flight processes in modern epidemics (bottom).

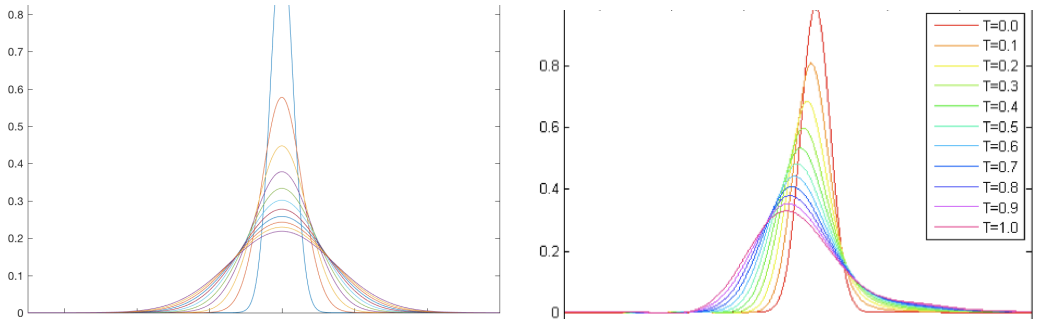

FIGURE 1.7: Solutions of the heat equation at $t = 0, 0.1, 0.2, ..., 1.0$ (left panel) versus the fractional heat equation of order $\frac{3}{2}$ (right panel).

by an object sliding without friction in uniform gravity to its lowest point is independent of its starting point. One can derive that this curve must be a cycloid, and the time is depending on the square root of the radius and the acceleration of gravity. The problem that describes this feature can be modeled by an integral equation of the form:

$$\frac{1}{\Gamma(\alpha)} \int_0^x \frac{y(s)}{(x-s)^{1-\alpha}}\, ds \; = h(x), \;\; 0 < \alpha < 1.$$

Abel solved this integral equation in an elegant way to obtain:

$$y(x) = \frac{1}{\Gamma(1-\alpha)} \frac{d}{dx} \int_0^x \frac{h(s)}{(x-s)^{\alpha}}\, ds \; = \mathcal{D}^{\alpha}_{RL} h(x).$$

Indeed, we recognize the Riemann-Liouville fractional derivative as the solution for this model.

Tensile and flexural strength of disorder materials

A relatively new application of fractional differential equations in mechanics is the size effect of some building material which aggregates like concrete [84]. This kind of material does not follow the classical rules of solid mechanics and fractional calculus is a significant tool to model this problem.

Fractional advection-dispersion equation

The fractional order form of the advection-dispersion equation [16] models particles which encounter very large transitions. These models play a role in transport in inhomogenous materials.

Bloch equations in MRI

In [102] the authors describe time-fractional Bloch equations and its application in magnetic resonance imaging (MRI). Adding the time-fractional term provides more flexibility in modeling the relaxation process.

Liquid containing gas bubbles

Time-fractional derivatives have been utilized in [52] to model nonlinear wave processes in a liquid containing gas bubbles. Solitary wave solutions are found that follow fractional order rules in the model.

Nonlinear optics

In [128] fractional calculus is entering the field of nonlinear optics to describe unconventional regimes, like disorder biological media and soft-matter. To model this behaviour, a

fractional Schrödinger equation is analyzed which also connects the traditional model to Lévy processes.

Long-distance optical communications

Fractional differentiation is of importance to model long-distance optical communications [126]. Caputo fractional derivatives are used in the modeling of optical pulse propagation in nonlinear fibers.

Neurodynamics

A fractional cable equation simulates the electrodiffusion of ions in neurodynamics. Researchers [129] have found that in nerve cells molecular diffusion can be replaced by anomalous subdiffusion.

Acoustics

The study of a fractional Burgers' equation in nonlinear acoustics is presented in [81]. The motivation to use fractional derivatives here comes from an elementary model of shock waves in brass wind instruments, that proves to be useful in musical acoustics.

Econometrics

Long-memory processes and fractional integration in econometrics provide new insights in the analysis of population characteristics [10]. In economics and finance the long-memory volatility is important to describe this behaviour.

Dielectric media

In [115] electromagnetic fields in dielectric media follow a fractional power-law dependence in a wide frequency range. This is modeled by differential equations with time derivatives of non-integer order.

Mechanics of solids

Applications of fractional calculus to nonlinear problems in hereditary mechanics of solids can be found in [108]. Fractional viscoelastic equations are used for modeling damped vibrations in elastic bodies.

Crime modeling

An interesting application arises in the modeling of crime with Lévy flights in [29]. Here, the movement of crime agents is related to a biased Brownian motion with a fractional Laplacian operator. Fractional derivatives are applied to model the formation of hotspots of criminal activity.

Fractional-order epidemic models

In [53] a system of fractional order reaction-diffusion equations is proposed to model the superdiffusive spread of modern epidemics due to Lévy flights. Theoretical analysis and numerical simulations show the potential of fractional derivatives to represent epidemic fronts.

This list of applications is just a brief overview of the recent emergence of fractional models in many different areas. For more applications, we would like to refer to [103, 33, 106, 103].

1.7 Numerical methods for fractional differential equations

Just as for ordinary differential equation models, analytical solutions can be constructed of fractional order differential equations only for special cases. Therefore, numerical methods to obtain approximate solutions need to be developed. Since fractional models in applications have only become of interest in the last half century, their numerical analysis has started up relatively recently. In the last couple of years, several articles and books have appeared which treat approximation techniques for this kind of models. Most of these are based on finite difference types of discretizations that approximate the integro-differential operators with weakly singular kernels. To illustrate this, we give a straightforward, first order, discretization of the Caputo derivative $\mathcal{D}_C^\alpha$ $(1 < \alpha < 2)$ of a function $u(x)$ at the grid point x_i:

$$\begin{aligned}
&\mathcal{D}_C^\alpha u|_{x=x_i} \\
&= \tfrac{1}{\Gamma(2-\alpha)} \int_0^{x_i} \tfrac{u''(s)}{(x_i-s)^{\alpha-1}} ds \\
&\approx \tfrac{1}{\Gamma(3-\alpha)} \textstyle\sum_{j=1}^{i-1} \{x_{j+1}^{2-\alpha} - x_j^{2-\alpha}\} \tfrac{u_{i-j+1}-2u_{i-j}+u_{i-j-1}}{h^2} \\
&= \tfrac{1}{\Gamma(3-\alpha)} \textstyle\sum_{j=1}^{i-1} \{\tfrac{j^{2-\alpha}-(j-1)^{2-\alpha}}{h^{\alpha-2}}\} \{\tfrac{u_{i-j+1}-2u_{i-j}+u_{i-j-1}}{h^2}\} \\
&= \tfrac{1}{\Gamma(3-\alpha)h^\alpha} \textstyle\sum_{j=1}^{i-1} \{j^{2-\alpha} - (j-1)^{2-\alpha}\} \{u_{i-j+1} - 2u_{i-j} + u_{i-j-1}\}.
\end{aligned} \tag{1.54}$$

In formula (1.54) we see that the resulting finite-difference matrix does not have a tridiagonal form anymore, which would be the case for a three-point approximation of the second derivative in the normal heat equation (see also (1.43)). This is typical for numerical approximations of fractional order equations. An overview of numerical methods can be found, for instance, in [12, 35, 35] and references therein. Here, we would like to mention just a few important articles on this subject. For instance, in [85, 86] the authors realized that fractional derivative models are strongly related to Abel-Volterra equations. They developed a framework for a discretized fractional calculus and convolution quadrature formulas in terms of fractional linear multistep methods. Meerschaert and co-authors extended the principle of finite difference techniques to many different fractional partial differential equations (see [15, 80, 110, 90]). Another important class of numerical methods was investigated and applied in [87, 23, 25, 25, 24].

This thesis is making use of approximating series solutions, instead of numerical solutions based on finite differences. Traditionally, basic methods like Taylor series or power series are included in this category. For special cases, one could apply extensions of these ideas, such as perturbation methods or methods with special parameters. Recently, Adomian decomposing methods and methods based on variational iterations came into play. For more details and an overview on this topic, one could consult [61, 59, 68, 122, 7, 78, 77]. A major drawback of such methods is their applicability and lack of convergence for linear and nonlinear differential equation models. One of the aims of this thesis is to numerically investigate recently developed series methods based on homotopy principles. The goal is, therefore, to numerically analyze their convergence properties and compare the experimental results with analytical solutions, that are available only in certain cases.

As an illustration of this idea and to show its relation with a traditional numerical method, we work this out for a homotopy based method and show its connection with Newton's method for solving nonlinear equations. The series methods in this thesis make us of step-wise approximations. In each next step, the approximating solution will be extended and, the aim is, to

improve its accuracy in this way. A typical example of such a series method can be described by sequences of approximations for the nonlinear equation $f(x) = 0$:

$$\begin{aligned}
&\text{step 0}: \ x \approx x_0, \\
&\text{step 1}: \ x \approx x_0 + x_1 = x_0 - \tfrac{f(x_0)}{f'(x_0)}, \\
&\text{step 2}: \ x \approx x_0 + x_1 + x_2 = x_0 - \tfrac{f(x_0)}{f'(x_0)} - \tfrac{f^2(x_0)f''(x_0)}{2[f'(x_0)]^3}, \\
&\text{step 3}: \ x \approx x_0 + x_1 + x_2 + x_3 = x_0 - \tfrac{f(x_0)}{f'(x_0)} - \tfrac{f^2(x_0)f''(x_0)}{2[f'(x_0)]^3} + ..., \\
&\text{step 4}: \ \text{etcetera.}
\end{aligned} \tag{1.55}$$

Step 0 is an initial approximation. We recognize in step 1 the, well-known, *quadratically* convergent Newton's method for solving the nonlinear equation. Step 2 can be viewed as the *cubically* convergent method developed by Olver [98], and so on. As we see, formulas become more complicated on the one hand and more accurate on the other hand. To obtain efficient numerical solutions, it is, of course, of importance to find a golden mean. Similar ideas are used for the treatment of nonlinear fractional differential equations in the remaining part of the thesis.

1.8 Outline of the thesis

The new contribution of this work consists of combining the ideas mentioned in the current chapter and applying them to time- and space-fractional differential equation models. To be more precise: a Homotopy Perturbation Method (HPM) is used for the numerical calculation of space-fractional (stationary) reaction-diffusion-advection models in chapter 2. Further, chapter 3 approximates a time-fractional partial differential equation model with an extension of this idea: the Homotopy Analysis Method (HAM). Finally, in chapter 4, HAM is further extended and its convergence is accelerated, by adding the concept of Padé approximations. Both stationary (non-fractional) and time-dependent (fractional) differential equations are treated. It must be stressed that investigating the numerical performance of these methods is the main goal of the research. Especially, we would like to discuss their dependence, not only on the numerical parameters, but also on the parameters in the model itself.

Chapter 2

A homotopy perturbation method for fractional-order advection-diffusion-reaction boundary-value problems[1]

Abstract

In this chapter we describe the application of the homotopy perturbation method (HPM) to two-point boundary-value problems with fractional-order derivatives of Caputo-type. We show that HPM is equivalent to the semi-analytical Adomian decomposition method when applied to a class of nonlinear fractional advection-diffusion-reaction models. A general expression is derived for the coefficients in the HPM series solution. Numerical experiments are given to demonstrate several properties of HPM, such as its dependence on the fractional order and the parameters in the model. In the case of more than one solution, HPM has difficulties to find the second solution in the model. Another example is given for which HPM seems to converge to a spurious numerical solution. However, the bifurcation theory connected to this model [11, 73] proves that there does not exist a solution at all for this situation.

2.1 Introduction

This chapter is devoted to the numerical study of a semi-analytical technique known as the homotopy perturbation method (HPM). The method was introduced by He [61, 59, 60, 62], For general nonlinear boundary-value models, it is almost impossible to derive exact solutions. Even if they are available, the calculations to obtain numerical values may be cumbersome, or it may be difficult to interpret the behavior of the solution. Recently, several new approximation methods in terms of infinite series have been proposed. These methods include the Adomian decomposition method [68], the variational iteration method [94], the *Exp*-function method [100] and HPM. Here, we analyze the application of HPM to a certain class of fractional-order boundary-value problems.

2.2 A fractional-order advection-diffusion-reaction model

We consider the following fractional-order BV-model of Bratu-type with damping and source term [59, 68, 109]:

$$\begin{cases} \epsilon\, \mathcal{D}_C^{\alpha} u + \gamma\, u' + f(u) = S(x),\ x \in (0,1), \\ u(0) = u_L,\ u(1) = u_R, \end{cases} \tag{2.1}$$

[1] This is joint work with P. A. Zegeling (Utrecht University). It has been published in the journal Applied Mathematical Modelling, Vol. 47, pages 425-441, 2017; http://dx.doi.org/10.1016/j.apm.2017.03.006.

with parameters $1 < \alpha \leq 2, 0 < \epsilon \leq 1$, and $\gamma \in \mathbb{R}$. The nonlinear source term $f : [0, \infty) \to [0, \infty)$ is assumed to be continuous. The function $S(x)$ represents a spatially dependent source term. The solution u is a function $u : [0, 1] \to [0, \infty)$. Applications stem, among others, from astrophysics and combustion theory. With $\mathcal{D}_C^\alpha$, we denote a fractional derivative defined in the Caputo sense (see Definition 4 below). The left three terms in differential equation (2.1) may be identified as fractional diffusion (corresponding to Lévy-flight processes), advection (with velocity γ) and a chemical reaction term represented by f. For simplicity, the boundary conditions are taken to be of Dirichlet type. To define the fractional derivative we need first to set up the function space of possible solutions and to derive some useful properties (see also [109]):

Definition 1. *A real function $g(x),\ x > 0$, lies in the function space $C_\gamma,\ \gamma \in \mathbb{R}$, if there exists a real number $p > \gamma$ such that g can be written as $g(x) = x^p g_1(x)$ with $g_1(x) \in C[0, \infty)$. It is clear that the property $C_{\gamma_1} \subset C_{\gamma_2}$ for $\gamma_2 \leq \gamma_1$ holds.*

Definition 2. *A function $g(x),\ x > 0$, lies in the function space $C_\gamma^m,\ m \in \mathbb{N} \cup \{0\}$, if $g^{(m)} \in C_\gamma$.*

Definition 3. *The left-sided Riemann-Liouville fractional integral $\mathcal{J}^\alpha$ of order $\alpha \geq 0$ of a function $g \in C_\gamma,\ \gamma \geq -1$ is defined as*

$$\begin{cases} \mathcal{J}^\alpha g(x) = \frac{1}{\Gamma(\alpha)} \int_0^x \frac{g(t)}{(x-t)^{1-\alpha}} dt,\ \alpha > 0,\ x > 0, \\ \mathcal{J}^0 g(x) = g(x), \end{cases} \tag{2.2}$$

where Γ denotes the Euler-gamma function that interpolates the factorial in integer values (with a shift of one unit): $\Gamma(m + 1) = m!,\ m \in \mathbb{N}$.

Definition 4. *Let $g \in C_{-1}^m,\ m \in \mathbb{N} \cup \{0\}$. Then the left-sided Caputo fractional derivative $\mathcal{D}_C^\alpha g$ is defined as:*

$$\mathcal{D}_C^\alpha g(x) = \mathcal{J}^{m-\alpha} g^{(m)}(x), \quad m - 1 < \alpha \leq m,\ m \in \mathbb{N}. \tag{2.3}$$

The following properties for $\mathcal{J}^\alpha$ and $\mathcal{D}_C^\alpha$ can be derived [109]:

$$\begin{cases} \mathcal{J}^\alpha \mathcal{J}^\nu g(x) = \mathcal{J}^\nu \mathcal{J}^\alpha g(x) = \mathcal{J}^{\alpha+\nu} g(x), \quad \alpha, \nu \geq 0,\ g \in C_\gamma,\ \gamma \geq -1, \\ \mathcal{J}^\alpha x^\delta = \frac{\Gamma(\delta+1)}{\Gamma(\delta+\alpha+1)} x^{\delta+\alpha}, \quad \alpha > 0,\ \delta > -1,\ x > 0, \\ \mathcal{D}_C^\alpha \mathcal{J}^\alpha g(x) = g(x), \\ \mathcal{J}^\alpha \mathcal{D}_C^\alpha g(x) = g(x) - \sum_{k=0}^{m-1} g^{(k)}(0^+) \frac{x^k}{k!}, \quad m - 1 < \alpha \leq m, x > 0, \\ \mathcal{D}_C^\alpha x^\delta = \frac{\Gamma(\delta+1)}{\Gamma(\delta-\alpha+1)} x^{\delta-\alpha}, \quad \alpha > 0,\ \delta > -1,\ x > 0, \end{cases} \tag{2.4}$$

where $g^{(k)}(0^+) := \lim_{x \downarrow 0} g^{(k)}(x)$. The first result shows the so-called semi-group property of fractional integrals. The second formula is a generalization of the integer counter-part: $\mathcal{J}^m x^k = \frac{k!}{(m+k)!} x^{k+m}$. The third and fourth properties indicate that $\mathcal{J}^\alpha$ and $\mathcal{D}_C^\alpha$ are not each other's inverses, unless a remainder term is zero. This can be forced, however, by further restricting the function space C_γ^m. The fifth property is the derivative counterpart of the second one. The consistency of the fractional derivative with respect to the traditional integer derivative can be expressed by the following result:

Theorem 1. *The Caputo fractional derivative $\mathcal{D}_C^\alpha$ with $m - 1 < \alpha \leq m$ is consistent with the integer-order derivative $\frac{d^m}{dx^m}$ for $m \in \mathbb{N}$.*

Proof. For $g \in C^{m+1}([0, \infty])$, we write:

$$\begin{aligned} \mathcal{D}_C^\alpha g(x) &= \tfrac{1}{\Gamma(m-\alpha)} \int_0^x \tfrac{g^{(m)}(s)}{(x-s)^{1-(m-\alpha)}} ds \\ &= \tfrac{1}{\Gamma(m-\alpha)} [-\tfrac{(x-s)^{m-\alpha}}{m-\alpha} g^{(m)}(s)|_{s=0}^{s=x} + \int_0^x \tfrac{(x-s)^{m-\alpha}}{m-\alpha} g^{(m+1)}(s) ds] \\ &= \tfrac{1}{\Gamma(m-\alpha+1)} [0 + x^{m-\alpha} g^{(m)}(0) + \int_0^x (x-s)^{m-\alpha} g^{(m+1)}(s) ds] \end{aligned}$$

and taking the limit: $\alpha \in \mathbb{R} \to m \in \mathbb{N}$ with $m-1 \leq \alpha \leq m$ yields:

$$= \frac{1}{\Gamma(1)}[g^{(m)}(0) + \int_0^x g^{(m+1)}(s)ds]$$
$$= g^{(m)}(0) + g^{(m)}(x) - g^{(m)}(0) = \frac{d^m g}{dx^m}(x).$$

□

Note that the solution of boundary-value model (2.1) does not necessarily need to have a unique solution. It is known, for example, that for exponential-type functions g there may be zero, one or two solutions, depending on a parameter in the model (see [11, 73]).

2.3 The Homotopy Perturbation Method (HPM)

In this section we describe a semi-analytical technique to approximate solutions of model (2.1). To explain the underlying concept of approximating solutions of the BV-problems (2.1), we first define a more general nonlinear differential equation by

$$D(u) = h(x), \quad x \in \Omega \subset \mathbb{R} \tag{2.5}$$

with boundary conditions

$$\mathcal{B}(u, \frac{\partial u}{\partial x}) = 0, \ x \in \partial\Omega. \tag{2.6}$$

Here, D describes a general differential operator, $\mathcal{B}$ a boundary operator, h a given analytic function and $\partial\Omega$ the boundary of the spatial domain Ω, respectively. It is useful to divide the operator D into two parts which we denote by $\mathcal{L}$ and $\mathcal{N}$, where $\mathcal{L}$ is a linear operator and $\mathcal{N}$ the remaining nonlinear part of the operator. Equation (2.5) may then be written as

$$\mathcal{L}(u) + \mathcal{N}(u) = h(x). \tag{2.7}$$

We construct a homotopy $u(x;p) : \Omega \times [0,1] \to \mathbb{R}$ which satisfies

$$\mathcal{H}(u;p) := (1-p)[\mathcal{L}(u) - \mathcal{L}(v_0)] + p[D(u) - h(x)] = 0.$$

This is equivalent to

$$\mathcal{H}(u;p) = \mathcal{L}(u) - \mathcal{L}(v_0) + p\mathcal{L}(v_0) + p[\mathcal{N}(u) - h(x)] = 0. \tag{2.8}$$

In equation (2.8), $p \in [0,1]$ represents a so-called embedding parameter, and v_0 can be viewed as an 'initial' approximation of the original model (2.5) which satisfies boundary condition (2.6). Obviously, from (2.7) and (2.8) it follows that

$$\begin{cases} \mathcal{H}(u;0) = \mathcal{L}(u) - \mathcal{L}(v_0) = 0 \\ \mathcal{H}(u;1) = D(u) - h(x) = 0. \end{cases} \tag{2.9}$$

The process of deforming p from zero to unity in (2.8) is just the deformation of $u(x;p)$ from the chosen function $u(x;0) = v_0(x)$ to the solution $u(x;1) = u(x)$ of differential equation (2.5). The term deformation stems from topology and the relation between the expressions $\mathcal{L}(u) - \mathcal{L}(v_0)$ and $D(u) - h(x)$ is called a homotopy. According to the homotopy perturbation method, the assumption is made that the solution of equation (2.8) can be written as a formal power series in the embedding parameter p:

$$u(x;p) = v_0(x) + v_1(x)p + v_2(x)p^2 + ... = \sum_{k=0}^{\infty} v_k(x)p^k. \tag{2.10}$$

Finally, on setting $p = 1$, this results in the formal solution

$$u(x) = \lim_{p\to 1} u(x;p) = \sum_{k=1}^{\infty} v_k(x). \tag{2.11}$$

Approximations to $u(x)$ are obtained by truncating the infinite series to:

$$u(x) \approx V_N(x) := \sum_{k=1}^{N} v_k(x). \tag{2.12}$$

The described approximation technique is called the homotopy perturbation method (HPM). This method has the *potential* advantage that it may overcome some limitations of traditional perturbation methods. The convergence of series (2.10) certainly depends on the nonlinear differential operator D. In general, one finds that the second derivative with respect to u of the nonlinear part $\mathcal{N}$ in the splitting (2.7) must be sufficiently small, since the parameter p may be relatively large, in fact we take $p \to 1$. Furthermore, to ensure convergence of the series the following estimate [61] must hold: $||\mathcal{L}^{-1}\frac{\partial \mathcal{N}}{\partial v}|| < 1$. For more details on the convergence of HPM we refer to [117, 61]. It may be clear from the construction above that the choice of the homotopy is not unique and therefore, the convergence (or divergence) also depends on that choice. Unfortunately, there exists no general theory yet to deal with this problem and each case has to be analyzed separately.
Next, we work out the described concept of HPM for boundary-value problem (2.1). For this model we take the homotopy defined by:

$$\begin{cases} \epsilon \mathcal{D}_C^{\alpha} u + p[\gamma u' + f(u) - S(x)] = 0, \;\; 1 < \alpha \leq 2, \\ u(0;p) = u_L, \; u(1;p) = u_R, \;\; p \in [0,1]. \end{cases} \tag{2.13}$$

To obtain subsequent approximations for $v_0, v_1, ...$, we use series (2.10), the linearity of the operator $\mathcal{D}_C^{\alpha}$ and a Taylor expansion of the function f around $u = 0$:

$$\begin{aligned} f(u) &= f(0) + f'(0)u + f''(0)\tfrac{u^2}{2!} + ... \\ &= f(0) + f'(0)v_0 + \tfrac{f''(0)}{2}v_0^2 + \tfrac{f'''(0)}{6}v_0^3 + ... \\ &\quad + p[f'(0)v_1 + v_0 v_1 f''(0) + \tfrac{5}{12}v_0^2 v_1 f'''(0) + ...] \\ &\quad + p^2[f'(0)v_2 + (2v_0v_2 + v_1^2)\tfrac{f''(0)}{2} + (\tfrac{5}{2}v_0^2 v_2 + 3v_0 v_1^2)\tfrac{f'''(0)}{6} + ...] \\ &\quad + p^3[f'(0)v_3 + (v_0v_3 + v_1v_2)f''(0) + (\tfrac{5}{2}v_0^2 v_3 + 6v_0v_1v_2 + v_1^3)\tfrac{f'''(0)}{6} + ...] \\ &\quad + \mathcal{O}(p^4). \end{aligned} \tag{2.14}$$

Note that this expansion can also be derived by applying the theory of Schur polynomials as described in [70]. Substituting (2.14) and (2.10) into (2.13) and collecting terms of equal power in the homotopy parameter p, we obtain:

$$\begin{cases} p^0: \;\; \epsilon \mathcal{D}_C^{\alpha} v_0 = 0, \\ v_0(0) = u_L, \; v_0(1) = u_R \;\; \Rightarrow v_0(x) = u_L + (u_R - u_L)x \end{cases} \tag{2.15}$$

$$\begin{cases} p^1: \;\; \epsilon \mathcal{D}_C^{\alpha} v_1 + \gamma v_0' + v_0 f'(0) + \tfrac{1}{2}v_0^2 f''(0) + \tfrac{1}{6}v_0^3 f'''(0) + ... - S(x) = 0, \\ v_1(0) = 0, \; v_1(1) = 0 \;\; \Rightarrow v_1(x) = ... \end{cases} \tag{2.16}$$

$$\begin{cases} p^2: \;\; \epsilon \mathcal{D}_C^{\alpha} v_2 + \gamma v_1' + v_1 f'(0) + v_0 v_1 f''(0) + \tfrac{5}{12}v_0^2 v_1 f'''(0) + ... = 0, \\ v_2(0) = 0, \; v_2(1) = 0 \;\; \Rightarrow v_2(x) = ... \end{cases} \tag{2.17}$$

$$\begin{cases} p^3: \;\; \epsilon \mathcal{D}_C^{\alpha} v_3 + \gamma v_2' + v_2 f'(0) + \tfrac{1}{2}(2v_0v_2 + v_1^2)f''(0) \\ \qquad\qquad + \tfrac{1}{6}(\tfrac{5}{2}v_0^2 v_2 + 3v_0 v_1^2)f'''(0) + ... = 0, \\ v_3(0) = 0, \; v_3(1) = 0 \;\; \Rightarrow v_3(x) = ... \end{cases} \tag{2.18}$$

$$\begin{cases} p^4: \ \epsilon \mathcal{D}_C^{\alpha} v_4 + \gamma v_3' + v_3 f'(0) + (v_0 v_3 + v_1 v_2) f''(0) \\ \qquad\qquad + \frac{1}{6}(\frac{5}{2} v_0^2 v_3 + 6 v_0 v_1 v_2 + v_1^3) f'''(0) + ... = 0, \\ v_4(0) = 0, \ v_4(1) = 0 \quad \Rightarrow v_4(x) = ..., etcetera. \end{cases} \tag{2.19}$$

In each step, we apply a fractional integral (see equations (2.2) and (2.4)) to obtain the intermediate solutions $V_0(x), \ V_1(x), ..., V_N(x)$. The first nonlinear term in (2.14) is u^2 and yields:

$$\begin{aligned} u^2 &= \Big(\textstyle\sum_{n=0}^{\infty} v_n p^n \Big) \Big(\textstyle\sum_{k=0}^{\infty} v_k p^k \Big), \\ &= \textstyle\sum_{n=0}^{\infty} \Big[\textstyle\sum_{i=0}^{n} v_i p^i v_{n-i} p^{n-i} \Big], \\ &= \textstyle\sum_{n=0}^{\infty} \Big[\textstyle\sum_{i=0}^{n} v_i v_{n-i} p^n \Big] = \textstyle\sum_{n=0}^{\infty} \Big[\textstyle\sum_{i=0}^{n} v_i v_{n-i} \Big] p^n := \textstyle\sum_{n=0}^{\infty} w_n^{(2)} p^n. \end{aligned} \tag{2.20}$$

where $w_n^{(2)}$ is a weight-function depending on products of the coefficients v_n. For the term with u^3 in (2.14) we set:

$$\begin{aligned} u^3 &= \textstyle\sum_{n=0}^{\infty} \Big[\textstyle\sum_{i=0}^{n} v_i v_{n-i} p^n \Big] \Big(\textstyle\sum_{k=0}^{\infty} v_k p^k \Big), \\ &= \textstyle\sum_{n=0}^{\infty} \Big[\textstyle\sum_{i=0}^{n} \Big(\textstyle\sum_{j=0}^{i} v_j v_{i-j} \Big) p^i v_{n-i} p^{n-i} \Big], \\ &= \textstyle\sum_{n=0}^{\infty} \Big[\textstyle\sum_{i=0}^{n} \Big(\textstyle\sum_{j=0}^{i} v_j v_{i-j} \Big) v_{n-i} \Big] p^n := \textstyle\sum_{n=0}^{\infty} w_n^{(3)} p^n, \end{aligned} \tag{2.21}$$

and following similar steps for higher powers of u we can write:

$$u^n = \sum_{r=0}^{\infty} w_n^{(r)} p^r, \tag{2.22}$$

where

$$w_n^{(r)} = \sum_{i=0}^{n} \Big[\sum_{j_1=0}^{i} \Big(\sum_{j_2=0}^{j_1} ... \Big(\sum_{j_{r-2}=0}^{j_{r-1}} v_{j_{r-1}} v_{j_{r-1}-j_{r-2}} \Big) ... \Big) \Big] v_{n-i}.$$

Next, we substitute these expressions into equation (2.14):

$$\begin{aligned} f(u) &= f(0) + f'(0) \textstyle\sum_{n=0}^{\infty} v_n p^n + f''(0) \frac{\sum_{n=0}^{\infty} w_n^{(2)} p^n}{2!} + f'''(0) \frac{\sum_{n=0}^{\infty} w_n^{(3)} p^n}{3!} + \cdots \\ &= \textstyle\sum_{m=0}^{\infty} [\frac{f^{(m)}(0)}{m!} \sum_{n=0}^{\infty} w_n^{(m)} p^n]. \end{aligned} \tag{2.23}$$

Equation (2.23) is a general formula which enables us to calculate the step solutions v_k in HPM. To our knowledge, this the first time such a general expression for the HPM solutions v_k is explicitly written out.

2.4 Theoretical results

2.4.1 A comparison between HPM and the Adomian Decomposition Method

In this section, we will compare HPM with another semi-analytical method: the Adomian Decomposition Method (ADM) (see [68, 122, 9, 2]). Although ADM provides us a series solution from a different perspective, it has a strong relation with the final HPM series. This is stated in the following lemma:

Theorem 2. *For boundary-value models of type (2.5) the series methods HPM and ADM yield equivalent expansions.*

Proof. We consider again the nonlinear BV-model (2.5). According to ADM, we write $u(x) = v_0(x) + \sum_{n=1}^{\infty} v_n(x)$. Here $u_0(x) = \mathcal{L}^{-1}[h(x)]$ and $u_n(x) = -\mathcal{L}^{-1}[A_{n-1}(x)]$, in which $\mathcal{L}^{-1}$ is the inverse operator of $\mathcal{L}$ and $A_n(x)$ are the so-called Adomian polynomials:

$$A_n(x) = \frac{1}{n!}\left[\frac{\partial^n}{\partial p^n}\mathcal{N}\left(v_0(x) + \sum_{n=1}^{\infty} v_n(x)p^n\right)\right]|_{p=0}. \tag{2.24}$$

On the other hand, the general HPM formula is as follows:

$$(1-p)\mathcal{L}[u(x;p) - v_0(x)] = -p\mathcal{N}[u(x;p) - h(x)], \tag{2.25}$$

where $u(x;p)$ is a unknown dependent variable. It clearly holds that $u(x;0) = v_0(x)$ and $u(x;1) = u(x)$. Then we expand $u(x;p)$ in a power series of p:

$$u(x;p) = v_0(x) + \sum_{n=1}^{\infty} v_n(x)p^n, \text{ and } V_n(x) = \frac{1}{n!}\frac{\partial^n u(x;p)}{\partial p^n}|_{p=0}. \tag{2.26}$$

Note that we have great freedom to choose the initial approximation in HPM. First, we substitute $p = 1$ in (2.10):

$$u(x) = v_0(x) + \sum_{n=1}^{\infty} v_n(x), \tag{2.27}$$

which becomes the same in ADM. Then, we differentiate (2.25) n times with respect to p, divide by $n!$ and finally set $p = 0$:

$$\mathcal{L}[v_1(x)] = -\mathcal{N}[v_0(x)] - h(x) \text{ when } n = 1, \text{ and} \tag{2.28}$$

$$\mathcal{L}[v_n(x) - v_{n-1}(x)] = -\frac{1}{(n-1)!}\frac{\partial^n \mathcal{N}[u(x;p)]}{\partial p^n}|_{p=0}, \text{ when } n \geq 1. \tag{2.29}$$

As we have mentioned before, we have great freedom to choose the auxiliary linear operator and the initial guess. Then we can choose:

$$\mathcal{L} = \mathcal{L}_0, \quad v_0(x) = \mathcal{L}_0^{-1}[g(x)]. \tag{2.30}$$

We reorganize (2.28) and (2.29) to obtain:

$$\mathcal{L}_0[v_1(x)] = h(x) - \mathcal{L}_0[v_0(x)] - \mathcal{N}_0[v_0(x)], \tag{2.31}$$

and

$$\begin{aligned}\mathcal{L}_0[v_n(x)] = \mathcal{L}_0[v_{n-1}(x)] - \tfrac{1}{(n-1)!}\tfrac{\partial^n \mathcal{L}_0[u(x;p)]}{\partial p^n}|_{p=0} \\ - \tfrac{1}{(n-1)!}\tfrac{\partial^n \mathcal{N}_0[u(x;p)]}{\partial p^n}|_{p=0}.\end{aligned} \tag{2.32}$$

We recognize that

$$h(x) - \mathcal{L}_0[v_0(x)] = 0, \tag{2.33}$$

from which it follows that

$$\mathcal{L}_0[v_1(x)] = -A_0(x), \tag{2.34}$$

according to the definition of Adomian polynomials. Making use of (2.26), it holds

$$\begin{aligned} &\mathcal{L}_0[v_{n-1}(x)] - \tfrac{1}{(n-1)!}\tfrac{\partial^n \mathcal{L}_0[u(x;p)]}{\partial p^n}|_{p=0} \\ &= \mathcal{L}_0[v_{n-1}(x)] - \mathcal{L}_0\left[\tfrac{1}{(n-1)!}\tfrac{\partial^n [u(x;p)]}{\partial p^n}|_{p=0}\right] \\ &= \mathcal{L}_0[v_{n-1}(x)] - \mathcal{L}_0[v_{n-1}(x)] \\ &= 0. \end{aligned} \tag{2.35}$$

Thus, equation (2.32) becomes

$$\mathcal{L}_0[v_n(x)] = -\frac{1}{(n-1)!}\frac{\partial^n \mathcal{N}_0[u(x;p)]}{\partial p^n}|_{p=0}. \tag{2.36}$$

We substitute (2.26) into the above expression, so that it becomes according to the definition of Adomian polynomials

$$\begin{aligned} &\mathcal{L}_0[v_n(x)] \\ &= -\tfrac{1}{(n-1)!}\left[\tfrac{\partial^n}{\partial p^n}\mathcal{N}_0\left(v_0(x) + \textstyle\sum_{n=1}^{\infty} v_n(x)p^n\right)|_{p=0}\right] \\ &= -A_{n-1}(x), \end{aligned} \tag{2.37}$$

which proves that ADM is equivalent with HPM. □

2.4.2 Convergence of HPM

Analyzing the convergence of series (2.11) in HPM is not trivial. It highly depends on the parameters in the underlying model. In some cases it even diverges. In the case of a convergent series, it can be shown to converge very fast to the exact solution of the nonlinear model. We will give an example to show the potentially fast convergence of HPM:

$$\begin{cases} u'' + u = g(x), \quad x \in (0,1) \\ u(0) = u(1) = 0. \end{cases} \tag{2.38}$$

The exact solution reads for a given $g(x)$:

$$u^*(x) = \sum_{n=1}^{\infty} b_n \sin(n\pi x) \quad \text{with} \quad b_n = 2\int_0^1 u^*(x)\sin(n\pi x)\,\mathrm{d}x \tag{2.39}$$

and we take

$$g(x) = \sum_{n=1}^{\infty}(1 - n^2\pi^2)b_n \sin(n\pi x). \tag{2.40}$$

Suppose that the exact solution u^* is bounded: $\|u^*\|_2 = M < \infty$. Then it follows that:

$$|b_n| \leq 2\int_0^1 |u^*(x)||\sin(n\pi x)|\,\mathrm{d}x = 2\int_0^1 |u^*(x)|\,\mathrm{d}x \tag{2.41}$$

$$\leq 2\,\|u^*\|_2\,\|1\|_2 = 2\,\|u^*\| = 2M. \tag{2.42}$$

The HPM solution is obtained in the way as described in section 2.3. First, we write the homotopy:

$$\begin{cases} u'' + p(u - g(x)) = 0, \\ u(0) = u(1) = 0. \end{cases} \tag{2.43}$$

Then we select the equations for equal powers of p:

$$p^0 : \begin{cases} (v_0)'' = 0, \\ v_0(0) = 0,\ v_0(1) = 0 \end{cases} \Rightarrow v_0(x) = 0. \tag{2.44}$$

$$p^1 : \begin{cases} (v_1)'' + v_0 = h(x), \\ v_1(0) = 0,\ v_1(1) = 0 \end{cases} \Rightarrow\ v_1(x) = \textstyle\sum_{n=1}^{\infty}(1 - \frac{1}{n^2\pi^2})b_n \sin(n\pi x). \tag{2.45}$$

$$p^2 : \begin{cases} (v_2)'' + v_1 = 0, \\ v_2(0) = 0,\ v_2(1) = 0 \end{cases} \Rightarrow\ v_2(x) = \textstyle\sum_{n=1}^{\infty}(\frac{1}{n^2\pi^2} - \frac{1}{n^4\pi^4})b_n \sin(n\pi x). \tag{2.46}$$

$$p^3 : \begin{cases} (v_3)'' + v_2 = 0, \\ v_3(0) = 0,\ v_3(1) = 0 \end{cases} \Rightarrow v_3(x) = \sum_{n=1}^{\infty}(\frac{1}{n^4\pi^4} - \frac{1}{n^6\pi^6})b_n \sin(n\pi x). \tag{2.47}$$

The HPM solution becomes: $u(x) = \sum_{k=1}^{\infty} v_k(x) = \lim_{N\to\infty} V_N(x)$

$$= \lim_{N\to\infty} \sum_{n=1}^{\infty} \left(1 - \frac{1}{(n\pi)^{2N}}\right) b_n \sin(n\pi x).$$

We can now easily find an estimate for the error as a function of N:

$$\mathrm{e}_N(x) := u^*(x) - V_N(x),$$

$$= \sum_{n=1}^{\infty} \frac{1}{(n\pi)^{2N}} b_n \sin(n\pi x),$$

which gives

$$\begin{aligned}
\|\mathrm{e}_N\|_2 &= \left\| \textstyle\sum_{n=1}^{\infty} \left(\frac{1}{(n\pi)^{2N}}\right) b_n \sin(n\pi x) \right\|_2, \\
&\leq \textstyle\sum_{n=1}^{\infty} \frac{|b_n|}{(n\pi)^{2N}} \left\|\sin(n\pi x)\right\|_2, \\
&\leq \textstyle\sum_{n=1}^{\infty} \frac{|b_n|}{(n\pi)^{2N}}, \\
&\leq \textstyle\sum_{n=1}^{\infty} \frac{2M}{(n\pi)^{2N}}, \\
&= \frac{2M}{\pi^{2N}} \textstyle\sum_{n=1}^{\infty} \frac{1}{n^{2N}}, \\
&= \frac{2M}{\pi^{2N}} \left[\frac{1}{1^{2N}} + \frac{1}{2^{2N}} + \frac{1}{3^{2N}} + ... \right], \\
&\leq \frac{2M}{\pi^{2N}} \left[\frac{1}{1^{2}} + \frac{1}{2^{2}} + \frac{1}{3^{2}} + ... \right], \\
&= \frac{2M}{\pi^{2N}} \frac{\pi^2}{6}, \\
&= \frac{M}{3\pi^{2N-2}}.
\end{aligned} \tag{2.48}$$

This example shows, at least for this specific example, 'spectral' convergence of the HPM approximations. In general, this is not necessarily the case, of course. The HPM series solution can converge (slowly, fast) or even diverge, depending on the situation. For this, we refer to [117, 19] in which more general convergence results for HPM are discussed.

2.5 Numerical examples

In this section, we present numerical experiments to show the different aspects of HPM when applied to models of type (2.1). The fractional differentiation computations are made by Maple using the command "*fracdiff*", which is based on the fractional integral formula connected to

the Riemann-Liouville definition [32]. For this purpose, Maple makes use, among others, of the Laplace transform (see [82]). Maple also enables us to make a symbolic calculation rather than computing only the numerical approximation.

2.5.1 Example 1: a linear fractional BV-model with a source term

First, we consider:

$$\begin{cases} \mathcal{D}_C^{\alpha} u + u = x^q + \frac{\Gamma(q+1)}{\Gamma(q-\alpha+1)} x^{q-\alpha}, \ q > \alpha, \\ u(0) = 0, \ u(1) = 1, \end{cases} \tag{2.49}$$

with the exact solution given by $u(x) = x^q$. We show the numerical HPM solutions for the cases $q = 10$ ($\alpha = 1.1$ and $\alpha = 1.7$) and $q = 20$ ($\alpha = 1.1$ and $\alpha = 1.7$) in Table 2.1. This table shows the effects of α and q values on the HPM solution. It can be observed that the lower α values and higher q values give higher maximum absolute errors. This example also demonstrates the fast convergence of HPM for linear fractional differential equations. In Figure 2.1, we present the effect of different α values on the HPM solution. It is clear that the quality of HPM approximation is directly related to the fractional order α and the power q in the solution.

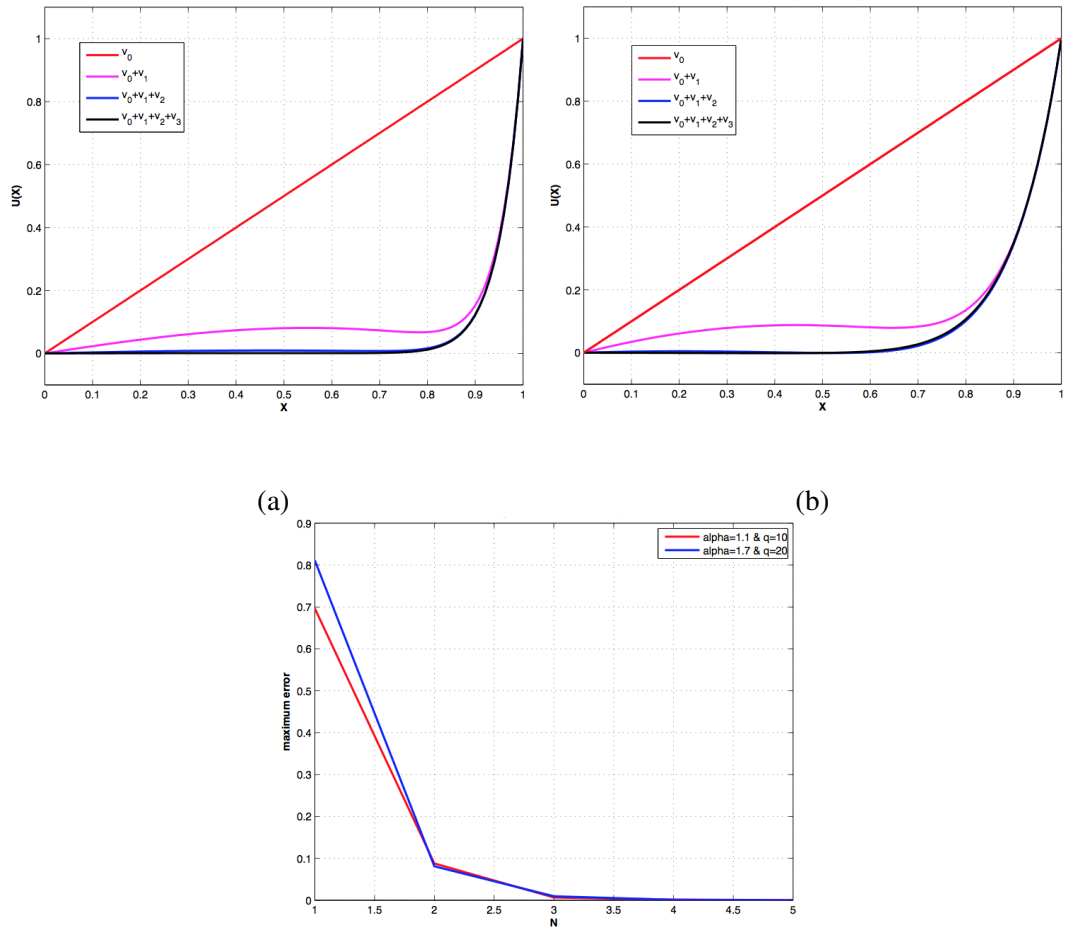

FIGURE 2.1: Panels (a) and (b) show HPM solutions as a function of the index N for different values of the fractional order α and the power q in model (2.49). Panel (a) presents the HPM solutions for $\alpha = 1.7$ and $q = 20$ and panel (b) shows the HPM solutions for $\alpha = 1.1$ and $q = 10$. In panel (c), the fast convergence of HPM for the two cases is displayed.

2.5.2 Example 2: an explicit HPM-solution

In this example, we study a linear fractional boundary-value model:

$$\begin{cases} \mathcal{D}_C^{\alpha} u + 1 + u = 0, \ 1 < \alpha \leq 2, \\ u(0) = 0, \ u(1) = 1. \end{cases} \tag{2.50}$$

For $\alpha = 2$ the exact solution reads $u(x) = \frac{1-\cos 1}{\sin 1} \sin x + \cos x - 1$. The lower plot in Figure 2.2 depicts the error for $N = 30$ of the HPM solution for $\alpha = 2$. The upper plots in Figure 2.2 illustrate the HPM solution for $N = 30$ (left plot) and the difference between two succeeding HPM solutions (right plot). For this model, we can derive an explicit formula for the series solution. Following the HPM steps in section 3, we separate the fractional derivative part and then multiply the remaining part with the parameter p:

$$\mathcal{D}_c^{\alpha} u = -p(1 + u) \tag{2.51}$$

Then we substitute assumption (2.10) into equation (2.51):

$$\mathcal{D}_c^\alpha(v_0 + pv_1 + p^2v_2 + p^3v_3 + ...) = -p(1 + v_0 + pv_1 + p^2v_2 + ...). \tag{2.52}$$

Collecting the equations for increasing powers of the parameter p, i.e. for p^0, p^1, p^2, p^3, ...; we find:

$$p^0: \ \mathcal{D}_c^\alpha v_0 = 0 \Rightarrow \begin{cases} v_0(x) - v_0'(0)x = c_0 \quad v_0'(0) = \beta_0 \\ v_0(x) = \beta_0 x + c_0 \\ v_0(0) = v_0(1) = 0 \ \Rightarrow \ \beta_0 = 0, \ c_0 = 0 \\ v_0(x) = 0. \end{cases} \tag{2.53}$$

$$p^1: \ \mathcal{D}_c^\alpha v_1 = -1 - v_0 \Rightarrow \begin{cases} v_1(x) - \underbrace{v_1'(0)}_{\beta_1} x = \frac{\Gamma(1)}{\Gamma(\alpha+1)}x^\alpha, \\ v_1(x) = -\frac{\Gamma(1)}{\Gamma(\alpha+1)}x^\alpha + \beta_1 x, \\ v_1(1) = 0 \ \Rightarrow \ \beta_1 = \frac{\Gamma(1)}{\Gamma(\alpha+1)}. \end{cases} \tag{2.54}$$

$$p^2: \ \mathcal{D}_c^\alpha v_2 = -v_1 = \frac{\Gamma(1)}{\Gamma(\alpha+1)}x^\alpha - \beta_1 x \Rightarrow \begin{cases} v_2(x) - \underbrace{v_2'(0)}_{\beta_2} x = \mathcal{J}_c^\alpha\left[\frac{\Gamma(1)}{\Gamma(\alpha+1)}x^\alpha - \beta_1 x\right], \\ v_2(x) = \frac{\Gamma(1)}{\Gamma(2\alpha+1)}x^{2\alpha} - \beta_1\frac{\Gamma(2)}{\Gamma(\alpha+2)}x^{\alpha+1} + \beta_2 x, \\ v_2(1) = 0 \ \Rightarrow \ \beta_2 = \frac{\Gamma(1)}{\Gamma(2\alpha+1)} - \beta_1\frac{\Gamma(2)}{\Gamma(\alpha+2)}. \end{cases} \tag{2.55}$$

$$p^3: \ \mathcal{D}_c^\alpha v_3 = -v_2 = -\frac{\Gamma(1)}{\Gamma(2\alpha+1)}x^{2\alpha} + \beta_1\frac{\Gamma(2)}{\Gamma(\alpha+2)}x^{\alpha+1} - \beta_2 x, \tag{2.56}$$

$$\Rightarrow \begin{cases} v_3(x) - \underbrace{v_3'(0)}_{\beta_3} x = \mathcal{J}_c^\alpha\left[-\frac{\Gamma(1)}{\Gamma(2\alpha+1)}x^{2\alpha} + \beta_1\frac{\Gamma(2)}{\Gamma(\alpha+2)}x^{\alpha+1} - \beta_2 x\right], \\ v_3(x) = -\frac{\Gamma(1)}{\Gamma(3\alpha+1)}x^{3\alpha} + \beta_1\frac{\Gamma(2)}{\Gamma(\alpha+2)}\frac{\Gamma(\alpha+2)}{\Gamma(2\alpha+2)}x^{2\alpha+1} - \beta_2\frac{\Gamma(2)}{\Gamma(\alpha+2)}x^{\alpha+1} + \beta_3, \\ v_3(1) = 0 \ \Rightarrow \ \beta_3 = \frac{\Gamma(1)}{\Gamma(3\alpha+1)} - \beta_1\frac{\Gamma(2)}{\Gamma(\alpha+2)}\frac{\Gamma(\alpha+2)}{\Gamma(2\alpha+2)} + \beta_2\frac{\Gamma(2)}{\Gamma(\alpha+2)}. \end{cases} \tag{2.57}$$

With induction we can generate the formula:

$$v_n(x) = (-1)^n\frac{\Gamma(1)}{\Gamma(1+n\alpha)}x^{n\alpha} + \left[\sum_{k=1}^{n-1}(-1)^{k+1}\beta_k\left(\prod_{i=1}^{n-k}\frac{\Gamma(2+\alpha(i-1))}{\Gamma(2+i\alpha)}\right)x^{\alpha(n-k)+1}\right] + \beta_n x,$$
$$\beta_n = (-1)^{n+1}\frac{\Gamma(1)}{\Gamma(1+n\alpha)} + \left[\sum_{k=1}^{n-1}(-1)^k\beta_k\left(\prod_{i=1}^{n-k}\frac{\Gamma(2+\alpha(i-1))}{\Gamma(2+i\alpha)}\right)\right]. \tag{2.58}$$

and finally we set $u(x) = u(x;1) = \sum_{n=1}^{\infty} v_n(x)$.
This generated formula could provide us with higher-order HPM solutions. However, from a practical point of view, the use of formula (2.58) is not very efficient. Instead, it could serve for theoretical considerations.

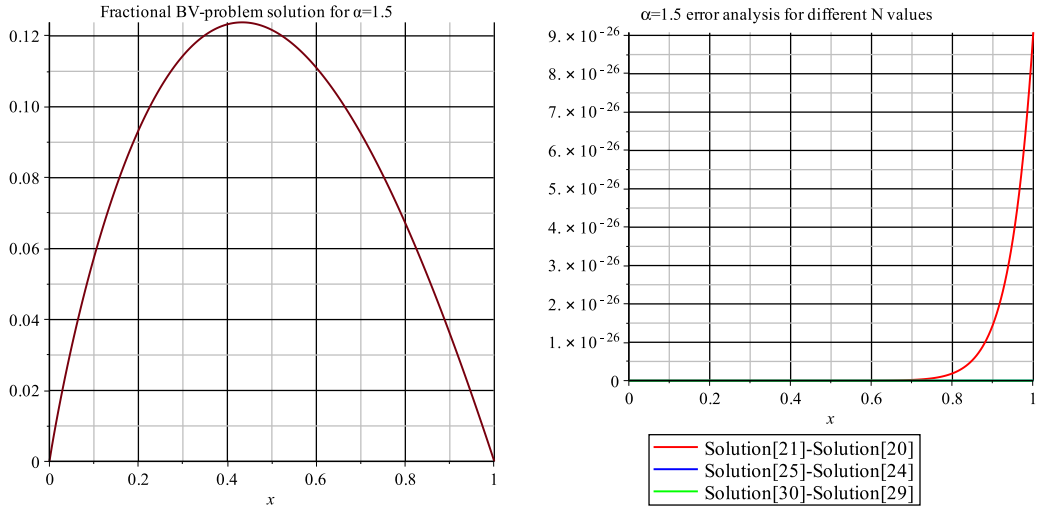

(a) (b)

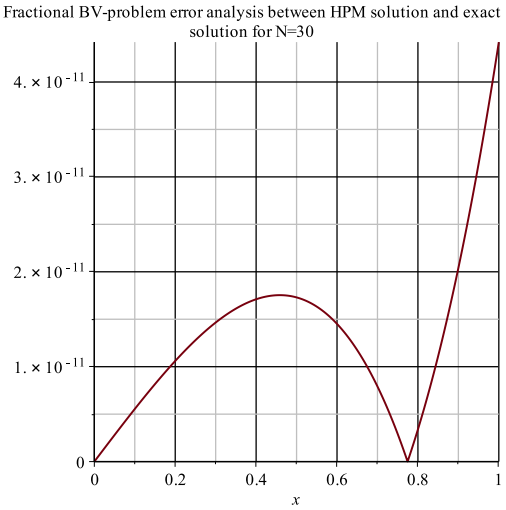

(c)

FIGURE 2.2: HPM solutions of model 2.50 for $\alpha = 1.5$ (upper two plots) and the error for $N = 30$ and $\alpha = 2$ (lower plot).

2.5.3 Example 3: a fractional Gelfand-Bratu model

The following example is the fractional Gelfand-Bratu model with parameter μ:

$$\begin{cases} \mathcal{D}_C^{\alpha} u + \mu e^u = 0, \ \mu > 0, \ 1 < \alpha \leq 2, \\ u(0) = u(1) = 0. \end{cases} \tag{2.59}$$

In this model, we expand the nonlinear term e^u into a Taylor series around 0 until the u^2 term to apply the fractional integral formulas in equations (2.15)...(2.19) more efficiently. Note that for $\alpha = 2$, there may be zero, one or two solutions for this model, depending on the value of μ [113]. We use here the initial HPM approximation $u(x) = A\, x(1-x)$ with $A \in \mathbb{R}$, which satisfies the boundary conditions. The effect of changing μ and A values on the HPM solution is presented in Tables 2.2, 2.3 and 2.4. These tables show us that for higher μ and A values we

need more steps to get a reasonable accuracy for $\alpha = 2$. We also included a 'ratio test' between differences of successive HPM approximations. These confirm clearly the convergence of HPM and its possible divergence in Table 2.4. In Table 2.5, we consider the case with $\alpha = 1.5$ for $\mu = 1$ and $A = 1$. If we compare the results in Tables 2.2 and 2.5, we conclude that HPM needs more steps for the fractional case than the ordinary case to reach a similar accuracy.

N	$\alpha = 1.1$	$\alpha = 1.7$
1	0.08582180	0.07493868
2	0.00486217	0.00851444
3	0.00158691	0.00089426
4	0.00013589	0.00009150
5	0.00002649	0.00000935

N	$\alpha = 1.1$	$\alpha = 1.7$
1	0.10386288	0.08023764
2	0.00696762	0.00930574
3	0.00171177	0.00098390
4	0.00017720	0.00010091
5	0.00002596	0.00001031

TABLE 2.1: Maximum HPM error for $q = 10$ (top) and for $q = 20$ (bottom).

TABLE 2.2: Errors in example 3 for $A = 1$, $\mu = 1$ and $\alpha = 2$

N	Maximum Error	Ratio Test
1	0.09609375	0.384375
2	0.01230238	0.128025
3	0.00109586	0.089077
4	0.00002895	0.026416
5	0.00001244	0.429618
6	0.00000295	0.237384
...	...	...
10	$1.51651970.10^{-9}$	0.236744
11	$1.72137047.10^{-10}$	0.113508
12	$4.68366748.10^{-13}$	0.001146

TABLE 2.3: Errors in example 3 for $A = 5$, $\mu = 1$ and $\alpha = 2$

N	Maximum Error	Ratio Test
1	0.92317708	0.477083
2	0.20311499	0.445347
3	0.00370464	0.298901
4	0.01602912	0.061214
5	0.00548413	2.595368
6	0.00009242	0.753362
...	...	...
23	$1.72124479.10^{-10}$	0.077870
24	$1.64598188.10^{-10}$	3.667836
25	$9.76579753.10^{-11}$	0.894541

TABLE 2.4: Errors in example 3 for $A = 5$, $\mu = 5$ and $\alpha = 2$

N	Maximum Error	Ratio Test
1	0.38411458	0.307292
2	0.39087528	1.017601
3	0.44169314	1.130010
4	0.52929314	1.198328
5	0.66284949	1.252330
6	0.85925246	1.296301
...	...	...
23	500.269910	1.519908
24	762.342906	1.523863
25	1164.49295	1.527519

TABLE 2.5: Errors in example 3 for $A = 1$, $\mu = 1$ and $\alpha = 1.5$

N	Maximum Error	Ratio Test
1	0.02809378	0.133318
2	0.00582333	0.214116
3	0.00136224	0.241065
4	0.00034055	1.627578
5	0.00008814	1.220158
6	0.00002348	0.737494
7	0.00000632	0.649958
8	0.00000171	0.654176
9	$4.62559720.10^{-7}$	0.744348
10	$1.25587544.10^{-7}$	1.113443

The HPM solutions for different values of α are also given in Figure 2.3. Figure 2.3(c) shows that HPM may converge to a non-existing solution, here for the values $\lambda = 4$ and $\alpha = 2$. Figure

2.3(d) displays a bifurcation diagram for this model. It remains unclear what would happen with the second solution for $1 < \alpha < 2$. In Figure 2.4 the effect of changing the parameter A on the convergence in the initial approximation of HPM is displayed.

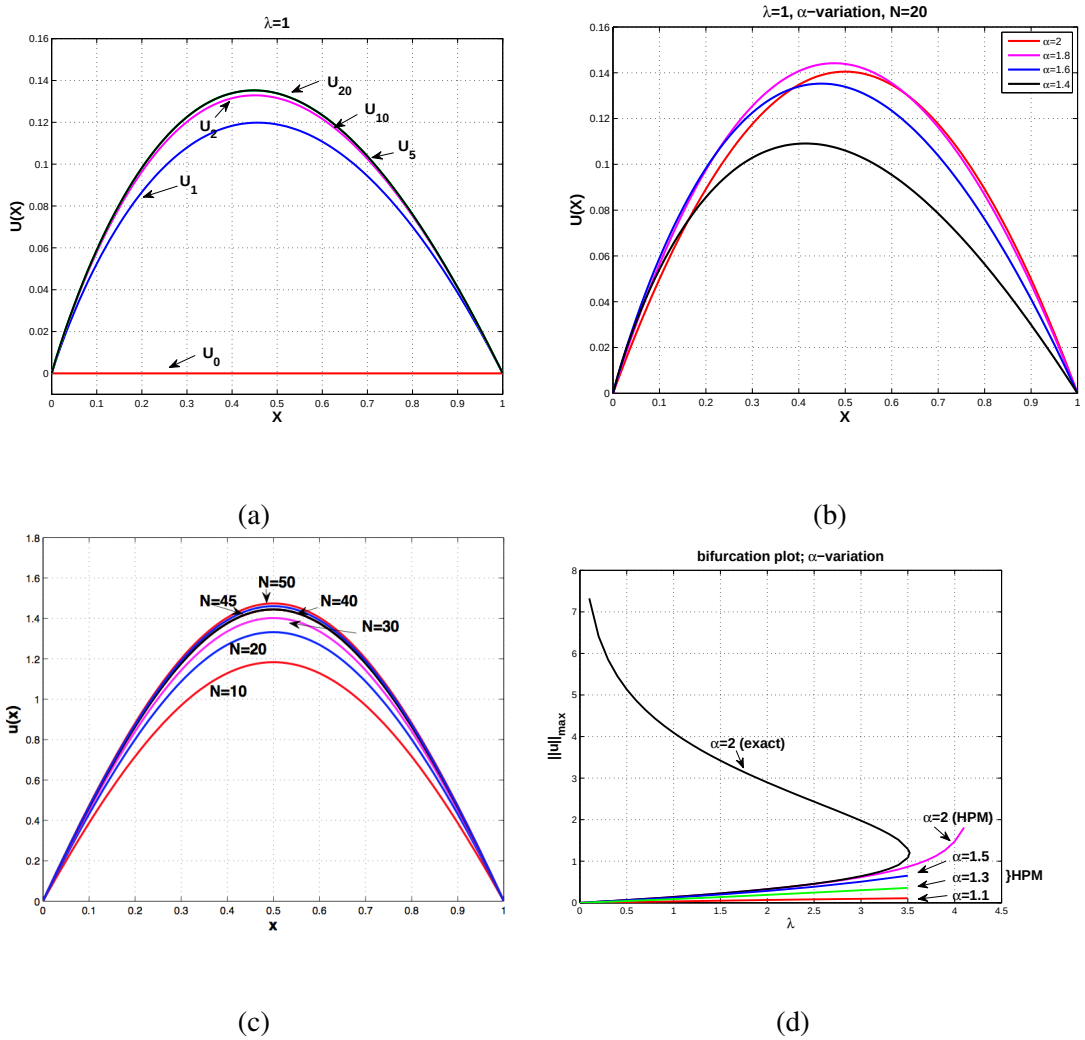

FIGURE 2.3: Numerical results for the Gelfand-Bratu model defined by equation (2.59). In panel (c), we can see that the HPM solution is converging for $\lambda = 4$ and $\alpha = 2$.

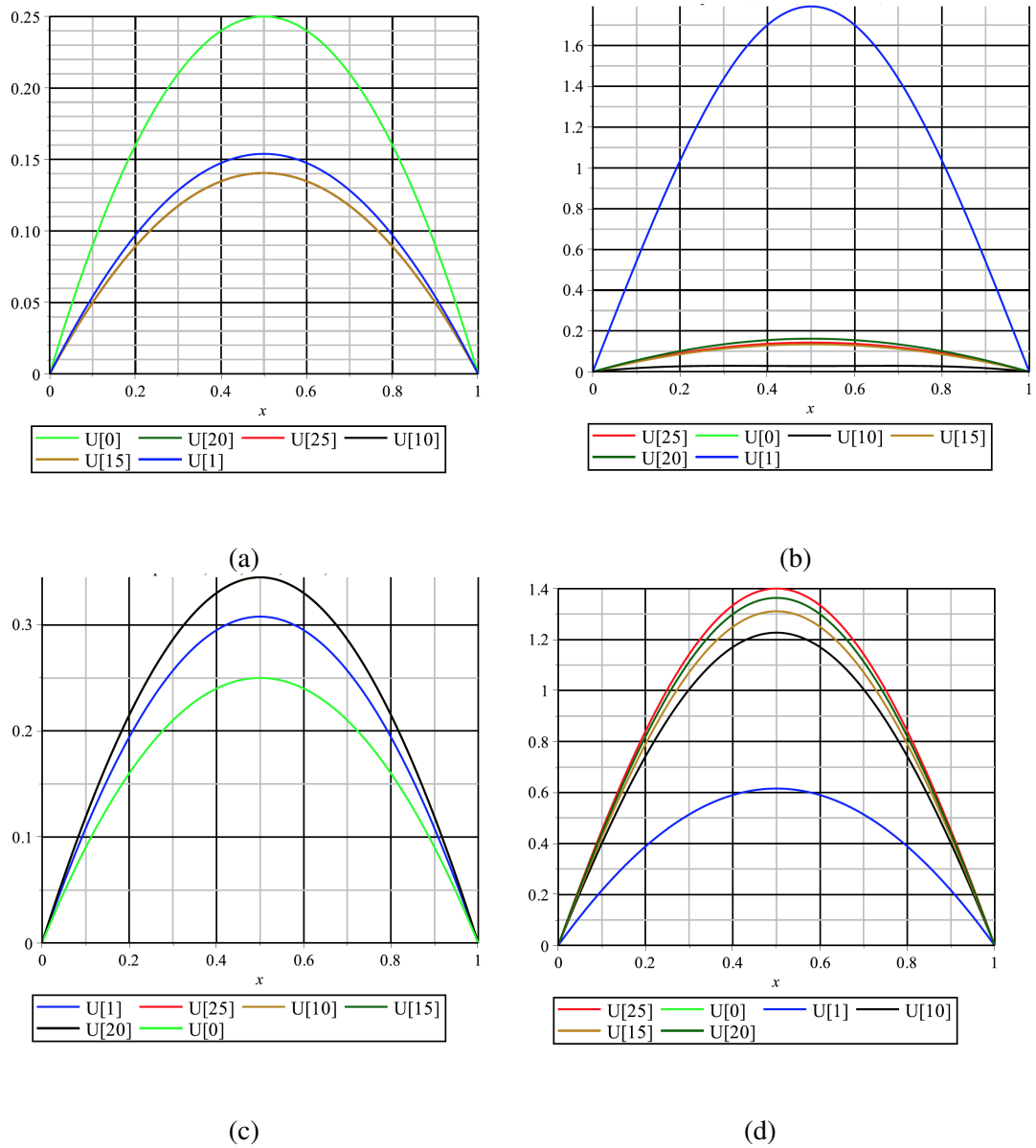

FIGURE 2.4: Influence on the convergence of HPM depending on the parameters μ and A in model (2.59). Panel (a) shows the HPM solution solutions for $A = 1$ and $\lambda = 1$, panel (b) shows for $A = 20$ and $\lambda = 1$, panel (c) shows for $A = 5$ and $\lambda = 2$ and finally panel (d) shows the results for $A = 1$ and $\lambda = 4$.

2.5.4 Example 4: a fractional Gelfand-Bratu model with damping

Similar to the description in [11], we consider the following nonlinear equation:

$$\begin{cases} \epsilon \mathcal{D}_C^{\alpha} u + 2u' + 1 + u + \frac{1}{2}u^2 = 0, \ 0 < \epsilon \leq 1, \\ u(0) = u(1) = 0. \end{cases} \tag{2.60}$$

This example includes a damping term and a quadratic approximation to the exponential compared to the previous example. Note that for $\alpha = 2$, there are two solutions for this model, but HPM can only produce one of them. Figures 2.5, 2.6 and 2.7 show different scenarios of the model. These are explained in the captions of the figures. The non-uniqueness of the solution is displayed for $\epsilon = 0.35$ and $\alpha = 2$: panels 2.6(a) and 2.6(b) were produced using a shooting method with Matlab. The right plot shows the two curves (in red and blue) in the phase plane

$(u, du/dx)$. It can also be clearly observed that the performance of HPM is very sensitive to the choice of the parameter ϵ in the model. Smaller values of ϵ slow down the convergence rate of the method dramatically (see panel 2.5(d)).

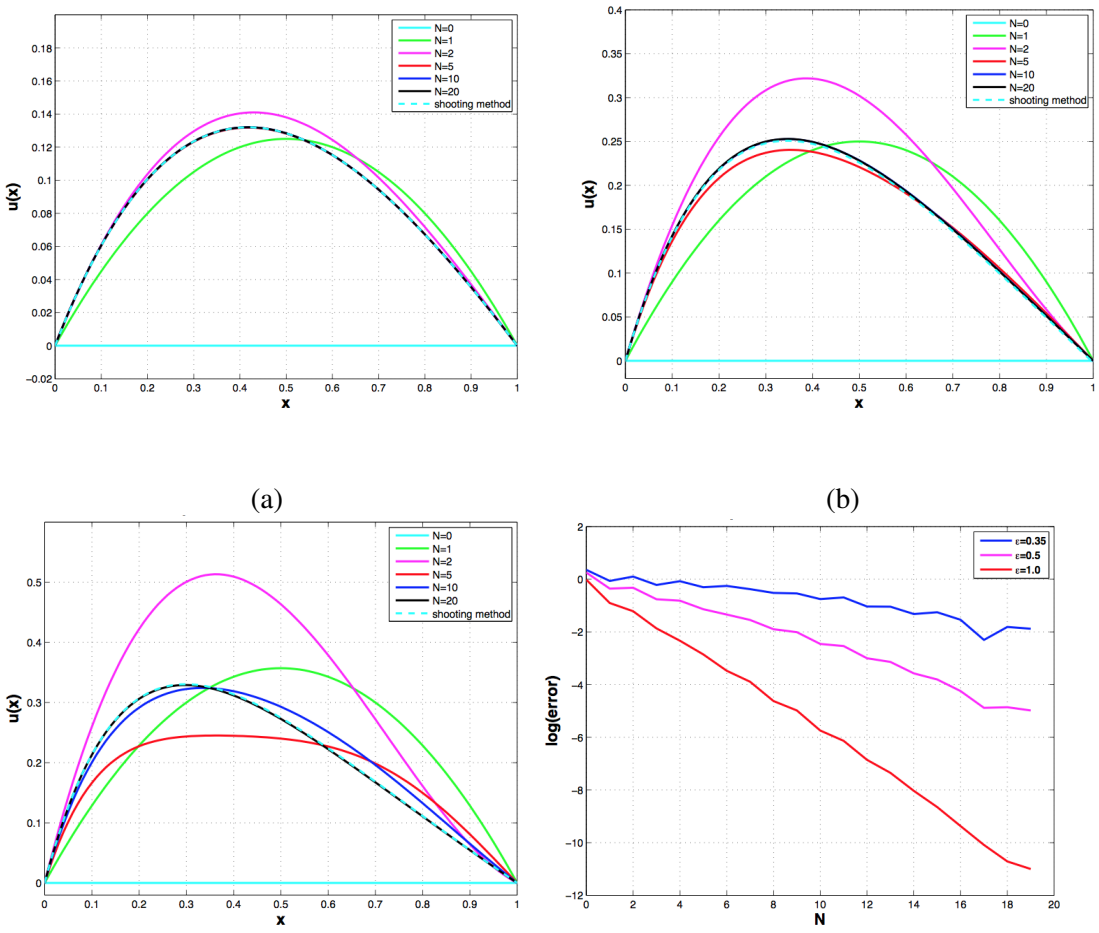

FIGURE 2.5: Numerical results for the fractional Gelfand-Bratu model with damping (2.60): HPM solutions for $\epsilon = 1.0$ (a), $\epsilon = 0.5$ (b), $\epsilon = 0.35$ (c), and the error in the maximum norm as a function of the number of terms N in the approximation, respectively.

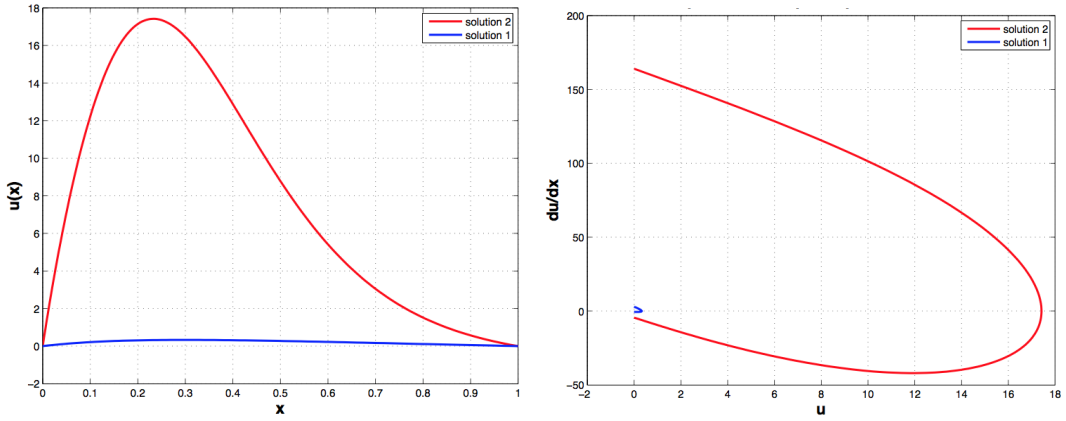

(a) (b)

FIGURE 2.6: Two different solutions in the fractional Gelfand-Bratu model with damping (2.60) for $\epsilon = 0.35$: in panel (a) these are displayed as a function of x and in panel (b) in the phase plane $(u, du/dx)$. These solutions were obtained by a shooting method and the existence is confirmed by analysis in [11]. Only the lower solution 1, shown in blue, can be detected by HPM.

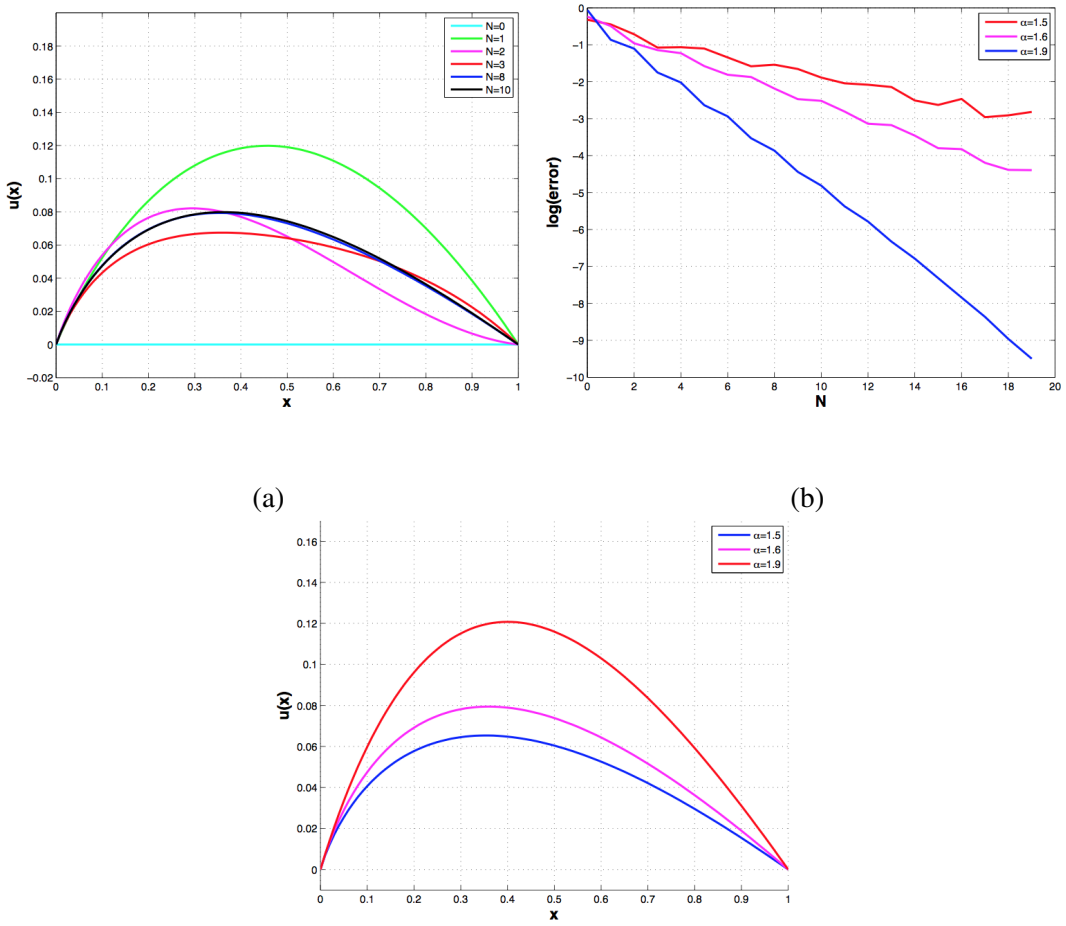

FIGURE 2.7: Panel (a) displays the convergence of HPM for the fractional Gelfand-Bratu model with damping (2.60) with $\epsilon = 1$ for the case $\alpha = 1.6$ as a function of N, panel (b) shows the dependence of the convergence rate on the fractional derivative α in the model, and panel (c) indicates the differences in solution behavior for three values of α for $\epsilon = 1$.

2.5.5 Example 5: a fractional boundary layer model

Our next example is a fractional boundary layer model:

$$\begin{aligned} &\epsilon \mathcal{D}_C^{\alpha} u + \gamma u' = 0, \quad 0 < \epsilon \leq 1, \quad \gamma > 0, \\ &u(0) = 0, \;\; u(1) = 1. \end{aligned} \tag{2.61}$$

For $\alpha = 2$ and $\gamma = -1$, it has an exact solution:

$$u(x) = \frac{\mathrm{e}^{\frac{x}{\epsilon}} - 1}{\mathrm{e}^{\frac{1}{\epsilon}} - 1}. \tag{2.62}$$

In Figure 2.8, we present the effect of ϵ on the convergence of the HPM method for $\alpha = 2$. It can be clearly seen that it depends on the small parameter ϵ: for smaller values of ϵ it converges slower or even diverges. This can be seen in panel 2.8(a) where we display the dependence of the value N (denoted by N^*) to obtain a similar accuracy equal to 0.01. Figure 2.9 shows HPM solutions for the fractional cases $\alpha = 1.7$ and $\alpha = 1.5$ with $\epsilon = 1.0$. Lower values of α tend to make the solution steeper for a fixed ϵ, but also let HPM converge slower.

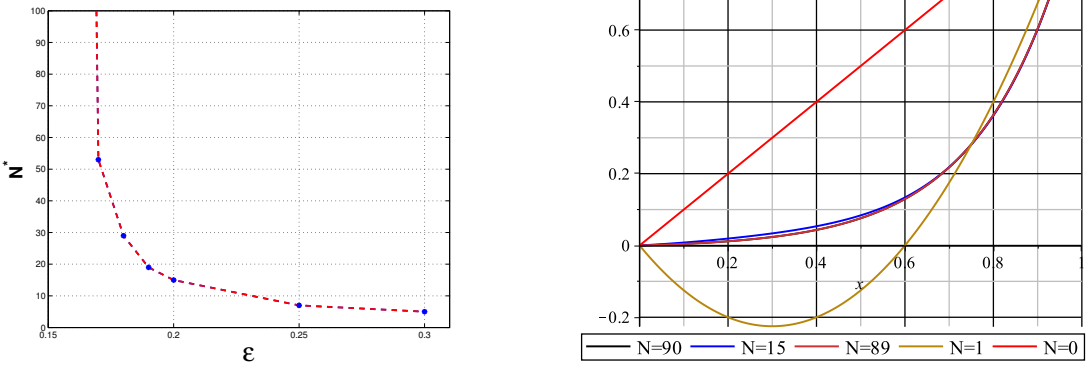

(a)

(b)

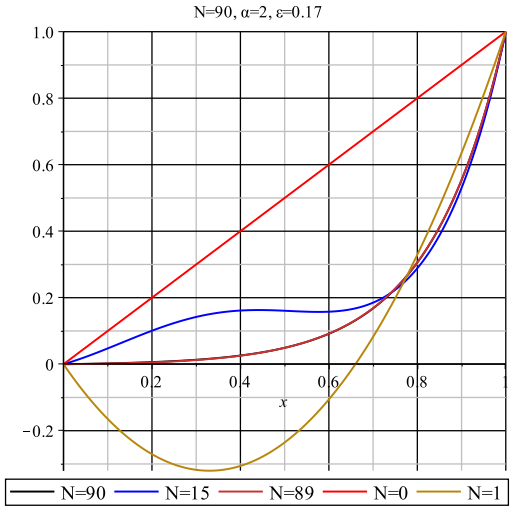

(c)

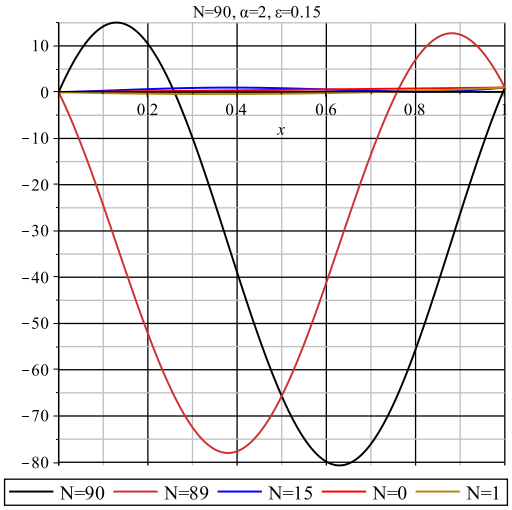

(d)

FIGURE 2.8: Panel (a) shows the convergence of HPM depending on the parameter ϵ in the fractional boundary layer model (2.61). Panel (b)-(d) show convergent and divergent solutions according to the value of ϵ.

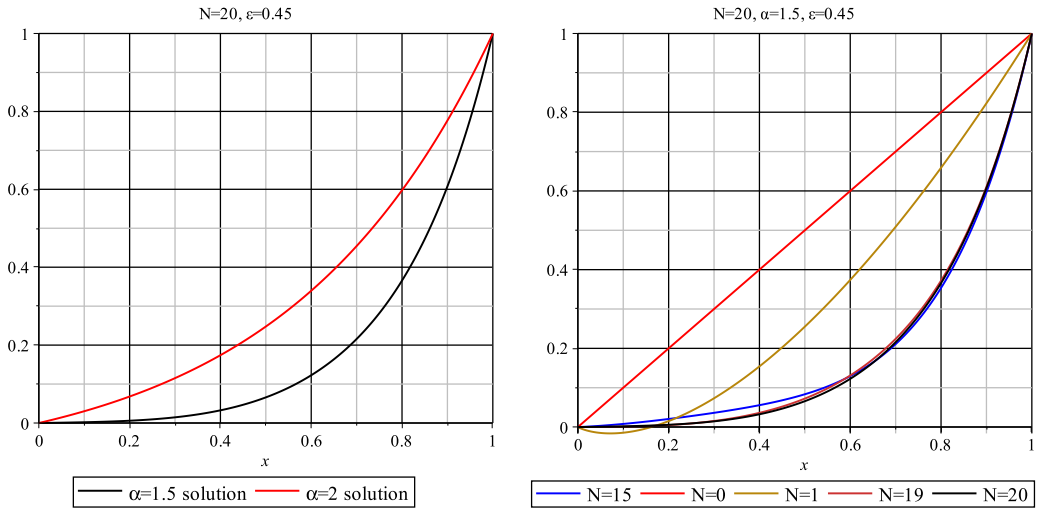

(a) (b)

FIGURE 2.9: The effect of varying the fractional order in the fractional boundary layer model (2.61) is depicted for a fixed value of $\epsilon = 0.45$. The right plot shows the fast convergence of HPM for $\alpha = 1.5$ The left plot displays the difference in solution behavior between the non-fractional $\alpha = 2$ and fractional $\alpha = 1.5$ case.

2.6 Summary

In this chapter we analyzed the Homotopy Perturbation Method (HPM) for fractional advection-dfiffusion-reaction equations. We showed the equivalence between HPM and ADM. A general expression for the coefficients in the series was derived in the case of a nonlinear source term. We applied HPM to a test set of models, both linear and nonlinear. Numerical experiments demonstrated the capability of HPM to find solutions up to high accuracy. However, in some cases the method converged slowly or even diverged. In the situation of non-existing or multiple solutions, HPM may converge to a non-existing one or has difficulties to find the second solution. Finally, the performance of HPM highly depends on the model parameters in the advection-diffusion-reaction equation.

Chapter 3

Traveling waves in time-fractional partial differential equations using the homotopy analysis method[1]

Abstract
This chapter is devoted to the numerical study of ordinary and fractional order Fisher equations. The homotopy analysis method (HAM) is used to produce approximate traveling wave solutions for time-fractional partial differential equations. An optimal value of the convergence parameter in HAM is determined by minimizing the square residual. Numerical experiments show that HAM could be an efficient way to find numerical approximations to solutions for both the ordinary and the fractional case.

3.1 Introduction

In the previous chapter, we presented the homotopy perturbation method (HPM) to solve fractional-order advection-diffusion-reaction boundary-value problems. HPM could be an efficient semi analytical series method in certain cases, but it has difficulties converging in some nonlinear cases. To overcome this challenge, we will use the homotopy analysis method in this chapter.

Liao proposed a semi-analytical method for nonlinear problems named the Homotopy Analysis Method [75, 77, 78] in 1992, which was mainly based on the idea of homotopy from topology. He and his co-authors claimed that, contrary to other series methods, HAM is independent of a small parameter. Furthermore, this property would enable HAM to overcome the restrictions and limitations of other methods. With this chapter, we would like to stress that this claim is widely exaggerated, in general. It has been shown, however, that there exist *special* nonlinear problems where the traditional methods fail, while HAM succeeded to give a reasonable semi-analytical solution [75]. Under certain circumstances, HAM may provide a faster converging solution with a higher accuracy and also a fewer number of calculations. For this reason, HAM has been applied to several nonlinear problems in science and engineering, such as wave equations, KdV-type equations, control problems [104, 112, 131, 125], etc.

The method HAM makes use of a convergence control parameter $\hbar$ in order to determine a convergent series solution. Via HAM, we can achieve explicit semi-analytic solutions of nonlinear problems. In this chapter, we apply HAM to Fisher- and Burger-Fisher type equations

[1]This is joint work with P. A. Zegeling (Utrecht University). It has been submitted to the Journal of Applied Mathematics and Computing (2017).

[104, 131] to obtain traveling wave approximations. We examine both ordinary and fractional order versions of these equations.

3.2 Time-fractional partial differential equations

We consider the following time fractional partial differential equation [5, 6, 13]:

$$\begin{cases} \mathcal{D}_t^{\alpha} u + (f(u))_x = d u_{xx} + S(u) + \tau u_{xxt}, \\ u(x,0) = u_0(x) \end{cases} \tag{3.1}$$

with parameters $0 < \alpha \leq 1$, $d > 0$. Here, S is a nonlinear source term and $f(u)$ is representing nonlinear convection. An example of the use of including the term τu_{xxt} is considered in [75] and applications of this term in geo-hydrology can be found in [55, 31, 38, 36] (see also [37, 127]). With $\mathcal{D}_t^{\alpha}$ we denote a fractional derivative defined in the Caputo sense in section 1.4.3. We also use the properties of the fractional derivative as already presented in section 2.2.

3.3 The Homotopy Analysis Method (HAM)

A general nonlinear differential equation is considered to describe the main steps in the homotopy analysis method (HAM):

$$\mathcal{N}[u(x,t)] = 0, \tag{3.2}$$

where $\mathcal{N}$ denotes the nonlinear operator, x and t denote the independent variables and $u(x,t)$ is the solution. This method was first proposed by Liao [77], where he first constructs the zeroth-order deformation equation as follows:

$$(1-p)\mathcal{L}[\phi(x,t;p) - u_0(x,t)] = p\hbar\mathcal{N}[\phi(x,t;p)], \tag{3.3}$$

where $p \in$ [0,1] is the embedding parameter, $\hbar \neq 0$ is an auxiliary parameter, $\mathcal{L}$ is an auxiliary linear operator, $\phi(x,t;p)$ is an unknown function and $u_0(x,t)$ is an initial approximation of $\phi(x,t;p)$, respectively. It should be mentioned that HAM allows us to choose both the auxiliary parameter and auxiliary linear operator. Further, we set:

$$\phi(x,t;0) = u_0(x,t), \qquad \phi(x,t;1) = u(x,t).$$

This means that while the parameter p increases from 0 to 1, the solution $\phi(x,t;p)$ changes from the initial guess $u_0(x,t)$ to the solution $u(x,t)$. The unknown function $\phi(x,t;p)$ is defined by expanding it into a Taylor series with respect to the embedding parameter p where N denotes how many steps we have calculated:

$$\phi(x,t;p) = u_0(x,t) + \sum_{m=1}^{\infty} u_m(x,t)p^m, \tag{3.4}$$

where

$$u_m(x,t) = \frac{1}{m!}\frac{\partial^m \phi(x,t;p)}{\partial p^m}|_{p=0} \text{ and } u(x,t) = \phi(x,t;1) \approx \sum_{m=0}^{N} u_m(x,t), \tag{3.5}$$

which therefore approximates the solution of the original model. By using equation (3.5), the governing function can be derived from the zeroth-order deformation equation (3.3). Differentiating equation (3.3) m times with respect to the embedding parameter p , then substituting $p = 0$ and finally dividing by $m!$, we obtain the so-called *m*th order deformation equation:

$$\mathcal{L}[u_m(x,t) - \chi_m u_{m-1}(x,t)] = \hbar R_m(u_{m-1}), \tag{3.6}$$

where

$$R_m(u_{m-1}) = \frac{1}{(m-1)!}\frac{\partial^{m-1}\mathcal{N}[\phi(x,t;p)]}{\partial p^{m-1}}|_{p=0}, \tag{3.7}$$

$$\chi_m = \begin{cases} 0, & m \leq 1 \\ 1, & m > 1. \end{cases} \tag{3.8}$$

It should be noted that if we substitute $\hbar = -1$ into equation (3.3), it reduces to:

$$(1-p)\mathcal{L}[\phi(x,t;p) - u_0(x,t)] + p\mathcal{N}[\phi(x,t;p)] = 0, \tag{3.9}$$

and it turns into the Homotopy Perturbation Method [60, 75]. However, choosing $\hbar = -1$ does not always yield a convergent solution, as we will see later on.

3.4 Analysis of HAM

In this section we discuss some convergence properties of the method and its dependence on the parameter $\hbar$ in equation (3.3).

3.4.1 Convergence of HAM

We show a convergence property of HAM for model (3.1), which is stated as follows:

Convergence result (see also [77]): As long as the series $u(x,t) = u_0(x,t) + \sum_{m=1}^{\infty} u_m(x,t)$ converges, where the functions $u_m(x,t)$ are calculated from (3.5)-(3.8), it must be the exact solution of the PDE model (3.1) .

***Sketch of a proof*:** If the series $\sum_{m=0}^{\infty} u_m(x,t)$ converges, we can write $u(x,t) = \sum_{m=0}^{\infty} u_m(x,t)$ and we know that $\lim_{m\to+\infty} u_m(x,t) = 0$. Then

$$\begin{aligned} &\textstyle\sum_{m=1}^{n}[u_m(x,t) - \chi_m u_{m-1}(x,t)] \\ &= u_1 + (u_2 - u_1) + (u_3 - u_2) + \ldots + (u_n - u_{n-1}) = u_n(x,t). \end{aligned}$$

and this gives

$$\sum_{m=1}^{\infty}[u_m(x,t) - \chi_m u_{m-1}(x,t)] = \lim_{m\to+\infty} u_m(x,t) = 0. \tag{3.10}$$

Using the linear operator $\mathcal{L}$ in (3.3), which represents the linear operator $\frac{\partial}{\partial t}$, we obtain

$$\sum_{m=1}^{\infty}[u_m(x,t) - \chi_m u_{m-1}(x,t)] = \hbar\sum_{m=1}^{\infty} R_m(u_{m-1}(x,t)) = 0, \tag{3.11}$$

which gives, since $\hbar \neq 0$

$$\sum_{m=1}^{\infty} R_m(u_{m-1}(x,t)) = 0. \tag{3.12}$$

The χ_m terms disappear and therefore we find,

$$R_m(u_{m-1}(x,t)) = \mathcal{D}_t^\alpha u_{m-1,t}(x,t) + (f(u_{m-1}(x,t))_x - d u_{m-1,xx}(x,t) \\ -S(u_{m-1}(x,t)) - \tau u_{m-1,xxt}(x,t)$$

Taking the infinite sum in all terms, we see that

$$\begin{aligned}\textstyle\sum_{m=1}^\infty R_m(u_{m-1}(x,t)) &= \textstyle\sum_{m=1}^\infty [\mathcal{D}_t^\alpha u_{m-1,t}(x,t) + (f(u_{m-1}(x,t))_x - d u_{m-1,xx}(x,t) \\ &\quad -S(u_{m-1}(x,t)) - \tau u_{m-1,xxt}(x,t) \\ &= \textstyle\sum_{m=1}^\infty \mathcal{D}_t^\alpha u_{m-1,t}(x,t) + \sum_{m=1}^\infty (f(u_{m-1}(x,t))_x - \sum_{m=1}^\infty d u_{m-1,xx}(x,t) \\ &\quad - \textstyle\sum_{m=1}^\infty S(u_{m-1}(x,t)) - \sum_{m=1}^\infty \tau u_{m-1,xxt}(x,t) \\ &= \textstyle\sum_{m=0}^\infty \mathcal{D}_t^\alpha u_{m,t}(x,t) + \sum_{m=0}^\infty (f(u_m(x,t))_x - \sum_{m=0}^\infty d u_{m,xx}(x,t) \\ &\quad - \textstyle\sum_{m=0}^\infty S(u_m(x,t)) - \sum_{m=0}^\infty \tau u_{m,xxt}(x,t) \\ &= \mathcal{D}_t^\alpha u + (f(u))_x - d u_{xx} - S(u) - \tau u_{xxt}.\end{aligned}$$

Using equation (3.12) it follows now that:

$$\mathcal{D}_t^\alpha u + (f(u))_x = d u_{xx} + S(u) + \tau u_{xxt}. \tag{3.13}$$

From this, we conclude that $u(x,t)$ from HAM equals the exact solution of model (3.1).

3.4.2 Remarks on the $\hbar$-curve

The Homotopy Analysis Method is based on a homotopy concept from topology [1]. We introduced the auxiliary parameter $\hbar$ with the so-called zeroth-order deformation equation. Thus, the auxiliary parameter $\hbar$ provides us with a family of solution expressions which contain $\hbar$. Note that the convergence region *strongly* depends on this auxiliary parameter and it allows us to control the convergence region in some way. While the Homotopy Perturbation Method [60, 75] can give solutions only when $\hbar = -1$, HAM can provide convergent approximations for different $\hbar$ values. These $\hbar$ values should be in the so-called flat interval. In this interval, the HAM-solution is represented as a function of $\hbar$ for given N, which denotes how many steps we compute, and for carefully chosen x and t values. Let $\delta(\vec{x},t)$ denote the residual error of the Nth order HAM approximation and $\Delta = \int\int \delta^2(x,t) dV dt$ denote the integral of residual error. If we plot the $\Delta \sim \hbar$-curve, then it is clear that it is useful to find an interval of $\hbar$-values for which Δ decreases to zero as the HAM approximation becomes more accurate (for more information see [76]). This $\hbar$-curve is produced by plotting the HAM approximation for chosen index N, evaluated at a specific x and t value.

3.4.3 An optimal $\hbar$ value

The goal of an optimal $\hbar$ value is to construct a convergent homotopy-series solution [76]. This aim is satisfied by minimizing the squared residual of the mth order homotopy approximation

$$E_m(\hbar) = \int_0^T [\mathcal{N}(\sum_{n=0}^m u_n(x_0,t;\hbar))]^2 dt. \tag{3.14}$$

This expression tends to zero as $m \to +\infty$ where x_0 is a selected value of x. The optimal homotopy approximation is given by the minimum of the squared residual E_m, and the optimal convergence parameter is determined by $\frac{\partial E_m}{\partial \hbar} = 0$.

An alternative way to determine the optimal $\hbar$ value is by examining the solution curve of u_N as a function of $\hbar$. When we calculate the final HAM approximation $u_N(x,t;\hbar)$, we can choose $x = 0$ and an arbitrary t_0 value in $[0,T]$. Then our function $u_N(0,t_0;\hbar)$ becomes a function of $\hbar$. We take the first derivative of this function $\frac{\partial u_N(0,t_0;\hbar)}{\partial \hbar} = 0$, in order to find the extremum points and finally to find the optimal $\hbar$ value. The idea of the optimal $\hbar$ value is to accelerate the convergence of the HAM solutions.

3.5 Numerical examples

In this section, we present both ordinary and fractional order models to show the applications of HAM.

3.5.1 Example 1: a non-fractional higher order PDE model

In this example we consider :

$$\begin{cases} u_t + u_x = 2u_{xxt}, \\ u(x,0) = \mathrm{e}^{-x}, \end{cases} \tag{3.15}$$

which has the exact solution e^{-x-t}. This example was also considered by Liang and Jeffrey [75]. We illustrate the use of the $\hbar$-curve from the previous section and the approximations depending on the index N and time t. HAM gives us a convergent $\hbar$-interval on the $\hbar$-axis and this enables us to choose different $\hbar$ values. The plots indicate that HAM may produce fast converging approximations for this model. As an example, we give the HAM solutions for this model, see also [75]:

$$\begin{aligned} &u_0(x,t) = \mathrm{e}^{-x}, \\ &u_1(x,t) = -\hbar \mathrm{e}^{-x} t, \\ &u_2(x,t) = \tfrac{\hbar \mathrm{e}^{-x} t}{2}(\hbar t + 2\hbar - 2), \\ &u_3(x,t) = -\tfrac{\hbar \mathrm{e}^{-x} t}{6}(\hbar^2 t^2 - 6\hbar t + 6\hbar^2 t + 6\hbar^2 - 12\hbar + 6), \\ &\text{etc.} \end{aligned}$$

We compare HAM with the Homotopy Perturbation Method (HPM) (see [60, 75]) which gives the same solution as HAM when $\hbar = -1$. The $\hbar$-curve in Figure 3.1 (a) shows that $\hbar = -1$ is outside of the convergence region which is indicated by the flat part. Indeed HPM gives a divergent solution for model (3.15). In Figure 3.1 (b), we also illustrate the convergence of HAM for model (3.15). Even in the second approximation, HAM can already give a reasonable solution. In Figure 3.2 (a), we depict the HAM solution for different time values. In Figure 3.2 (b) a comparison between the exact solution and HAM approximation is given.

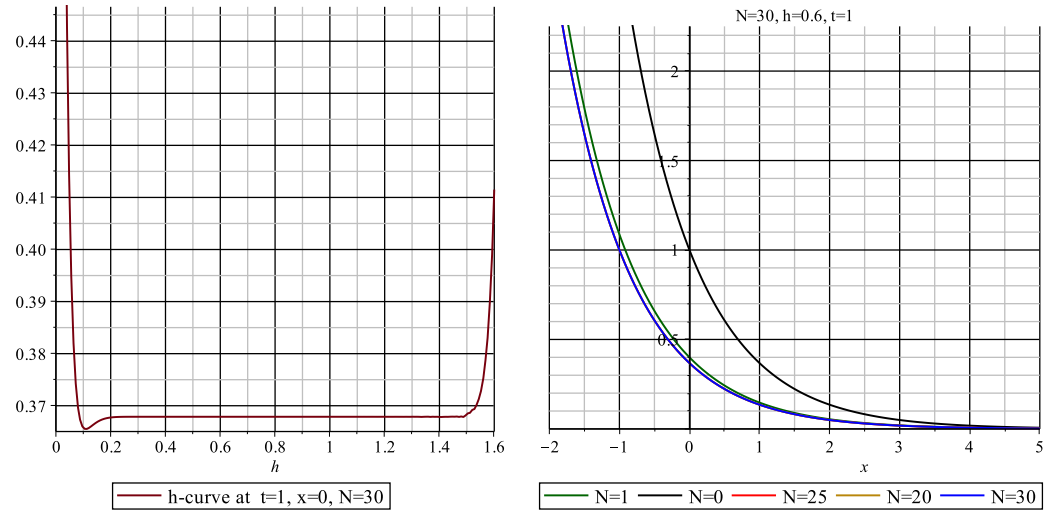

(a) (b)

FIGURE 3.1: The $\hbar$-curve in panel (a) and HAM approximations for different N values in panel (b) are shown for the non-fractional higher order PDE model (3.15).

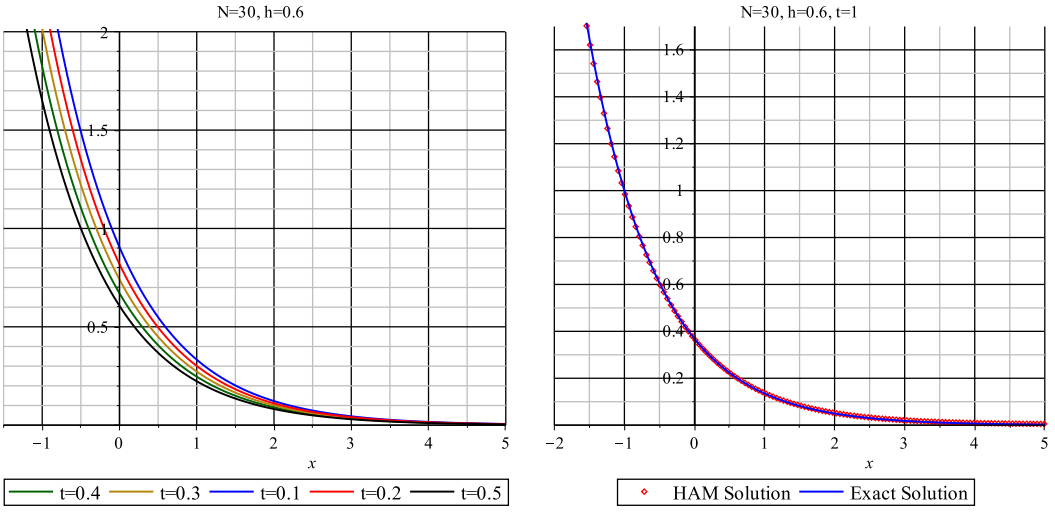

(a) (b)

FIGURE 3.2: Panel (a) illustrates HAM solutions of the non-fractional higher order PDE model (3.15) for different time values. The comparison between the exact solution and HAM solution is shown in panel (b).

3.5.2 Example 2: a fractional higher order PDE model

This example is an extended time-fractional version of model (3.15):

$$\begin{cases} \mathcal{D}_t^{\alpha} u + u_x = 2u_{xxt}, & 0 < \alpha \leq 1 \\ u(x,0) = \mathrm{e}^{-x}, \end{cases} \tag{3.16}$$

In Figure 3.3, 3.4 and 3.5, we present HAM approximations for different fractional orders α. The $\hbar$-curve, the optimal $\hbar_{\text{opt}}$ and HAM approximations for a chosen index N are presented. We conclude that if the fractional order α decreases, the $\hbar$-curve provides wider intervals. It can clearly be seen that the fractional order case gives flatter solutions than the ordinary case. In the ordinary case, we find a wider $\hbar$-interval whereas, for the fractional case, we can only use a restricted interval of $\hbar$ values.

First, we construct the zeroth-order deformation equation as follows:

$$(1-p)\mathcal{L}[\phi(x,t;p)-u_0(x,t)] = p\hbar\mathcal{N}[\phi(x,t;p)], \tag{3.17}$$

where $\mathcal{L}[\phi(x,t;p)-u_0(x,t)] = \mathcal{D}_t^{\alpha}(u_0(x,t)+\sum_{m=1}^{\infty}u_m(x,t)p^m)-u_0(x,t)$ and $\mathcal{N}[\phi(x,t;p)] = \mathcal{D}_t^{\alpha}(\phi(x,t;p))+(\phi(x,t;p))_x-2(\phi(x,t;p))_{xxt}$.
And the mth order deformation equation becomes:

$$\mathcal{L}[u_m(x,t)-\chi_m u_{m-1}(x,t)] = \hbar R_m(u_{m-1}), \tag{3.18}$$

where

$$R_m(u_{m-1}) = \frac{1}{(m-1)!}\frac{\partial^{m-1}(\mathcal{D}_t^{\alpha}(\phi(x,t;p))+(\phi(x,t;p))_x-2(\phi(x,t;p))_{xxt})}{\partial p^{m-1}}|_{p=0}. \tag{3.19}$$

Here, we start with the initial condition as a first approximation $u_0(x,t) = \mathrm{e}^{-x}$. It can be observed that the fractional case (3.16) is rather different than the ordinary case (3.15). If we compare the $\hbar$-curves of both cases (see Figure 3.1 and 3.3), the ordinary case has a wider $\hbar$-interval.

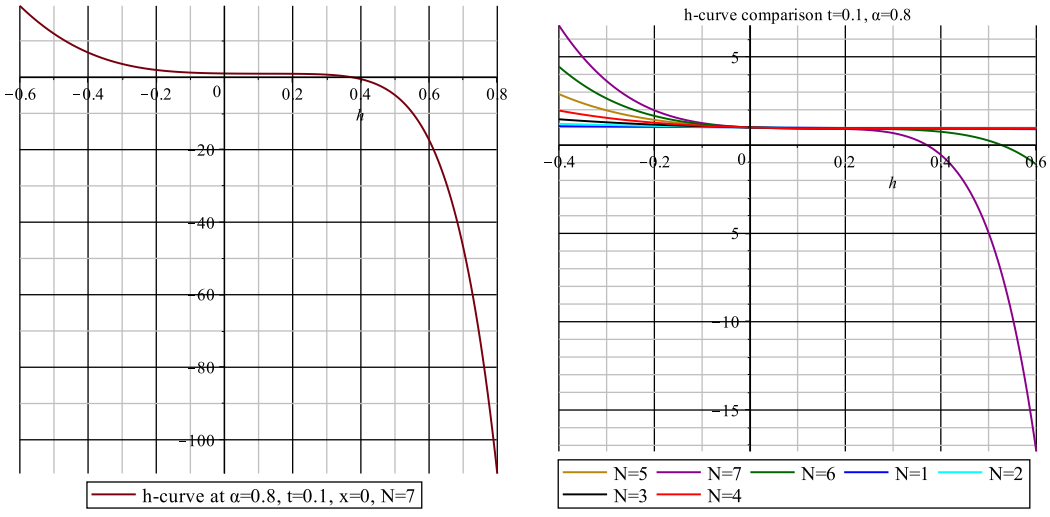

(a) (b)

FIGURE 3.3: $\hbar$-curves of HAM for the fractional higher order PDE model (3.16) for different N values are shown.

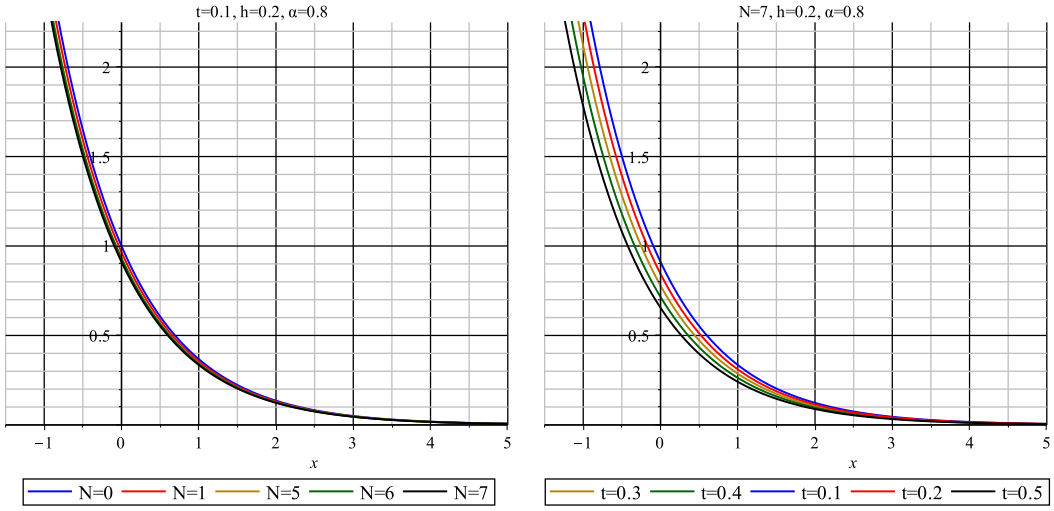

(a) (b)

FIGURE 3.4: HAM solutions for both different N values and time values are illustrated for the fractional higher order PDE model (3.16).

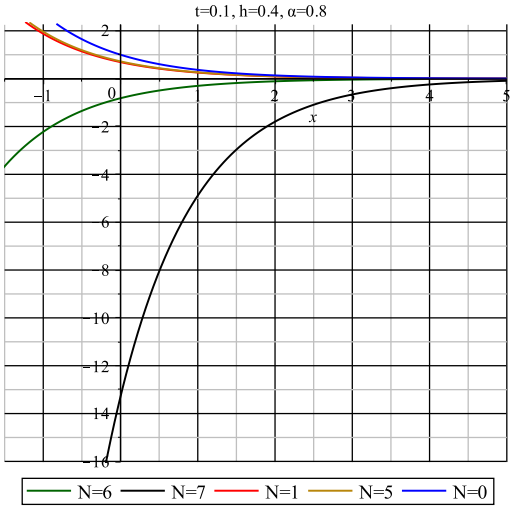

FIGURE 3.5: A divergent solution for $\hbar = 0.4$ is illustrated to show the effect of $\hbar$-value on HAM solution for the fractional higher order PDE model (3.16).

We illustrate the final HAM solution for different N and time values for $\alpha = 0.8$ in Figure 3.4 (a) and (b). HAM can produce an accurate approximation even for small N values. We also show a divergent HAM solution for $\hbar = 0.4$ in Figure 3.5, which is outside of the convergence interval. This emphasizes the role of the $\hbar$-value.

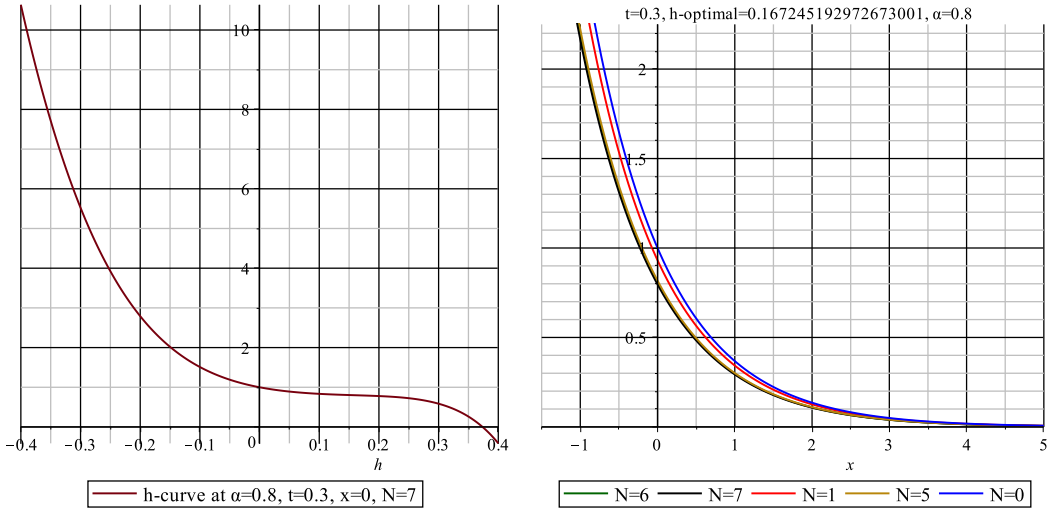

(a) (b)

FIGURE 3.6: Panel (a) shows the $\hbar$-curve of the fractional higher order PDE model (3.16) for $\alpha = 0.8$ and $t = 0.3$. Panel (b) shows the HAM approximations for optimal $\hbar = 0.167245$.

In Figure 3.6, we illustrate the HAM approximations with optimal $\hbar_{\text{opt}} = 0.16724$. Figure 3.6 (a) shows the $\hbar$-curve for $t = 0.3$. For this time value there is no clear $\hbar$-value we can choose from the interval. We calculated the optimal $\hbar$-value by formula (3.14): $\hbar_{\text{opt}} = 0.16724$ and show the HAM solutions with this optimal value in Figure 3.6 (b).

3.5.3 Example 3: a Fisher equation

Here we apply HAM to the Fisher equation [8, 5, 6, 13]:

$$\begin{cases} u_t = u_{xx} + 6u(1-u), & 0 < \alpha \leq 1 \\ u(x,0) = \frac{1}{(1+\mathrm{e}^x)^2}. \end{cases} \tag{3.20}$$

First, we suppose that our HAM solution is of the form of equation (3.4). Then we substitute equation (3.4) into the equation (3.6) and collect terms of equal powers in the embedded parameter p. We start with the initial condition $u_0(x,t) = \frac{1}{(1+\mathrm{e}^x)^2}$ as an initial guess. The following approximations are obtained in this way:

$$u_0 = \frac{1}{(1+\mathrm{e}^x)^2}, \tag{3.21}$$

$$u_1 = -\frac{10\hbar \mathrm{e}^x t}{(1+\mathrm{e}^x)^3}, \tag{3.22}$$

$$u_2 = \frac{5\hbar \mathrm{e}^x t(-2\hbar \mathrm{e}^x - 2\mathrm{e}^x + 10\hbar \mathrm{e}^x t - 2 - 5\hbar t - 2\hbar)}{(1+\mathrm{e}^x)^4}, \tag{3.23}$$

$$\vdots \tag{3.24}$$

The $\hbar$ value should be selected from the convergence interval derived by the so-called $\hbar$-curve. For example, $\hbar = -1$ (in this case HAM coincides with HPM) gives the solution:

$$u(x,t) = \frac{1}{(1+e^x)^2} + \frac{10e^x t}{(1+e^x)^3} + \frac{25e^x t^2(-1+2e^x)}{(1+e^x)^4} + \dots, \tag{3.25}$$

which is the Taylor expansion of the exact solution $u(x,t) = \frac{1}{(1+e^{x-5t})^2}$.

In this example, HAM gives fast convergent traveling wave approximations already in a few steps. It shows the potential efficiency of the method.

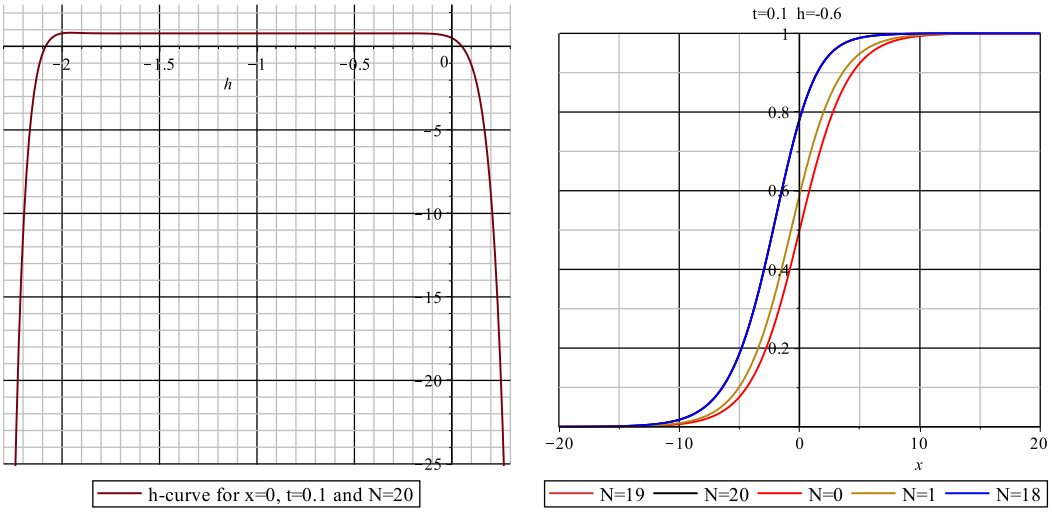

(a) (b)

FIGURE 3.7: $\hbar$-curve and traveling wave HAM solutions for different N values of the Fisher equation (3.20).

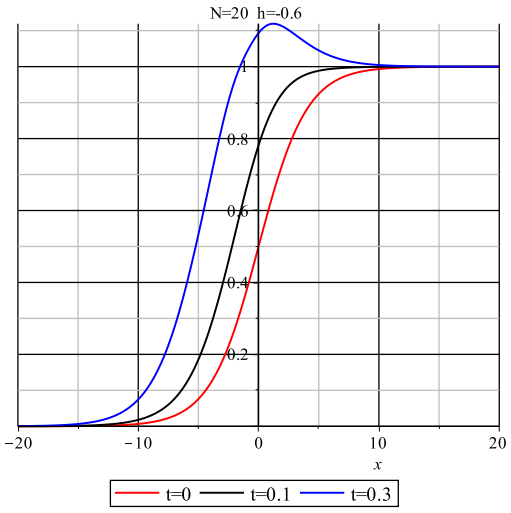

FIGURE 3.8: The time range of the Fisher equation (3.20).

In Figure 3.7 we show the $\hbar$-curve and the final HAM approximations. These approximations depict a fast convergent solution. In Figure 3.8 we illustrate HAM solutions for different

time values. The approximations are convergent until $t = 0.1$, when they start to become divergent.

3.5.4 Example 4: a time-fractional Fisher equation

Finally, HAM is applied to the time-fractional Fisher equation:

$$\begin{cases} \mathcal{D}_t^{\alpha} u = u_{xx} + u(1-u), & 0 < \alpha \leq 1 \\ u(x,0) = \frac{1}{2} + \frac{1}{2}\tanh(\frac{x}{4}). \end{cases} \tag{3.26}$$

Here we start with the initial guess $u_0(x,t) = \frac{1}{2} + \frac{1}{2}\tanh(\frac{x}{4})$ and the following approximation is as follows:

$$u_1(x,t) = \frac{1}{8}\frac{\hbar\sqrt{t}(-4\cosh(\frac{x}{4}) + \sinh(\frac{x}{4}))}{\sqrt{\pi}\cosh(\frac{x}{4})^3} \tag{3.27}$$

etc...

In this model, we also want to show the role of the factor "6" in model (3.20). Even if we have a small interval of time in model (3.20), now we can consider a much wider one.

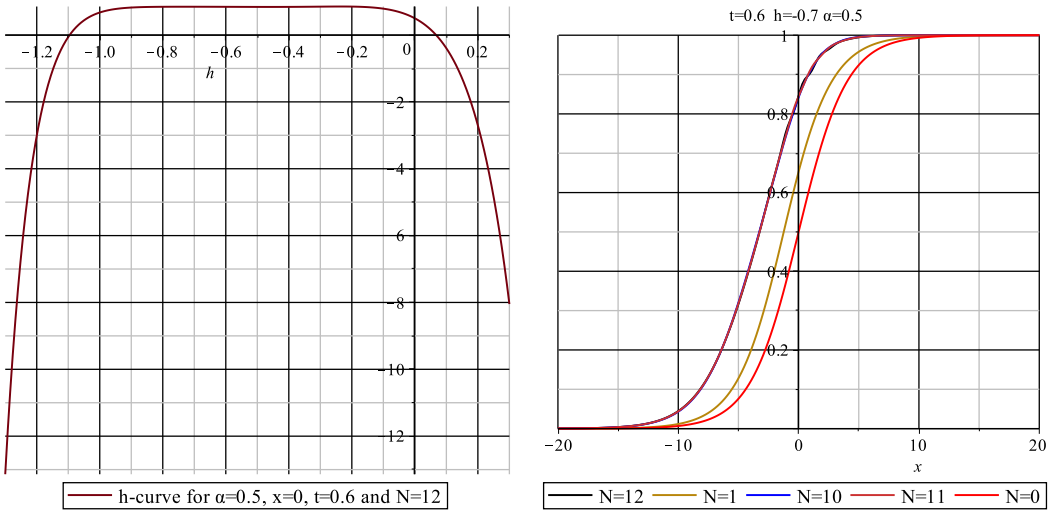

(a) (b)

FIGURE 3.9: The left panel shows the $\hbar$-curve and the right panel shows numerical results of the time-fractional Fisher model (3.26) for $\alpha = \frac{1}{2}$, $t = 0.6$ and $N = 12$.

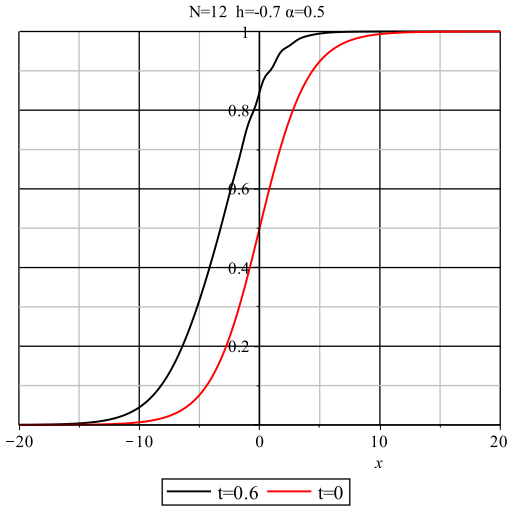

FIGURE 3.10: Traveling wave HAM approximations for different time values for the time-fractional Fisher model (3.26) with $\alpha = 0.5$. It shows the effect of the time value on the final approximation.

In Figure 3.9 and 3.10, we present the traveling wave approximations for $\alpha = \frac{1}{2}$. As you can see in panel (a) in the $\hbar$-curve, we have a wide flat area to choose the $\hbar$ value. Panel (b) shows that even in lower steps HAM can give a convergent solution. And it is also illustrated that our final approximation moves to the left with higher time values.

3.6 Summary

In this chapter we analyzed approximate solutions of ordinary and fractional order partial differential equations using the Homotopy Analysis Method (HAM). HAM is employed to determine a convergent solution which is provided by an optimal convergence parameter derived via minimizing the square residual. The results confirm that the Homotopy Analysis Method has the potential to be an efficient technique for this kind of models. The calculations are made by Maple. It can be observed that if we choose the value $\hbar = -1$ in the HAM solution, the approximations match exactly with the ones given by the Homotopy Perturbation Method (HPM) in chapter 2. It is also shown that the choice $\hbar = -1$ as in HPM may not always give a convergent solution. We need the parameter $\hbar$ in HAM to improve the convergence properties.

Chapter 4

Padé approximations in semi-analytic methods[1]

4.1 Introduction

Padé approximations [21, 83, 26, 27, 50, 116] are rational approximations of a function. This technique was developed by Henri Padé [99], but in fact F. Georg Frobenius [47] already described this concept by featuring the rational approximations of power series. The Padé approximant gives, in general, more accurate approximations than for example using the Taylor series and it can still converge even if the Taylor series does not.

We introduce the Padé approximant of a function $f(x)$ over a portion of its domain. Let's suppose, as an example, that $f(x) = \cos x$, and we approximate it on the interval $[0, \pi/2]$.

A rational approximation of the function $f(x)$ on $[a, b]$, which contains the value 0, consists of two polynomials named $P_N(x)$ and $Q_M(x)$ with degrees N and M. Their quotient is defined by:

$$R_{N,M}(x) = \frac{P_N(x)}{Q_M(x)}, \quad \text{for } a \leq x \leq b. \tag{4.1}$$

The primary requirement for a Padé approximation is that $f(x)$ and its derivative $f'(x)$ should be continuous at $x = 0$, which lies in the interval $[a, b]$. The reason behind the choice $x = 0$ is that it can be controlled easier. The polynomials defined in (4.1) are as follows:

$$P_N(x) = p_0 + p_1 x + p_2 x^2 + ... + p_N x^N, \tag{4.2}$$

and

$$Q_M(x) = 1 + q_1 x + q_2 x^2 + ... + q_M x^M. \tag{4.3}$$

The polynomials in (4.2) and (4.3) are defined such that $f(x)$, $R_{N,M}(x)$ and their derivatives agree at $x = 0$. For $Q_0(x) = 1$, the approximation turns into just the Maclaurin expansion for $f(x)$. It can be also observed that for a fixed value of $N + M$, the error becomes smaller when $P_N(x)$ and $Q_M(x)$ have the same degree or $P_N(x)$ has one degree higher.

We impose $q_0 = 1$, but there is no restriction to use $q_0 = 1$ in $Q_N(x)$. The important point in $Q_N(x)$ is that the constant term should be nonzero. In (4.1), we have totally $N + M + 1$ unknown coefficients. Suppose that $f(x)$ is analytic and the Maclaurin expansion of $f(x)$ is valid. Then,

$$f(x) = a_0 + a_1 x + a_2 x^2 + ... + a_k x^k + ... ,$$

[1] Sections 4.2, 4.3 and 4.4 are based on a paper published in International Journal of Computational Methods with joint authors H. Vazquez-Leal and H. Koçak, Vol. 13(6), 14 pages, 2016; DOI: 10.1142/S0219876216500390.

and we establish the difference $f(x)Q_M(x) - P_N(x) = Z(x)$:

$$\left(\sum_{j=0}^{\infty} a_j x^j\right)\left(\sum_{j=0}^{M} q_j x^j\right) - \sum_{j=0}^{N} p_j x^j = \sum_{j=N+M+1}^{\infty} c_j x^j. \tag{4.4}$$

The first $N + M$ derivatives of $f(x)$ and $R_{N,M}$ agree at $x = 0$. Because of this we choose the starting index $j = N + M + 1$ in (4.4) at the right side.

We first multiply out the left hand side of (4.4) and then equalize the powers of x^j to zero. It results in a system consisting of $N + M + 1$ linear equations:

$$a_0 - p_0 = 0$$

$$a_1 - p_1 + q_1 a_0 = 0$$

$$a_2 - p_2 + q_1 a_1 + q_2 a_0 = 0$$

$$a_3 - p_3 + q_1 a_2 + q_2 a_1 + q_3 a_0 = 0$$

$$a_N - p_N + ... + q_{M-1} a_{N-M+1} + q_M a_{N-M} = 0$$

and the second part

$$q_M a_{N-M+1} + q_{M-1} a_{N-M+2} + \cdots + q_1 a_N + a_{N+1} = 0$$

$$q_M a_{N-M+2} + q_{M-1} a_{N-M+3} + \cdots + q_1 a_{N+1} + a_{N+2} = 0$$

$$\vdots \qquad\qquad \vdots$$

$$q_M a_N + q_{M-1} a_{N+1} + \cdots + q_1 a_{N+M-1} + a_{N+M} = 0.$$

We first consider the M equations in the second part to solve for $q_1, q_2, ..., q_M$, then find $p_0, p_1, ..., p_N$ and produce the Padé approximation.

Let's establish the Padé approximation of cos x on the interval $[-5, 5]$ for $R_{4,4}(x)$. As we mentioned before, we will have $M+N+1$ equations with $M+N+1$ unknowns if we start with the Maclaurin expansion of cos x. It means that we have nine equations and nine unknowns. We can simplify these computations by starting $f(x) = \cos(x^{1/2})$ because both cos x and $R_{4,4}(x)$ are even functions and involve powers of x^2. The Maclaurin expansion of $f(x) = \cos(x^{1/2})$ is:

$$f(x) = 1 - \frac{1}{2}x + \frac{1}{24}x^2 - \frac{1}{720}x^3 + \frac{1}{40,320}x^4 - ... \tag{4.5}$$

and substituting (4.5) into (4.4) yields:

$$\left(1 - \frac{1}{2}x + \frac{1}{24}x^2 - \frac{1}{720}x^3 + \frac{1}{40,320}x^4 - ...\right)\left(1 + q_1 x + q_2 x^2\right) - p_0 - p_1 x - p_2 x^2$$

$$= 0 + 0x + 0x^2 + 0x^3 + 0x^4 + c_5 x^5 + c_6 x^6 + ...$$

We gather the coefficients according to the powers of x:

$$1 - p_0 = 0,$$

$$-\frac{1}{2} + q_1 - p_1 = 0,$$

$$\frac{1}{24} - \frac{1}{2}q_1 + q_2 - p_2 = 0,$$
$$-\frac{1}{720} + \frac{1}{24}q_1 - \frac{1}{2}q_2 = 0,$$
$$\frac{1}{40,320} - \frac{1}{720}q_1 + \frac{1}{24}q_2 = 0.$$

We first solve the last two equations above to find q_1 and q_2 and they become $q_2 = \frac{13}{15,120}$ and $q_1 = \frac{11}{252}$. It is obvious that $p_0 = 1$. Then we calculate $p_1 = -\frac{115}{252}$ and $p_2 = \frac{313}{15,120}$.

According to the Padé formula, we can write the approximation of $f(x) = \cos(x^{1/2})$ as follows:

$$f(x) \approx \frac{1 - \frac{115}{252}x + \frac{313}{15,120}x^2}{1 + \frac{11}{252}x + \frac{13}{15,120}x^2}. \tag{4.6}$$

If we substitute x^2 into (4.6), we can produce the $R_{4,4}(x)$ Padé expansion of cos x:

$$\cos x \approx R_{4,4}(x) = \frac{15,120 - 6900x^2 + 313x^4}{15,120 + 660x^2 + 13x^4}.$$

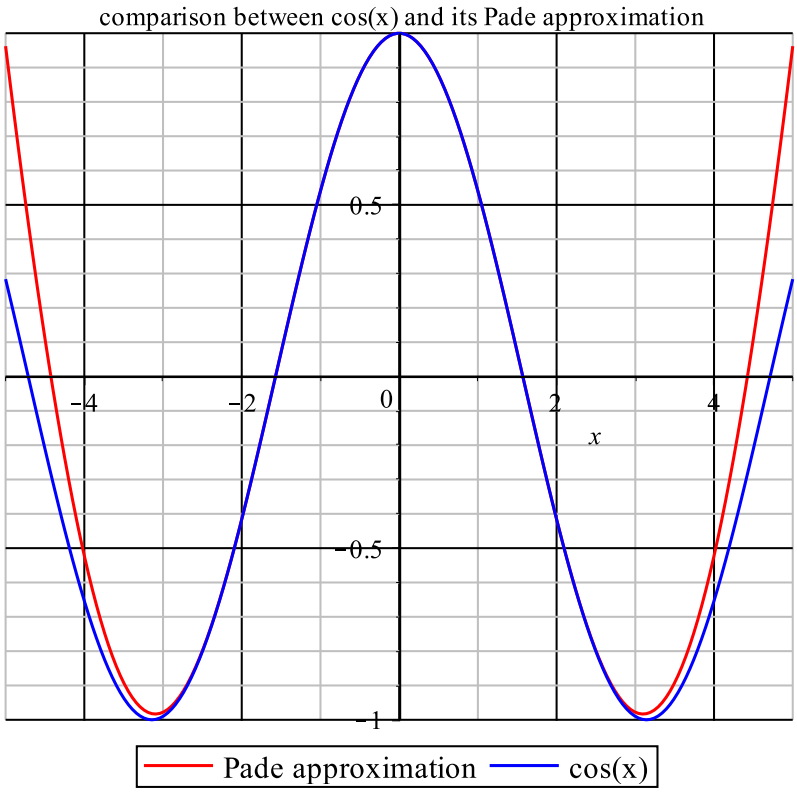

FIGURE 4.1: The difference between the function cos x and its Padé approximation

The accuracy of the Padé approximation is shown in Figure 4.1 by comparing the analytic function cos x and its Padé approximation.

4.2 Rational approximations for heat radiation and Troesch's equations

In this section, the rational homotopy perturbation method (RHPM) for the solution of nonlinear differential equations is presented. It may deliver a higher precision representation of the nonlinear differential equation using a few linear algebraic terms. In order to assess the benefits of this tool, three nonlinear problems are solved and compared against other semi-analytic methods or numerical methods. Furthermore, in order to deal with boundary-value problems (BVP), we propose a modification of the RHPM method. The obtained results show that RHPM is a powerful tool capable of generating highly accurate rational solutions.

Recently, homotopy based methods [19, 118, 58, 39, 120] have been extended with the introduction of an additional rational approximation, resulting in the, so-called, Rational Homotopy Perturbation Method (RHPM) [118, 121]. In RHPM, we assume that the approximate solution of a differential equation can be represented by the quotient of two power series in the homotopy parameter p. This quotient of power series transforms the nonlinear differential equation into a series of linear differential equations. In literature, one can find different applications of RHPM, like the Zakharov-Kuznetsov [18] equations, nonlinear systems of mixed Volterra-Fredholm [17] integral equations and stiff systems of ODEs, for example. We propose the application of this method to solve three nonlinear problems: one differential equation model, the so-called Troesch model and two other problems connected with heat radiation. Moreover, in order to deal with BVPs, we propose a modification of the original RHPM method which is based on the use of extra adjustment parameters from the RHPM divisor to fulfill the boundary conditions. To assess the potential of the proposed methodology, we compare the results to other approximated solutions reported in literature.

This section is organized as follows. In Section 4.2.1, we introduce the basic concept of the RHPM method. Section 4.3 shows the solution of three nonlinear differential equations of different kinds. Numerical simulations and a discussion about the results are provided in Section 4.4. Finally, a brief conclusion is given in Section 4.4.1.

4.2.1 The basic concept of the RHPM method

We can consider a nonlinear differential equation expressed as

$$\mathcal{L}(u) + \mathcal{N}(u) - f(r) = 0, \qquad \text{where} \qquad r \in \Omega, \tag{4.7}$$

having as boundary condition

$$B(u, \frac{\partial u}{\partial \eta}) = 0, \qquad \text{where} \qquad r \in \Gamma, \tag{4.8}$$

and where $\mathcal{L}$ and $\mathcal{N}$ are a linear and a non-linear operator, respectively; $f(r)$ is a known analytic function, B is a boundary operator, Γ is the boundary of domain Ω, and $\partial u/\partial \eta$ denotes differentiation along the normal drawn outwards from Ω [120].
Now, a possible homotopy formulation is

$$H(v,p) = (1-p)[\mathcal{L}(v) - \mathcal{L}(u_0)] + p(\mathcal{L}(v) + \mathcal{N}(v) - f(r)) = 0, \qquad p \in [0,1], \tag{4.9}$$

where u_0 is the initial approximation for (4.7) which satisfies the boundary conditions and p is known as the perturbation homotopy parameter. Analyzing (4.9), it can be concluded that

$$H(v,0) = \mathcal{L}(v) - \mathcal{L}(u_0) = 0, \tag{4.10}$$

and

$$H(v,1) = \mathcal{L}(v) + \mathcal{N}(v) - f(r) = 0. \tag{4.11}$$

Until this point, RHPM uses the same concept and the same notation used in HPM in section 2.3. Now, we assume that the solution for (4.9) can be written as power series quotient [118, 121] of p

$$v = \frac{p^0 v_0 + p^1 v_1 + p^2 v_2 + \cdots}{1 + p^1 w_1 + p^2 w_2 + \cdots}, \tag{4.12}$$

where $v_1, v_2, \ldots$ are unknown functions to be determined by the RHPM method and $w_1, w_2, \ldots$ are known (arbitrary) analytic functions of the independent variable, which are going to be represented by $w_i = k_i x^i$.
From (4.12), we calculated the limit when $p \to 1$ to obtain the solution for (4.7)

$$u = \lim_{p \to 1} v = \frac{v_0 + v_1 + v_2 + \cdots}{1 + w_1 + w_2 + \cdots}. \tag{4.13}$$

A convergence study of the method can be found in [118, 121].

4.3 Case studies

In this section, we will present three case studies to show the usefulness of the RHPM method to solve nonlinear differential equations.

4.3.1 Example 1: an unsteady nonlinear convective-radiative equation

The governing equation for heat transfer in a lumped system of combined convective-radiative heat transfers [48] is the following initial value problem, where we use the notation $\theta = \theta(\tau)$ instead of u:

$$\theta' + \theta + \epsilon_1 \theta\theta' + \epsilon_2 \theta^4 = 0, \qquad \theta(0) = 1, \tag{4.14}$$

where prime denotes differentiation with respect to τ and ϵ_1, ϵ_2 are parameters of the equation. From (4.14) we establish the following homotopy equations

$$(1-p)\left(v' + v\right) + p\left(v' + v + \epsilon_1 v v' + \epsilon_2 v^4\right) = 0, \tag{4.15}$$

From (4.12) we assume that the solution for (4.15) has the following quotient form (the number of terms in the denominator and the numerator are chosen such that an efficient computation can be made)

$$v = \frac{v_0 + v_1 p + v_2 p^2}{1 + k_1 x p^1 + k_2 x^2 p^2 + k_3 x^3 p^3}. \tag{4.16}$$

Substituting (4.16) into (4.15), regrouping and rearranging the terms of the same order of p, we obtain

$$\begin{aligned}
p^0: &\quad v_0' + v_0 = 0, && v_0(0) = 1,\\
p^1: &\quad v_1' + v_1 - v_0 k_1 + 3 v_0 k_1 x + \epsilon_2 v_0^4 + v_0 \epsilon_1 (v_0') + 3 (v_0') k_1 x = 0, && v_1(0) = 0,\\
p^2: &\quad v_2' + v_2 - v_1 k_1 - \epsilon_1 v_0^2 k_1 + 2 v_0 \epsilon_1 (v_0') k_1 x + 3 v_0 k_1^2 x^2 - 2 v_0 k_1^2 x \\
&\quad + 3 (v_0') k_1^2 x^2 + 4 \epsilon_2 v_0^3 v_1 + 3 (v_1') k_1 x + 3 v_1 k_1 x - 2 v_0 k_2 x + 3 v_0 k_2 x^2 \\
&\quad + 3 (v_0') k_2 x^2 + v_0 \epsilon_1 (v_1') + v_1 \epsilon_1 (v_0') = 0, && v_2(0) = 0.
\end{aligned} \tag{4.17}$$

Then, solving (4.17), results in

$$\begin{aligned}
v_0 = &\ \exp(-\tau),\\
v_1 = &\ \frac{1}{3}\Big(3k_1\tau + \epsilon_2\exp(-3\tau) - 3\epsilon_1\exp(-\tau) - \epsilon_2 + 3\epsilon_1\Big)\exp(-\tau),\\
v_2 = &\ \frac{3}{2}\epsilon_1^2\exp(-3\tau) - \frac{17}{12}\epsilon_1\epsilon_2\exp(-5\tau) - \exp(-2\tau)\epsilon_1 k_1\tau\\
&+\frac{1}{3}\epsilon_2\exp(-4\tau)k_1\tau + \exp(-\tau)k_2\tau^2 - \frac{1}{3}k_1\tau\exp(-\tau)\epsilon_2\\
&+\epsilon_1 k_1\tau\exp(-\tau) + \frac{2}{9}\epsilon_2^2\exp(-7\tau) + \frac{4}{3}\epsilon_2\exp(-4\tau)\epsilon_1\\
&+\frac{2}{3}\epsilon_1\exp(-2\tau)\epsilon_2 - \frac{4}{9}\epsilon_2^2\exp(-4\tau) - 2\epsilon_1^2\exp(-2\tau) + \frac{1}{2}\epsilon_1^2\exp(-\tau)\\
&-\frac{7}{12}\epsilon_1\epsilon_2\exp(-\tau) + \frac{2}{9}\exp(-\tau)\epsilon_2^2.
\end{aligned} \tag{4.18}$$

Substituting (4.18) into (4.16) and calculating the limit when $p \to 1$, we obtain the second-order approximation

$$\theta(\tau) = \lim_{p\to 1} v = \frac{v_0 + v_1 + v_2}{1 + k_1\tau + k_2\tau^2 + k_3\tau^3}, \tag{4.19}$$

with the parameters of k_1, k_2 and k_3.
If we use $\epsilon_1 = 0.05$ and $\epsilon_2 = 0.7$ as reported in [48], then the adjustment parameters are determined as follows: $k_1 = 1.4863852932$, $k_2 = 0.5165065093$, and $k_3 = 0.01581897788$. Here, the parameters are calculated using the NonlinearFit [118, 121, 119, 120] command from Maple Release 15 (given a total of k-samples from the exact model, the NonlinearFit command enables us to find values of the approximate model parameters such that the sum of the squared k-residuals is minimized).

4.3.2 Example 2: a nonlinear convective-radiative conduction equation

The governing equation of the one dimensional heat transfer in a straight fin [48], where one fin surface transfers heat through both convection and radiation, is the following boundary value problem with $\theta = \theta(x)$

$$\theta'' - \mathrm{N}^2\theta + \epsilon_1(\theta')^2 + \epsilon_1\theta\theta'' - \epsilon_2\theta^4 = 0, \qquad \theta'(0) = 0, \quad \theta(1) = 1 \tag{4.20}$$

where N denotes the fin parameter, prime denotes differentiation with respect to X and ϵ_1, ϵ_2 are parameters of the equation.

From (4.14) we establish the following homotopy equation

$$(1-p)\left(v'' - \mathrm{N}^2 v\right) + p\left(v'' - \mathrm{N}^2 v + \epsilon_1(v')^2 + \epsilon_1 v v'' - \epsilon_2 v^4\right) = 0, \tag{4.21}$$

From (4.12), we assume that the solution for (4.15) has the following form

$$v = \frac{v_0 + v_1 p}{1 + k_1 X p + k_2 X^2 p^2}, \tag{4.22}$$

Substituting (4.22) into (4.21), regrouping and rearranging the terms having same order of p, we obtain

$$\begin{aligned} p^0: &\quad v_0'' - \mathrm{N}^2 v_0 = 0, && v_0'(0) = 0, v_0(1) = 1, \\ p^1: &\quad v_1'' + \epsilon_1 v_0 v_0'' - 3\mathrm{N}^2 v_0 k_1 X - \epsilon_2 v_0^4 - \mathrm{N}^2 v_1 + \epsilon_1 (v_0')^2 \\ &\quad +3 v_0'' k_1 X - 2 v_0' k_1 = 0, && v_1'(0) = 0, v_1(1) = 0, \end{aligned} \tag{4.23}$$

Then, we solve (4.23), resulting in

$$\begin{aligned} v_0 &= (\exp(\mathrm{N}X) + \exp(-\mathrm{N}X))/l, \\ v_1 &= \frac{1}{30}\Bigg\{ -\Bigg[20\Bigg((\epsilon_1 \mathrm{N}^2 l^2 - 2\epsilon_2)\exp(2\mathrm{N}X) - \frac{3}{2}\mathrm{N}k_1(\mathrm{N}X + 1/2) l^3 \exp(3\mathrm{N}X) \\ &\quad -\frac{3}{2}\mathrm{N}k_1(\mathrm{N}X - 1/2) l^3 \exp(5\mathrm{N}X) + (\epsilon_1 \mathrm{N}^2 l^2 - 2\epsilon_2)\exp(6\mathrm{N}X) \\ &\quad +\Big[9\Big(\exp(4\mathrm{N}X) - \frac{1}{90} - \frac{1}{90}\exp(8\mathrm{N}X)\Big)\Big]\epsilon_2\Bigg)\Bigg] l\exp(-4\mathrm{N}X) \\ &\quad +\Bigg[\Bigg((20\epsilon_1 \mathrm{N}^2 l^2 - 40\epsilon_2)\exp(2\mathrm{N}) - 30\mathrm{N}k_1(\mathrm{N} + 1/2) l^3 \exp(3\mathrm{N}) \\ &\quad -30\mathrm{N}k_1(\mathrm{N} - 1/2) l^3 \exp(5\mathrm{N}) + (20\epsilon_1 \mathrm{N}^2 l^2 - 40\epsilon_2)\exp(6\mathrm{N}) \\ &\quad +\Big[180\Big(\exp(4\mathrm{N}) - \frac{1}{90} - \frac{1}{90}\exp(8\mathrm{N})\Big)\Big]\epsilon_2\Bigg)\exp(-4\mathrm{N}) + 30\mathrm{N}k_1 l^3 \exp(\mathrm{N})\Bigg]\exp(-\mathrm{N}X) \\ &\quad +\Bigg[20\Bigg(\Big\{(\epsilon_1 \mathrm{N}^2 l^2 - 2\epsilon_2)\exp(2\mathrm{N}) - \frac{3}{2}\mathrm{N}k_1(\mathrm{N} + 1/2) l^3 \exp(3\mathrm{N}) \\ &\quad -\frac{3}{2}\mathrm{N}k_1(\mathrm{N} - 1/2) l^3 \exp(5\mathrm{N}) + (\epsilon_1 \mathrm{N}^2 l^2 - 2\epsilon_2)\exp(6\mathrm{N}) + \Big[9\Big(\exp(4\mathrm{N}) - \frac{1}{90} \\ &\quad -\frac{1}{90}\exp(8\mathrm{N})\Big)\Big]\epsilon_2\Big\}\exp(-4\mathrm{N}) - \frac{3}{2}\mathrm{N}l^3 k_1 \exp(-\mathrm{N})\Bigg)\Bigg]\exp(\mathrm{N}X)\Bigg\}/(\mathrm{N}^2 l^5), \end{aligned} \tag{4.24}$$

where $l = \exp(\mathrm{N}) + \exp(-\mathrm{N})$. These formulas have been calculated by Maple.

Substituting (4.24) into (4.22) and calculating the limit when $p \to 1$, we obtain the first-order approximation

$$\theta(X) = \lim_{p \to 1} v = \frac{v_0 + v_1}{1 + k_1 X + k_2 X^2}, \tag{4.25}$$

If we use $N = 1$, $\epsilon_1 = 0.2$, and $\epsilon_2 = 0.2$ as reported in [48]; the adjustment parameters are chosen as: $k_1 = 0.0098534568628$, $k_2 = -0.0098534568628$. In fact, k_2 was set to $k_2 = -k_1$ to satisfy the boundary condition $\theta(1) = 1$ and k_1 was calculated using the numerical procedure given for the first case study.

4.3.3 Example 3: Troesch's problem

Troesch's equation is a boundary value problem that arises in the investigation of confinement of a plasma column by a radiation pressure [123] and also in the theory of gas porous electrodes [49, 89].

The problem is expressed as

$$y'' = n\sinh(ny), \qquad y(0) = 0, \quad y(1) = 1, \tag{4.26}$$

where prime denotes differentiation with respect to x and n is known as Troesch's parameter.

Straightforward application of RHPM to solve (4.26) is not possible due to the hyperbolic sine term of the dependent variable. Nevertheless, the polynomial type nonlinearities are easier to handle by the RHPM method. Therefore, in order to apply RHPM successfully, we convert the hyperbolic-type nonlinearity in Troesch's problem into a polynomial type nonlinearity using the variable transformation reported in [28, 120]

$$u(x) = \tanh\left(\frac{n}{4}y(x)\right). \tag{4.27}$$

After using (4.27), we obtain the following transformed problem

$$\left(1-u^2\right)u'' + 2u(u')^2 - n^2u(1+u^2) = 0, \tag{4.28}$$

where the boundary conditions are obtained by using variable transformation (4.27).

Substituting the original boundary conditions $y(0) = 0$ and $y(1) = 1$ into (4.27), results in

$$u(0) = 0, \qquad \text{and} \qquad u(1) = \tanh\left(\frac{n}{4}\right). \tag{4.29}$$

From (4.9) and (4.28), we can formulate the following homotopy [61, 58, 57]

$$H(v,p) = (1-p)v'' + p\left(\left(1-v^2\right)v'' + 2v(v')^2 - n^2v(1+v^2)\right), \tag{4.30}$$

where p is the homotopy parameter.

From (4.12), we assume that the solution for (4.30) has the following form

$$v = \frac{v_0 + v_1p + v_2p^2 + v_3p^3}{1 + k_1xp^1 + k_2x^2p^2 + k_3x^3p^3}, \tag{4.31}$$

where k_1, k_2 and k_3 are coefficients.

Substituting (4.31) into (4.30) and equating identical powers of p terms, we obtain

$$\begin{aligned}
p^0: &\quad v_0'' = 0, \qquad v_0(0) = 0, v_0(1) = \gamma,\\
p^1: &\quad v_1'' + 2v_0(v_0')^2 - v_0^2v_0'' - 2(v_0')k_1 - n^2v_0 - n^2v_0^3 + 3v_0''k_1x = 0, \qquad v_1(0) = 0, v_1(1) = 0,\\
p^2: &\quad v_2'' - 2v_0^2(v_0')k_1 - 3n^2v_0^2v_1 + 2v_1(v_0')^2 - 4(v_0')k_2x - 2(v_1')k_1 - 2v_0k_2\\
&\quad -n^2v_0^3k_1x + 3v_1''k_1x - 3n^2v_0k_1x - 2v_0v_1v_0'' + 3v_0''k_1^2x^2 - n^2v_1\\
&\quad +2v_0(v_0')^2k_1x - v_0^2v_0''k_1x + 2v_0k_1^2 + 3v_0''k_2x^2\\
&\quad +4v_0(v_1')(v_0') - v_0^2v_1'' - 4(v_0')k_1^2x = 0, \qquad v_2(0) = 0, v_2(1) = 0.\\
p^3: &\quad \cdots
\end{aligned} \tag{4.32}$$

where $\gamma = \tanh\left(\frac{n}{4}\right)$.

We solve (4.32) by using Maple, resulting in

$$\begin{aligned} v_0 &= \gamma x, \\ v_1 &= \frac{1}{20}(x-1)\left(\left(x^2n^2 - \tfrac{20}{3} + n^2\right)(x+1)\gamma^2 + 20k_1 + 10/3n^2x + \frac{10}{3}n^2\right)\gamma x, \\ &\vdots \end{aligned} \tag{4.33}$$

Substituting (4.33) into (4.31) and calculating the limit when $p \to 1$, we obtain the third-order approximated solution for (4.28)

$$u_3(x) = \lim_{p\to 1} v = \frac{v_0 + v_1 + v_2 + v_3}{1 + k_1x + k_2x^2 + k_3x^3}. \tag{4.34}$$

Finally, from (4.27) and (4.34), the proposed solution for Troesch's problem is

$$y(x) = \frac{4}{n}\tanh^{-1}(u_3(x)), \qquad 0 \le x \le 1, \tag{4.35}$$

Considering $n = 0.5$ and $n = 1$, we choose the adjustment parameters $[k_1, k_2, k_3]$ as: [0.0008714504846,-0.0008670617014,-0.0000043887833] and [0.01265746050997,-0.0121666681719,-0.000490792338] respectively, by using the procedure explained for the first case study. In fact, for both cases, k_2 was set to $k_2 = -k_1 - k_3$ to fulfil the boundary condition of (4.26) at $x = 1$.

4.4 Numerical simulations and discussion

For all case studies, we employed built-in numerical routines from Maple 13 for comparison purposes. For the boundary-value problem, it utilized the scheme based on the trapezoidal rule combined with Richardson extrapolation. For the initial value problems, it used the Fehlberg fourth-fifth order Runge-Kutta method with degree four interpolant (RKF45) [40, 43]. For both types of algorithms, an absolute error (A.E.) tolerance of 10^{-12} was selected.

For the first case study, we solve the heat radiation problem (4.14) obtaining a highly accurate solution as shown in Figure 4.2 and Figure 4.3. In those figures, we can observe a comparison between the proposed solution, HPM [48] and PM [48]; showing higher precision for the proposed solution. For the second case study, we solved with high accuracy another heat radiation equation (4.20) as depicted in Figure 4.4 and Figure 4.5. Again, in those figures, we can observe a comparison with HPM [48], showing higher precision for the RHPM solution. This higher precision of the RHPM method is due to its ability to produce rich rational expressions that can potentially fit a wider scope of non-linearities. For instance, it is well known that Padé approximants [116], being rational expressions, can represent with more efficiency approximate solutions than simple series solutions.

The Troesch's BVP is a benchmark equation for numerical [42, 79] and semi-analytical methods [28, 120, 34, 44, 54, 72, 92] which has been solved by RHPM to obtain the approximated solution (4.35). Tables 4.1 and 4.2 show a comparison between the results obtained and other semi-analytical methods like: homotopy perturbation method (HPM)[92, 44, 120], decomposition method approximation (DMA)[34, 44], homotopy analysis method (HAM)[54], and Laplace transform decomposition method (LTDM)[72]. The comparison shows that the average absolute relative error (A.A.R.E.) for (4.35) is lower than the reported results for $n = 0.5$ and $n = 1$. In addition, these results show that RHPM can produce rapidly convergent approximations, even when few steps are employed, while the other finite difference scheme based methods [42] need more than ten steps.

Finally, in order to deal with BVPs, we proposed a modification of the RHPM method that is based on the use of the adjustment parameters (k_1, $k_2, \cdots$) of the RHPM divisor to fulfil the boundary conditions. This modification was efficient as seen in the results for case studies two and three. Therefore, further research is required in order to exploit the proposed modification to solve more challenging BVPs.

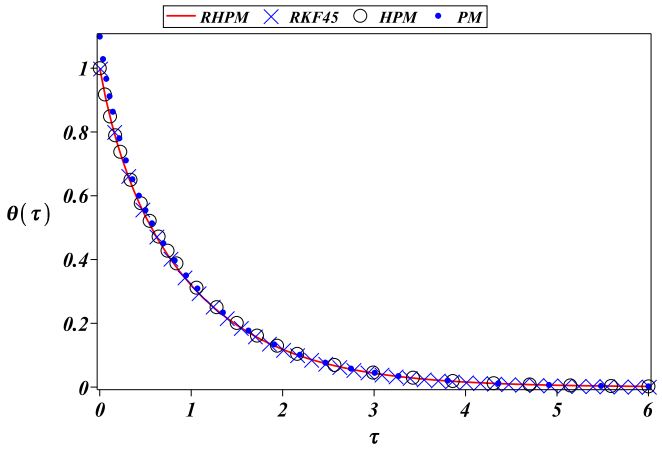

FIGURE 4.2: RKF45 solution for (4.14) (diagonal cross) and its approximations obtained by using: RHPM (4.19) (solid line), HPM [48] (circles), and PM [48] (dots).

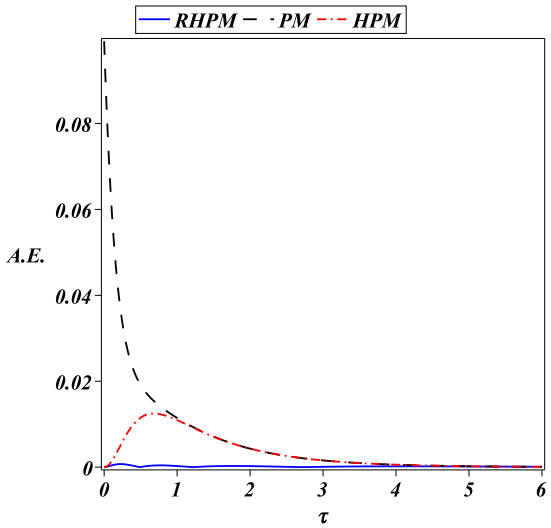

FIGURE 4.3: Absolute error (A.E.) of approximations RHPM (4.19) (solid line), HPM [48] (dash-dot), and PM [48] (dash) with respect to RKF45 solution for (4.14). The PM starts with a higher absolute error because of its initial approximation. Note the rapid convergence of RHPM compared with the other methods.

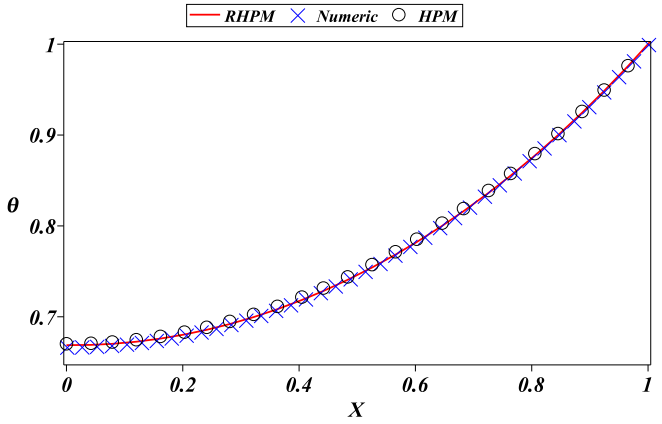

FIGURE 4.4: Numerical solution for (4.20) (diagonal cross) and its approximations obtained by using: RHPM (4.25) (solid line) and HPM [48] (circles).

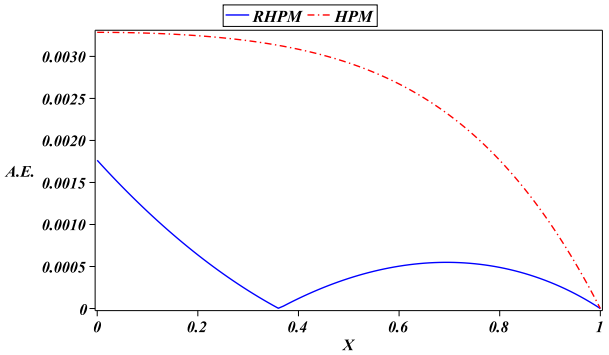

FIGURE 4.5: Absolute error (A.E.) of approximations RHPM (4.25) (solid line) and HPM [48] (dash-dot) with respect to RKF45 solution for (4.20). It shows that RHPM can give a better approximation than HPM for the same step value $N = 20$.

x	Exact[42, 79]	This work (4.35)	HPM [120]	DMA[34]	HPM[44]	HPM[92]	HAM[54]	LDTM[72]
0.1	0.0959443493	0.0959443499	0.0959443155	0.0959383534	0.0959395656	0.095948026	0.0959446190	0.0959443520
0.2	0.1921287477	0.1921287486	0.1921286848	0.1921180592	0.1921193244	0.192135797	0.1921292845	0.1921287539
0.3	0.2887944009	0.2887944015	0.2887943176	0.2887803297	0.2887806940	0.288804238	0.2887952148	0.2887944107
0.4	0.3861848464	0.3861848461	0.3861847539	0.3861687095	0.3861675428	0.386196642	0.3861859313	0.3861848612
0.5	0.4845471647	0.4845471637	0.4845470753	0.4845302901	0.4845274183	0.4845599	0.4845485110	0.4845471832
0.6	0.5841332484	0.5841332476	0.5841331729	0.5841169798	0.5841127822	0.584145785	0.5841348222	0.5841332650
0.7	0.6852011483	0.6852011484	0.6852010943	0.6851868451	0.6851822495	0.685212297	0.6852028604	0.6852011675
0.8	0.7880165227	0.7880165234	0.7880164925	0.7880055691	0.7880018367	0.788025104	0.7880181729	0.7880165463
0.9	0.8928542161	0.8928542159	0.8928542059	0.8928480234	0.8928462193	0.892859085	0.8928553997	0.8928542363
	Order	3	2	6	2	2	6	3
	A.A.R.E.	2.05378E(-9)	1.83327E(-07)	3.47802E(-05)	3.57932E(-05)	2.44418E(-05)	2.51374E(-06)	3.10957E(-08)

TABLE 4.1: Comparison between (4.35), exact solution [42, 79], and other reported approximate solutions. Using $n = 0.5$. This table gives the accuracy of the RHPM and also shows that RHPM is a more efficient method than the other methods for this model.

x	Exact[42]	This work (4.35)	HPM [120]	ADM[34]	HPM[44]	HPM[92]	HAM[54]	LDTM[72]
0.1	0.0846612565	0.0846612846	0.08466075858	0.084248760	0.0843817004	0.084934415	0.0846732692	0.08466308972
0.2	0.1701713582	0.1701715279	0.1701704581	0.169430700	0.1696207644	0.170697546	0.1701954538	0.1701750442
0.3	0.2573939080	0.2573941007	0.2573927827	0.256414500	0.2565929224	0.258133224	0.2574302342	0.2573994845
0.4	0.3472228551	0.3472228892	0.3472217324	0.346085720	0.3462107378	0.348116627	0.3472715981	0.3472303763
0.5	0.4405998351	0.4405996642	0.4405989511	0.439401985	0.4394422743	0.44157274	0.4406610140	0.4406093753
0.6	0.5385343980	0.5385341875	0.5385339413	0.537365700	0.5373300622	0.539498234	0.5386072529	0.5385460046
0.7	0.6421286091	0.6421285932	0.6421286573	0.641083800	0.6410104651	0.642987984	0.7526899495	0.6421421393
0.8	0.7526080939	0.7526082657	0.7526085475	0.751788000	0.7517335467	0.753267551	0.7526899495	0.7526226886
0.9	0.8713625196	0.8713625063	0.8713630450	0.870908700	0.8708835371	0.871733059	0.8714249118	0.8713748860
Order		3	2	6	2	2	6	3
A.A.R.E.		3.58118E(-07)	2.54568E(-06)	0.002714577	0.002320107	0.002044737	0.019244326	2.05E(-05)

TABLE 4.2: Comparison between (4.35), exact solution [42, 79], and other reported approximate solutions. Using $n = 1$.

4.4.1 Summary

This work presented the Rational Homotopy Perturbation Method (RHPM) as a novel tool with potential to solve nonlinear differential equations. We were able to obtain highly accurate rational numerical solutions for different types of problems: two nonlinear boundary value problems (BVPs) and a highly nonlinear initial value problem. The high precision of RHPM solutions is due to the generated rational expressions that can, potentially, fit a wider scope of non-linearities. We proposed a modification for the RHPM method to solve nonlinear BVPs by using extra adjustment parameters and, thus, fulfill the boundary conditions. A comparison of RHPM with other semi-analytic methods exhibited the flexibility of the new method to generate higher accurate numerical solutions.

4.5 Semi-analytical solutions of the time-fractional Fisher equation by using a Padé approximation

4.5.1 Introduction

The Homotopy Analysis Method (HAM), as described and applied in Chapter 3, may provide us with explicit semi-analytic solutions of nonlinear problems in certain cases. In this section, we apply HAM to the time-fractional Fisher equation [5, 6, 13, 37, 127] and examine both the ordinary and fractional order versions. Further, we apply a Padé approximation (see previous sections) to improve the accuracy of the numerical solution compared to the basic method HAM.

4.5.2 The time-fractional Fisher equation

We consider the following time fractional Fisher type equation:

$$\begin{cases} \mathcal{D}_t^{\alpha} u(x,t) = u_{xx}(x,t) + 6u(1-u), \qquad 0 < \alpha \leq 1, \\ u(x,0) = \frac{1}{(1+\mathrm{e}^{x})^2}, \end{cases} \tag{4.36}$$

which has the exact solution $\frac{1}{(1+\mathrm{e}^{x-5t})^2}$ for $\alpha = 1$.
In this example, we will use HAM and then apply a Padé approximation to find a good approximate solution. As it was mentioned in section 4.1, we consider (3.3) to construct the homotopy. Then it follows from the theory of HAM that we can obtain the step solutions (3.4) by using formula (3.6). We suppose that the initial condition $u(x,0) = \frac{1}{(1+\mathrm{e}^{x})^2}$ is our initial guess u_0 for HAM. The rest of the process can be calculated by Maple, and it gives the following first two step solutions:

$$u_1 = -\frac{1.07367\,\hbar t^{\alpha}\mathrm{e}^{x}(7\,\mathrm{e}^{x}+5)}{1+3\,\mathrm{e}^{x}+3\,\mathrm{e}^{2x}+\mathrm{e}^{3x}},$$

$$u_2 = \frac{t^{2\alpha}(34.27473\,\mathrm{e}^{3x}+0.69948\,\mathrm{e}^{2x}-34.27473\,\mathrm{e}^{x}-17.48711)\,\mathrm{e}^{x}}{(1+\mathrm{e}^{x})^2(1+3\,\mathrm{e}^{x}+3\,\mathrm{e}^{2x}+\mathrm{e}^{3x})}.$$

Then, the final HAM solution is obtained by the summation $U(x,t) = u_0(x,t) + \sum_{m=1}^{\infty} u_m(x,t)p^m$. We first consider the case $\alpha = 1$. For this case, the $\hbar$-curve (see section 3.4.2) and the HAM solutions for the time values $t = 0.1, 0.2, 0.3, 0.4$ and 0.5 are presented in Figure 4.6:

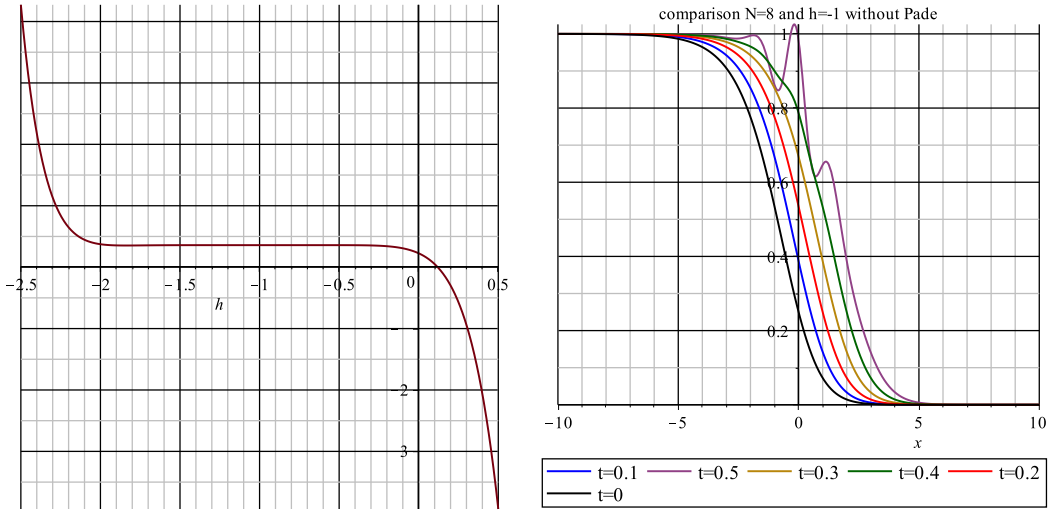

(a) (b)

FIGURE 4.6: Panel (a) shows the $\hbar$-curve. Panel (b) illustrates the HAM solutions for different time values for $\alpha = 1$.

In Figure 4.6 (a), we see clearly a flat interval for choosing an appropriate $\hbar$ value for the HAM solution (see section 3.4.2). HAM can produce accurate approximations even for $N = 8$ and $\hbar = -1$. But it is clear from Figure 4.6 that the HAM solution becomes divergent for $t = 0.5$ (the black curve). Here, we apply the Padé[5,5] approximation to smooth the solution.

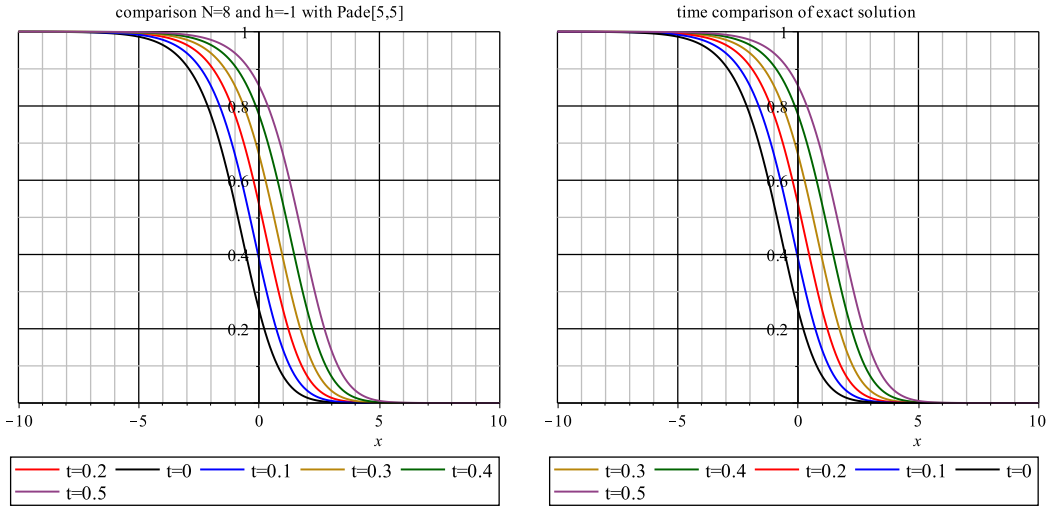

(a) (b)

FIGURE 4.7: HAM solution with Padé[5,5] approximation for $\alpha = 1$ (left) and the exact solution of (4.36) (right).

In Figure 4.7, the HAM solution is clearly improved by applying the Padé[5,5] approximation and we can produce accurate approximations even for higher time values.

Let's consider the fractional case and take $\alpha = 0.8$. In this case, we decided to stop the loop in the 4th step, because we could manage to obtain accurate approximations.

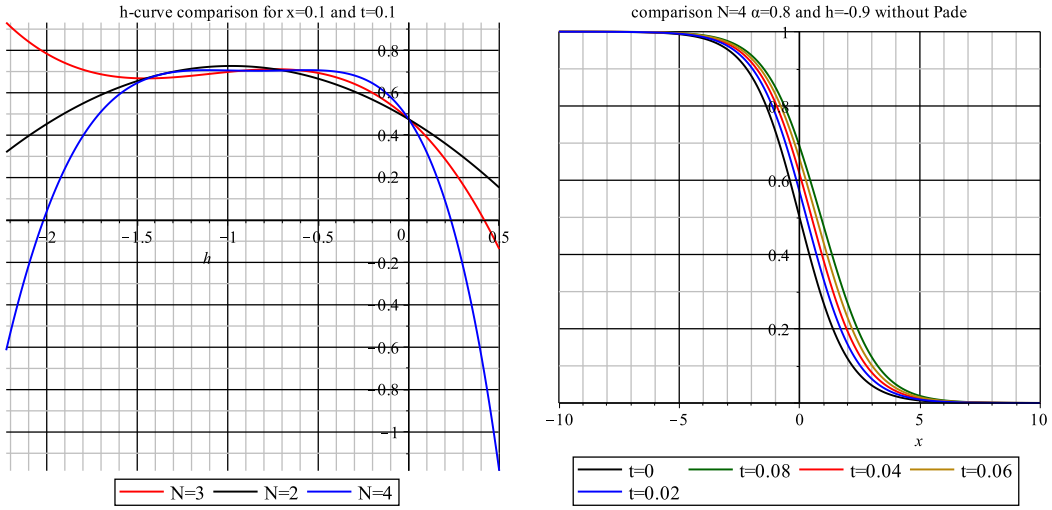

(a) (b)

FIGURE 4.8: In the fractional case $\alpha = 0.8$, the different $\hbar$-curves for different N values are shown in Panel (a) and the traveling wave solutions for $N = 4$ are presented in Panel (b).

We can observe in Figure 4.8 (a) that $\hbar = -0.9$ is the intersection point for different N values (see section 3.4.3) and it gives smooth traveling waves solutions for different time values (see Figure 4.8 (b)).

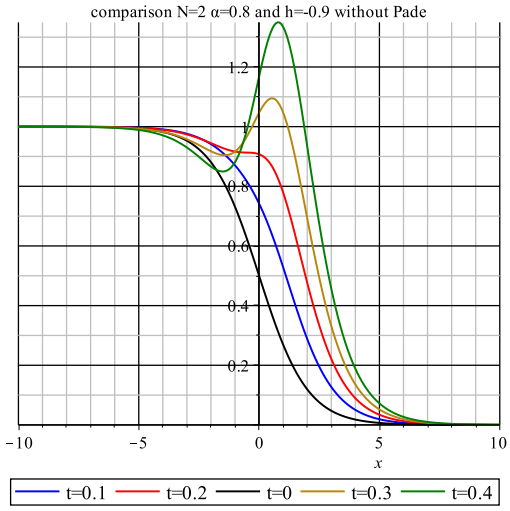

(a)

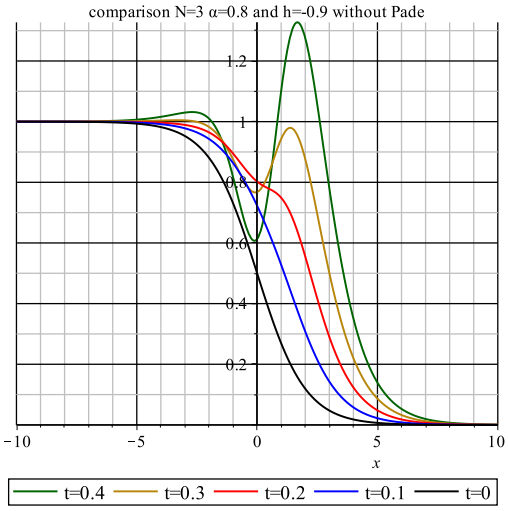

(b)

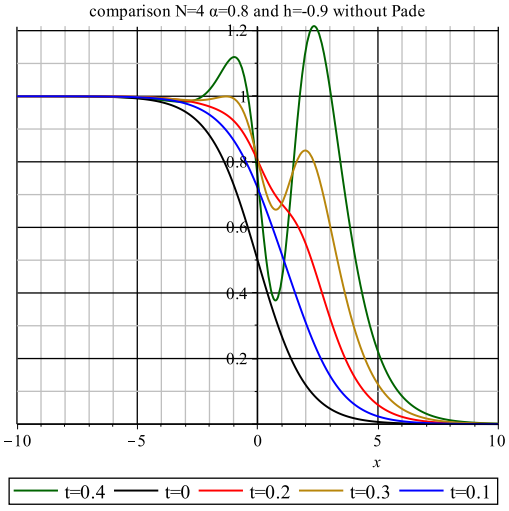

(c)

FIGURE 4.9: The HAM solutions for $N = 2, 3$ and 4 for different time values are displayed.

In Figure 4.9, we present the HAM solutions for steps 2, 3 and 4 when $\alpha = 0.8$ and $\hbar = -0.9$ without using the Padé approximation. We can observe from the red curves (for $t = 0.2$), from the brown curves ($t = 0.3$) and also from the green curves (t=0.4) in Figure 4.9 (a), (b), (c) that HAM needs more steps to smooth the solution. Then, we apply the Padé approximation to improve the solution.

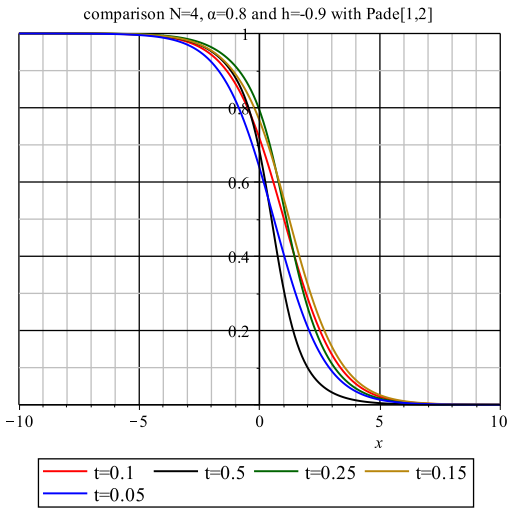

FIGURE 4.10: HAM solution with Padé[1,2] approximation for $\alpha = 0.8$.

In Figure 4.10 it is depicted that the Padé[1,2] approximation helps to produce better approximations for higher time values. There, we apply different types of Padé approximations for different N values. While we are using Padé[1,2] for $N = 2$ and $N = 4$, we use Padé[2,2] for $N = 3$. As it was mentioned in section 4.1, we construct the Padé approximations as follows:

$$R_{1,2}(x) = \frac{P_1(x)}{Q_2(x)} = \frac{p_0 + p_1 x}{1 + q_1 x + q_2 x^2} : \quad \text{Padé[1,2]}$$

and

$$R_{2,2}(x) = \frac{P_2(x)}{Q_2(x)} = \frac{a_0 + a_1 x + a_2 x^2}{1 + b_1 x + b_2 x^2} : \quad \text{Padé[2,2].}$$

Before we apply the Padé approximation, we use a variable transformation in the HAM solution to change the fractional order x^α into an integer order:

$$x^\alpha = z, \;\; x^{2\alpha} = z^2, \;\; x^{3\alpha} = z^3, etc.$$

After that, we establish the difference (4.4) and then the powers of x^j are equalized to determine the unknown coefficients of $R_{1,2}(x)$ and $R_{2,2}(x)$. Finally, we apply the inverse transformation:

$$z = x^\alpha, \;\; z^2 = x^{2\alpha}, \;\; z^3 = x^{3\alpha}, etc.$$

and obtain the fractional HAM Padé solution.

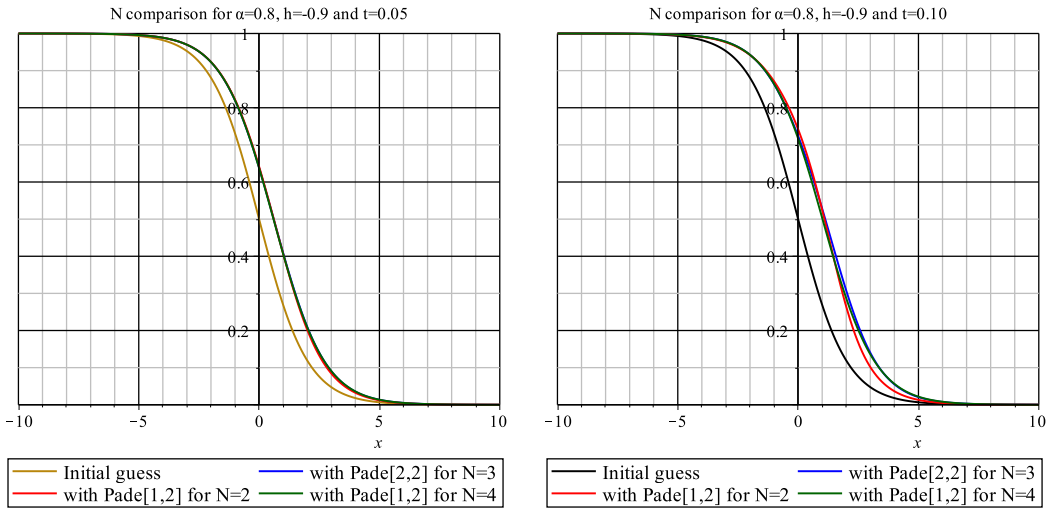

(a) (b)

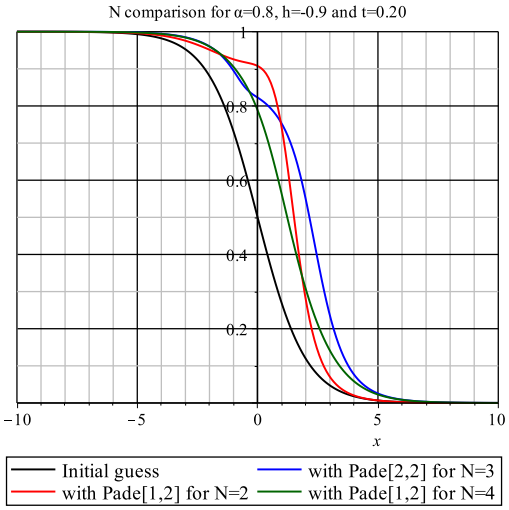

(c)

FIGURE 4.11: The HAM Padé solutions for different N values are shown. We see that the Padé approximation gives a faster convergence for $t = 0.05$ and $t = 0.1$. For $t = 0.2$ in frame (c), HAM with Padé seems to converge, but there we would need higher N-values.

We can observe in Figure 4.11(a) and in Figure 4.11(b) that the Padé approximation helps us to find a fast convergent solution for $t = 0.05$ and $t = 0.1$ even in two steps. But, if we explore the solutions for higher time values like $t = 0.2$ presented in Figure 4.11(c), we should compute more steps to find a convergent solution. We also compare the solutions between HAM with Padé and HAM without Padé.

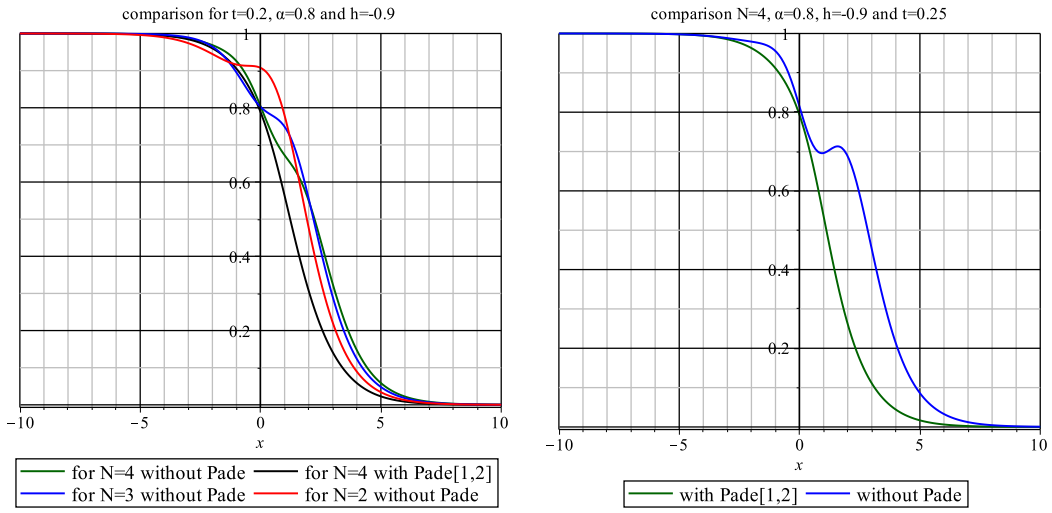

(a) (b)

FIGURE 4.12: The impact of the Padé approximation on HAM for $t = 0.2$ is shown in the left plot and for $t = 0.25$ in the right plot when $\alpha = 0.8$.

The effect of the Padé approximation is presented in Figure 4.12 for different time values and these plots show how the Padé approximation can help to improve the convergence properties of HAM. In Figure 4.12, HAM can not produce convergent solutions and creates oscillations. To overcome this problem, we applied Padé approximations. The Padé approximation enables us to smooth the solutions. Also, it is clear that in Figure 4.12 (a), if we evaluate the HAM for higher step values, we can obtain an even better Padé approximation.

4.5.3 Summary

In the previous chapter we have used the concept of Padé approximations to improve the numerical performance of the Homotopy Analysis Method (HAM). We managed to obtain a higher accuracy in the non-fractional case, when applied to traveling wave solutions of the Fisher equation. It may be obvious, however, that more research is needed to develop efficient Padé approximations, especially, for time-fractional (partial) differential equations. The Padé technique could be an efficient tool to improve the approximation, but, unfortunately, we can not generalize this idea for all fractional models. The major disadvantage of the Padé approximation is the high computation time. For nonlinear models, it is, in general, hard to estimate the needed computation time. Future research would be required to optimize the application of Padé approximation for fractional differential equations.

Bibliography

[1] S. Abbasbandy, E. Shivanian, and K. Vajravelu. Mathematical properties of h-curve in the frame work of the homotopy analysis method. *Commun Nonlinear Sci Numer Simulat* 16 (2011), pp. 4268–4275.

[2] G. Adomian. A review of the decomposition method in applied mathematics. *Journal of Mathematical Analysis and Application* 135 (1998), pp. 501–544.

[3] R. P. Agarwal. A propos d'une note de M. Pierre Humbert. *Comptes Rendus Acad. Sci. Paris* 236 (1953), pp. 2031–2032.

[4] M. A. Al-Bassam. On fractional calculus and its applications to the theory of ordinary differential equations of generalized order. *nonlinear analysis and applications* 80 (1981), pp. 305–331.

[5] M. Alquran, K. Al-Khaled, T. Sardar, and J. Chattopadhyay. Revisited Fisher's equation in a new outlook: A fractional derivative approach. *Physics A: Statistical Mechanics and its Applications* 438 (2015), pp. 81–93.

[6] A. Atangana. On the new fractional derivative and application to nonlinear Fisher's reaction–diffusion equation. *Applied Mathematics and Computation* 273 (2016), pp. 948–956.

[7] K. A. Atkinson. *An Introduction to Numerical Analysis.* 2nd edition. New York: John Wiley and Sons, 1989.

[8] E. Babolian and J. Saeidian. Analytic approximate solutions to Burgers, Fisher, Huxley equations and two combined forms of these equations. *Communications in Nonlinear Science and Numerical Simulation* 14(5) (2009), pp. 1984–1992.

[9] E. Babolian, A. R. Vahidi, and Z. Azimzadeh. A comparison between the Homotopy Perturbation Method and Adomian's Decomposition Method for Solving Nonlinear Volterra Integral Equations. *J. Sci. Tarbiat University* 11(2) (2012).

[10] R. T. Baillie. Long memory processes and fractional integration in econometrics. *Journal of Econometrics* 73(1) (1996), pp. 5–59.

[11] T. Bakri, Y. A. Kuznetsov, F. Verhulst, and E. Doedel. Multiple solutions of a generalized singular perturbed Bratu problem. *International Journal of Bifurcation and Chaos in Applied Sciences and Engineering* 22(4) (2012), p. 10.

[12] D. Baleanu, K. Diethelm, E. Scalas, and J. J. Trujillo. *Fractional Calculus: Models and Numerical Methods.* Series on Complexity, Nonlinearity and Chaos, 2012.

[13] V. K. Baranwal, R. K. Pandey, M. P. Tripathi, and O. P. Singh. An analytic algorithm for time fractional nonlinear reaction–diffusion equation based on a new iterative method. *Communications in Nonlinear Science and Numerical Simulation* 17(10) (2012), pp. 3906–3921.

[14] E. Barkai and I. M. Sokolov. On fractional diffusion and continuous time random walks. *Physica A: Statistical Mechanics and its Applications* 373 (2007), pp. 231–236.

[15] D. A. Benson, M. M. Meerschaert, and J. Revielle. Fractional calculus in hydrologic modeling: A numerical perspective. *Advances in Water Resources* 51 (2013), pp. 479–497.

[16] D. A. Benson, S. W. Wheatcraft, and M. M. Meerschaert. Application of a fractional advection-dispersion equation. *Water Resources Research* 36(6) (2000), pp. 1403–1412.

[17] J. Biazar, M. A. Asadi, and F. Salehi. Rational Homotopy Perturbation Method for solving stiff systems of ordinary differential equations. *Applied Mathematical Modelling* 39 (2015), pp. 1291–1299.

[18] J. Biazar, F. Badpeima, and F. Azimi. Application of the homotopy perturbation method to Zakharov-Kuznetsov equations. *Computers and Mathematics with Applications* 58(11-12) (2009), pp. 2391–2394.

[19] J. Biazar and G. Ghazvini. Convergence of the homotopy perturbation method for partial differential equations. *Nonlinear Analysis: Real World Applications* 10(5) (2009), pp. 2633–2640.

[20] H. Bohr and J. Mollerup. *Lærebog i Kompleks Analyse vol. III, Copenhagen*. Textbook in Complex Analysis, 1922.

[21] C. Brezinski and M. Redivo-Zaglia. New representations of Padé, Padé-type, and partial Padé approximants. *Journal of Computational and Applied Mathematics* 284 (2015), pp. 69–77.

[22] M. Caputo. Linear model of dissipation whose Q is almost frequency independent-II. *Geophys. J. R. Astron. Soc.* 13(5) (1967), pp. 529–539.

[23] D. del Castillo-Negrete, B. A. Carreras, and V. E. Lynch. Fractional diffusion in plasma turbulence. *Physics of Plasmas* 11(8) (2004), pp. 3854–3864.

[24] D. del Castillo-Negrete, B. A. Carreras, and V. E. Lynch. Front dynamics in reaction-diffusion systems with Levy flights: a fractional diffusion approach. *Physical Review Letters* 91(1) (2003), doi: https://doi.org/10.1103/PhysRevLett.91.018302.

[25] D. del Castillo-Negrete, P. Mantica, V. Naulin, and J. J. Rasmussen. Fractional diffusion models of non-local perturbative transport: numerical results and application to JET experiments. *Nuclear Fusion* 48(7):075009 (2008), doi: 10.1088/0029–5515/48/7/075009.

[26] O. Catà. Padé approximants and the prediction of non-perturbative parameters in particle physics. *Applied Numerical Mathematics* 60(12) (2010), pp. 1273–1285.

[27] E. Celik and M. Bayram. On the numerical solution of differential-algebraic equations by Padé series. *Applied Mathematics and Computation* 137(1) (2003), pp. 151–160.

[28] S. H. Chang. A variational iteration method for solving Troesch's problem. *Journal of Computational and Applied Mathematics* 234(10) (2010), pp. 3043–3047.

[29] S. Chaturapruek, J. Breslau, D. Yazdi, T. Kolokolnikov, and S. G. McCalla. Crime modeling with Levy flights. *SIAM Journal on Applied Mathematics* 73(4) (2013), pp. 1703–1720.

[30] A. Chechkin, R. Metzler, J. Klafter, and V. Y. Gonchar. Introduction to the theory of Levy flights. *ResearchGate* https://www.researchgate.net/publication/228030356 (2008), doi: 10.1002/9783527622979.ch5.

[31] C. Cuesta, C. J. van Duijn, and J. Hulshof. Infiltration in porous media with dynamic capillary pressure: travelling waves. *European Journal of Applied Mathematics* 11 (2000), pp. 381–397.

[32] M. Davison and C. Essex. Fractional differential equations and initial value problems. *The Mathematical Scientist* 23(2) (1998), pp. 108–116.

[33] L. Debnath. Recent applications of fractional calculus to science and engineering. *International Journal of Mathematics and Mathematical Sciences* 2003(54) (2003), pp. 3413–3442.

[34] E. Deeba, A. A. Khuri, and S. Xie. An Algorithm for Solving Boundary Value Problems. *Journal of Computational Physics* 159(2) (2000), pp. 125–138.

[35] K. Diethelm. *The Analysis of Fractional Differential Equations: An Application-Oriented Exposition Using Differential Operators of Caputo Type (Lecture Notes in Mathematics).* Springer, 2010.

[36] C. J. van Duijn, Y. Fan, L. A. Peletier, and I. S. Pop. Travelling wave solutions for degenerate pseudo-parabolic equations modelling two-phase flow in porous media. *Nonlinear Analysis: Real World Applications* 14.3 (2013), pp. 1361–1383.

[37] C. J. van Duijn, S. M. Hassanizadeh, I. S. Pop, and P. A. Zegeling. Non-equilibrium models for two phase flow in porous media: the occurence of saturation overshoots. *Proceedings of the Fifth International Conference on Application of Porous Media, Babes-Bolyai University, Cluj-Napoca* (2013), p. 12.

[38] C. J. van Duijn, L. A. Peletier, and I. S. Pop. A new class of entropy solutions of the Buckley-Leverett equation. *SIAM Journal on Mathematical Analysis* 39.2 (2007), pp. 507–536.

[39] A. M. A. El-Sayed, A. Elsaid, I. L. El-Kalla, and D. Hammad. A homotopy perturbation technique for solving partial differential equations of fractional order in finite domains. *Applied Mathematics and Computation* 218(17) (2012), pp. 8329–8340.

[40] W. H. Enright, K. R. Jackson, S. P. Norsett, and P. G. Thomsen. Interpolants for Runge-Kutta formulas. *ACM Trans. Math. Softw.* 12 (1986), pp. 193–218.

[41] A. Erdelyi and H. Kober. On fractional integrals and derivatives. *The Quarterly Journal of Mathematics (Oxford Series)* 11(1) (1940), pp. 193–211.

[42] U. Erdogan and T. Ozis. A smart nonstandard finite difference scheme for second order nonlinear boundary value problems. *Journal of Computational Physics* 230(17) (2011), pp. 6464–6474.

[43] E. Fehlberg. Klassische Runge–Kutta-formeln vierter und niedrigerer Ordnung mit schrittweiten-kontrolle und ihre Anwendung auf Waermeleitungsprobleme. *Computing* 6 (2011), pp. 61–71.

[44] X. Feng, L. Mei, and G. He. An efficient algorithm for solving Troesch's problem. *Applied Mathematics and Computation* 189(1) (2007), pp. 500–507.

[45] G. M. Figueiredo and G. Siciliano. Positive solutions for the fractional Laplacian in the almost critical case in a bounded domain. *Nonlinear Analysis: Real World Applications* 36 (2017), pp. 89–100.

[46] E. Flores and T. J. Osler. The Tautochrone Under Arbitrary Potentials Using Fractional Derivatives. *American Journal of Physics* 67 (1999), pp. 718–722.

[47] F. G. Frobenius. Ueber Relationen zwischem den Naherungsbruchen von Potenzreihen. *Journal fur die reine und angewandte Mathematik (Crelle's Journal)* 90 (1881), pp. 1–17.

[48] D.D. Ganji and A. Rajabi. Assessment of homotopy–perturbation and perturbation methods in heat radiation equations. *International Communications in Heat and Mass Transfer* 33(3) (2006), pp. 391–400.

[49] D. Gidaspow and B. S. Baker. A model for discharge of storage batteries. *Journal of the Electromechanical Society* 120 (1973), pp. 1005–1010.

[50] J. Gilewicz and M. Pindor. Padé-type approximants and errors of Padé approximants. *Journal of Computational and Applied Mathematics* 99(1-2) (1998), pp. 155–165.

[51] J. F. Gomez-Aguilar, R. Razo-Hernandez, and D. Granados-Lieberman. A physical interpretation of fractional calculus in observables terms: analysis of the fractional time constant and the transitory response. *Revista Mexicana de Fısica* 60 (2014), pp. 32–38.

[52] A. K. Gupta and S. S. Ray. On the solitary wave solution of fractional Kudryashov–Sinelshchikov equation describing nonlinear wave processes in a liquid containing gas bubbles. *Applied Mathematics and Computation* 298 (2017), pp. 1–12.

[53] E. Hanert, E. Schumacher, and E. Deleersnijder. Front dynamics in fractional-order epidemic models. *Journal of Theoretical Biology* 279 (2011), pp. 9–16.

[54] H. N. Hassana and M. A. El-Tawil. An efficient analytic approach for solving two-point nonlinear boundary value problems by homotopy analysis method. *Mathematical Methods in the Applied Sciences* 34(8) (2011), pp. 977–989.

[55] S. M. Hassanizadeh and W. G. Gray. Thermodynamic basis of capillary pressure in porous media. *Water Resources Research* 29.10 (1993), pp. 3389–3405.

[56] H. J. Haubold, A. M. Mathai, and R. K. Saxena. Mittag-Leffler functions and their applications. *Journal of Applied Mathematics* 2011 (2011), p. 51.

[57] J. H. He. An elementary introduction to the homotopy perturbation method. *Computers and Mathematics with Applications* 57(3) (2009), pp. 410–412.

[58] J. H. He. Comparison of homotopy perturbation method and homotopy analysis method. *Applied Mathematics and Computation* 156(2) (2004), pp. 527–539.

[59] J. H. He. Homotopy perturbation method: a new nonlinear analytical technique. *Applied Mathematics and Computation* 135(1) (2003), pp. 73–79.

[60] J. H. He. Homotopy perturbation method for solving boundary value problems. *Physics Letters A* 350(1-2) (2006), pp. 87–88.

[61] J. H. He. Homotopy perturbation technique. *Computer Methods in Applied Mechanics and Engineering* 178(3-4) (1999), pp. 257–262.

[62] J. H. He. New Interpretation of homotopy perturbation method. *International Journal of Modern Physics B* 20(18) (2006), pp. 2561–2568.

[63] T. P. Higgins. *The Use of Fractional Integral Operators for Solving Nonhomogeneous Differential Equations.* Defense Technical Information Center, Boeing Scientific Research Laboratories, Seattle, 1967.

[64] R. Hilfer. Fractional time evolution. *Applications of Fractional Calculus in Physics* doi: http://dx.doi.org/10.1142/9789812817747-0002 (2000), p. 89.

[65] R. Hilfer. On fractional diffusion and continuous time random walks. *Physica A: Statistical Mechanics and its Applications* 329(1-2) (2003), pp. 35–40.

[66] R. Hilfer. Remarks on fractional time. *Time, Quantum and Information* Springer-Verlag (2003), pp. 235–241.

[67] F. Hoefling and T. Franosch. Anomalous transport in the crowded world of biological cells. *Reports on Progress in Physics* 76(4) (2013), doi:10.1088/0034–4885/76/4/046602.

[68] H. Jafari and V. Daftardar-Gejji. Positive solutions of nonlinear fractional boundary value problems using Adomian decomposition method. *Applied Mathematics and Computation* 180 (2006), pp. 700–706.

[69] B. B. Jaimini, N. Shrivastava, and H. M. Srivastava. The integral analogue of the Leibniz rule for fractional calculus and its applications involving functions of several variables. *Computers and Mathematics with Applications* 41(1-2) (2001), pp. 149–155.

[70] V. G. Kac and A. K. Raina. *Advanced Series in Mathematical Physics: Volume 2,Bombay Lectures on Highest Weight Representations of Infinite Dimensional Lie Algebras*. 2nd. Word Scientific, 1987.

[71] L. Kexue and P. Jigen. Laplace transform and fractional differential equations. *Applied Mathematics Letters* 24(12) (2011), pp. 2019–2023.

[72] S. A. Khuri. A numerical algorithm for solving Troesch's problem. *International Journal of Computer Mathematics* 80(4) (2003), pp. 493–498.

[73] S.A. Khuri. A new approach to Bratu's problem. *Applied Mathematics and Computation* 147 (2004), pp. 131–136.

[74] C. Li, D. Qian, and Y. Chen. On Riemann-Liouville and Caputo Derivatives. *Discrete Dynamics in Nature and Society* 2011 (2011), p. 15.

[75] S. Liang and D. J. Jeffrey. Comparison of homotopy analysis method and homotopy perturbation method through an evolution equation. *Communications in Nonlinear Science and Numerical Simulation* 14(12) (2009), pp. 4057–4064.

[76] P. Liao. Notes on the homotopy analysis method: Some definitions and theorems. *Commun Nonlinear Sci Numer Simulat* 14 (2009), pp. 983–997.

[77] S. Liao. *Beyond Perturbation: Introduction to the Homotopy Analysis Method*. CRC Press LLC, 2004.

[78] S. Liao. *Homotopy Analysis Method in Nonlinear Differential Equations*. Higher Education Press, 2012.

[79] Y. Lin, J. A. Enszer, and M. A. Stadtherr. Enclosing all solutions of two-point boundary value problems for ODEs. *Computers and Chemical Engineering* 32(8) (2008), pp. 1714–1725.

[80] F. Liu, M. M. Meerschaert, R. J. McGough, P. Zhuang, and Q. Liu. Numerical methods for solving the multi-term time-fractional wave-diffusion equations. *Fractional Calculus and Applied Analysis* 16(1) (2013), pp. 9–25.

[81] B. Lombard, D. Matignon, and Y. L. Gorrec. A fractional Burgers equation arising in nonlinear acoustics: theory and numerics. *IFAC Proceedings Volumes* 46(23) (2013), pp. 406–411.

[82] J. L. López, P. Pagola, and E. P. Sinusía. A simplification of Laplace's method: Applications to the Gamma function and Gauss hypergeometric function. *Journal of Approximation Theory* 161(1) (2009), pp. 280–291.

[83] L. Lorentzen. Padé approximation and continued fractions. *Applied Numerical Mathematics* 60(12) (2010), pp. 1364–1370.

[84] A. Loverro. Fractional Calculus: History, Definitions and Applications for the Engineer (2004).

[85] Ch. Lubich. Discretized Fractional Calculus. *SIAM Journal on Mathematical Analysis* 17(3) (1986), pp. 704–719.

[86] Ch. Lubich. Fractional linear multistep methods for Abel-Volterra integral equations of the second kind. *Mathematics of Computation* 45 (1985), pp. 463–469.

[87] V. E. Lynch, B. A. Carreras, D. del Castillo-Negrete, K. M. Ferreira-Mejias, and H. R. Hicks. Numerical methods for the solution of partial differential equations of fractional order. *Journal of Computational Physics* 192(2) (2003), pp. 406–421.

[88] J. T. Machado, V. Kiryakova, and F. Mainardi. Recent history of fractional calculus. *Communications in Nonlinear Science and Numerical Simulation* 16(3) (2011), pp. 1140–1153.

[89] V. S. Markin, A. A. Chernenko, Y. A. Chizmadehev, and Y. G. Chirkov. Aspects of the theory of gas porous electrodes. *in Fuel Cells: Their Electrochemical Kinetics, Consultants Bureau (Wiley, New York)* (1966), pp. 22–23.

[90] M. M. Meerschaert, R. L. Magin, and A. Q. Ye. Anisotropic fractional diffusion tensor imaging. *Journal of Vibration and Control* 22(9) (2016), pp. 2211–2221.

[91] M. Mikolas. On recent trends in development, theory and applications of fractional calculus. *Fractional Calculus and Its Applications (Proc. Conf. Held in New Haven, 1974) Lecture Notes in Math. 457, Springer-Verlag* (1975), pp. 357–375.

[92] S. H. Mirmorad, I. Hosseinpour, S. Ghanbarpour, and A. Barari. Application of an Approximate Analytical Method to Nonlinear Troesch's Problem. *Applied Mathematical Sciences* 3(32) (2009), pp. 1579–1585.

[93] Mittag-Leffler. M.G.: Sur la nouvelle fonction E(x). *C. R. Acad. Sci. Paris* 137 (1903), pp. 554–558.

[94] S. Momani and Z. Odibat. Comparison between the homotopy perturbation method and the variational iteration method for linear fractional partial differential equations. *Computers and Mathematics with Applications* 54(7-8) (2007), pp. 910–919.

[95] R. Musina and A. I. Nazarov. On fractional Laplacians. *Communications in Partial Differential Equations* 39(9) (2014), pp. 1780–1790.

[96] R. Musina and A. I. Nazarov. On fractional Laplacians–2. *Annales de l'Institut Henri Poincaré (C) Non Linear Analysis* 33(6) (2016), pp. 1667–1673.

[97] K. B. Oldham and J. Spanier. *The Fractional Calculus: Theory and Applications of Differentiation and Integration to Arbitrary Order.* Dover Books on Mathematics, 1974.

[98] F. W. Olver. The evaluation of zeros of high-degree polynomials. *Phil. Trans. Roy. Soc. London A* 244 (1952), pp. 385–415.

[99] H. Padé. Sur la representation approchée d'une fonction par des fractions rationelles. *Thesis* 9 (1892), pp. 1–93.

[100] K. Parand and J. A. Rad. Exp-function method for some nonlinear PDE's and a nonlinear ODE's. *Journal of King Saud University - Science* 24(1) (2012), pp. 1–10.

[101] I. Podlubny. *Fractional Differential Equations. An Introduction to Fractional Derivatives, Fractional Differential Equations, Some Methods of Their Solution and Some of Their Applications.* Academic Press, San Diego-Boston-New York-London-Tokyo-Toronto, 1999.

[102] S. Qin, F. Liu, I. Turner, V. Vegh, Q. Yu, and Q. Yang. Multi-term time-fractional Bloch equations and application in magnetic resonance imaging. *Journal of Computational and Applied Mathematics* 319 (2017), pp. 308–319.

[103] M. Rahimy. Applications of fractional differential equations. *Applied Mathematical Sciences* 4 (2010), pp. 2453–2461.

[104] M. M. Rashidi, G. Domairry, and S. Dinarvand. Approximate solutions for the Burger and regularized long wave equations by means of the homotopy analysis method. *Communications in Nonlinear Science and Numerical Simulation* 14(3) (2009), pp. 708–717.

[105] A. P. Riascos and J. L. Mateos. Fractional dynamics on networks: emergence of anomalous diffusion and Levy flights. *Physical Review E* 90(3) (2014), doi: 10.1103/PhysRevE.90.032809.

[106] B. Ross. *Fractional Calculus and Its Applications*. Lecture Notes in Mathematics 457. Springer-Verlag, New York-Berlin, 1974.

[107] B. Ross. The development of fractional calculus 1695–1900. *Historia Mathematica* 4(1) (1977), pp. 75–89.

[108] Y. A. Rossikhin and M. V. Shitikova. Applications of fractional calculus to dynamic problems of linear and nonlinear hereditary mechanics of solids. *Applied Mechanics Reviews* 50(1) (1997), pp. 15–67.

[109] S. G. Samko, A. A. Kilbas, and O. I. Marichev. *Fractional Integrals and Derivatives: Theory and Applications*. 1st edition. CRC Press, 1993.

[110] R. Schumer, M. M. Meerschaert, and B. Baeumer. Fractional advection-dispersion equations for modeling transport at the Earth surface. *Journal of Geophysical Research* 114 (2009), p. F00A07, doi:10.1029/2008JF001246.

[111] P. Singh. A study on fractional calculus and their problems. *International Journal of Multidisciplinary Research and Development* 1(2) (2014), pp. 152–154.

[112] L. Song and H. Zhang. Application of homotopy analysis method to fractional KdV–Burgers–Kuramoto equation. *Physics Letters A* 367(1-2) (2007), pp. 88–94.

[113] M. I. Syam and A. Hamdan. An efficient method for solving Bratu equations. *Applied Mathematics and Computation* 176(2) (2006), pp. 704–713.

[114] V. E. Tarasov. Fractional Derivative as Fractional Power of Derivative. *International Journal of Mathematics* 18 (2007), pp. 281–299.

[115] V. E. Tarasov. Fractional integro-differential equations for electromagnetic waves in dielectric media. *Theoretical and Mathematical Physics* 158(3) (2009), pp. 355–359.

[116] M. Torabi and H. Yaghoobi. Novel solution for acceleration motion of a vertically falling spherical particle by HPM–Padé approximant. *Advanced Powder Technology* 22(5) (2011), pp. 674–677.

[117] M. Turkyilmazoglu. Convergence of the homotopy perturbation method. *Int. J. Nonlinear Sci. Numer. Simul.* 12 (2011), pp. 9–14.

[118] H. Vázquez-Leal. Rational Homotopy Perturbation Method. *Journal of Applied Mathematics* Article ID 490342 (2012), doi:10.1155/2012/490342.

[119] H. Vázquez-Leal, U. Filobello-Nino, R. Castaneda-Sheissa, L. Hernandez-Martinez, and A. Sarmiento-Reyes. Modified HPMs Inspired by Homotopy Continuation Methods. *Mathematical Problems in Engineering* (2012), p. 19.

[120] H. Vázquez-Leal, Y. Khan, G. Fernandez-Anaya, A. Herrera-May, A. Sarmiento-Reyes, U. Filobello-Nino, V.-M. Jimenez-Fernández, and D. Pereyra-Diaz. A general solution for Troesch's problem. *Mathematical Problems in Engineering* Article ID 208375 (2012), doi:10.1155/2012/208375.

[121] H. Vázquez-Leal, A. Sarmiento-Reyes, Y. Khan, U. Filobello-Nino, and A. Diaz-Sanchez. Rational Biparameter Homotopy Perturbation Method and Laplace-Padé Coupled Version. *Journal of Applied Mathematics* Article ID 923975 (2012), doi:10.1155/2012/923975.

[122] A. Wazwaz. Adomian decomposition method for a reliable treatment of the Bratu-type equations. *Applied Mathematics and Computation* 166 (2005), pp. 652–663.

[123] E. S. Weibel. On the confinement of a plasma by magnetostatic fields. *Phys. Fluids* 2(1) (1959), p. 5.

[124] A. Wiman. Über den fundamental Satz in der Theorie der Funktionen E(x). *Acta Math.* 29 (1905), pp. 191–201.

[125] M. S. Zahedi and H. S. Nik. On homotopy analysis method applied to linear optimal control problems. *Applied Mathematical Modelling* 37(23) (2013), pp. 9617–9629.

[126] L. I. Zaidan and M. T. Darvishi. Numerical simulation for fractional nonlinear (1+1)-dimensional Biswas–Milovic equation. *Optik-International Journal for Light and Electron Optics* 136 (2017), pp. 390–402.

[127] P. A. Zegeling. An adaptive grid method for a non-equilibrium PDE model from porous media. *Journal of Mathematical Study* 48(2) (2015), pp. 93–104.

[128] L. Zhang, Z. He, C. Conti, Z. Wang, Y. Hu, D. Lei, Y. Li, and D. Fan. Modulational instability in fractional nonlinear Schroedinger equation. *Communications in Nonlinear Science and Numerical Simulation* 48 (2017), pp. 531–540.

[129] Y. Zheng and Z. Zhao. The discontinuous Galerkin finite element method for fractional cable equation. *Applied Numerical Mathematics* 115 (2017), pp. 32–41.

[130] A. Zoia, A. Rosso, and M. Kardar. Fractional Laplacian in bounded domains. *Physical Review E* 76(2) (2007), doi: 10.1103/PhysRevE.76.021116.

[131] L. Zou, Z. Zong, Z. Wang, and L. He. Solving the discrete KdV equation with homotopy analysis method. *Physics Letters A* 370(3-4) (2007), pp. 287–294.

Summary

This thesis discusses numerical methods for models with fractional order derivatives. These methods make use of infinite series, which are based on the notion of homotopy with an additional method parameter to accelerate the convergence properties.

In Chapter 1, we start with a brief motivation and history of fractional calculus. Next, we introduce the Gamma function and the Mittag-Leffler function, which play an important role in the theory of fractional derivatives. There exist many definitions of fractional order derivatives. Among the most important ones, we present four definitions: the Riesz, the Riemann-Liouville, the Caputo, and the Grünwald-Letnikov derivative. Properties, relations and differences between these are mentioned to show the different aspects and consequences. Furthermore, the importance of fractional calculus is emphasized and the background for using fractional differential equations is briefly described. The widespread application of fractional order derivatives is discussed and a series of fractional order models from many different application areas is given. At the end of chapter 1, an outline of the new contribution to this area is shortly indicated.

In Chapter 2, we focus on a fractional order advection-diffusion-reaction model. We introduce the homotopy perturbation method to solve the model. First, we analyze the convergence of the method and compare it with the Adomian decomposition method to understand its effectivity for different models. Some theoretical results are given and are explained in terms of convergence tables and graphics. Numerical experiments illustrate the performance of this method, when applied to a test set of boundary-value problems. Both convergent and divergent numerical solutions are presented.

In Chapter 3, we deal with traveling wave solutions in time-fractional partial differential equations. This is done by using the homotopy analysis method which is an extension of the homotopy perturbation method. Primarily, we explain the importance of the convergence parameter $\hbar$ in the so-called $\hbar$-curve. This curve enables us, somehow, to control the convergence region of the method. Especially, for this curve, the role of an optimal $\hbar$ value is emphasized. Numerical results for a special partial differential equation are given: the time-fractional Fisher equation. The effect of changing the fractional order on the solution behavior is shown.

In Chapter 4, we study Padé approximations to improve the numerical solutions which were obtained by the homotopy analysis method in the previous chapter. A Padé approximation has the potential to produce more accurate numerical solutions not only for higher time values in the differential equation, but also speeds up the computation time of the series. First, we introduce the rational homotopy perturbation method which makes use of a Padé approximation for stationary problems. For example, it is applied to a convective-radiative equation and to Troesch's model. Finally, we apply a Padé approximation with the homotopy analysis method to a time-fractional Fisher partial differential equation and show its usefulness in several experiments.

Samenvatting

Dit proefschrift behandelt numerieke methoden voor modellen met fractionele (gebroken) afgeleiden. Deze methoden, die gebruik maken van oneindige reeksen, zijn gebaseerd op het begrip homotopie met een methode parameter die de convergentie tracht te versnellen.

In hoofdstuk 1 beginnen we met een motivatie en een korte geschiedenis van fractionele calculus. Vervolgens introduceren we de Gamma-functie en de Mittag-Leffler functie, die een belangrijke rol spelen in de theorie van fractionele (gebroken) afgeleiden. Er bestaan vele definities van fractionele orde afgeleiden. De vier belangrijkste worden hier gepresenteerd: de Riesz, de Riemann-Liouville, de Caputo, en de Grünwald-Letnikov afgeleide. Enkele eigenschappen, overeenkomsten en verschillen worden uitgewerkt om de diversiteit van dit onderwerp te laten zien. Verder wordt het nut van fractionele calculus benadrukt en de achtergronden bij de toepassing van fractionele differentiaalvergelijkingen beschreven. De wijdverbreide toepassing van modellen met fractionele orde afgeleiden wordt genoemd en verschillende toepassingsgebieden hiervan worden behandeld. Aan het einde van dit hoofdstuk staat een overzicht van de nieuwe bijdragen op dit gebied in het kort vermeld.

In hoofdstuk 2 richten we ons op een fractioneel advectie-diffusie-reactie-model. We introduceren de homotopie verstorings methode om het model op te lossen. Eerst analyseren we de convergentie van de methode en vergelijken we deze met een andere methode: de Adomian decompositie methode. Enkele theoretische resultaten worden bevestigd in termen van numerieke convergentie tabellen en grafieken. Numerieke experimenten illustreren de eigenschappen van deze methode, wanneer deze worden toegepast op een testset van randwaarde problemen. Zowel convergente als divergente numerieke oplossingen worden gepresenteerd.

In hoofdstuk 3 behandelen we lopende golfoplossingen voor tijds-fractionele partiële differentiaalvergelijkingen. Dit wordt uitgevoerd met de homotopie analyse methode, die een uitbreiding is van de homotopie verstorings methode uit hoofdstuk 2. In de eerste plaats leggen we het belang uit van de convergentie parameter $\hbar$ in de zogenaamde $\hbar$-kromme. Deze kromme stelt ons, in zekere zin, in staat om het convergentiegebied van de methode te controleren. Numerieke resultaten voor enkele partiële differentiaalvergelijkingen worden gegeven, o.a. voor de tijds-fractionele Fisher vergelijking. Het effect van het veranderen van de fractionele order op het gedrag van de oplossing wordt getoond.

In hoofdstuk 4 bestuderen we Padé benaderingen om de numerieke oplossingen te verbeteren, die werden verkregen met de homotopie analyse methode in hoofdstuk 3. Een Padé benadering heeft de mogelijkheid om nauwkeurigere numerieke oplossingen te verkrijgen voor latere tijdstippen in de tijdafhankelijke differentiaalvergelijking. Bovendien kan dit ook de rekentijd van de reeksoplossing versnellen. Als eerste toepassing introduceren we de rationele homotopie verstorings methode die gebruik maakt van een Padé benadering voor stationaire problemen. Deze wordt toegepast op een convectie-radiatieve vergelijking en het model van Troesch. Tot slot passen we een Padé benadering, in combinatie met de homotopie analyse methode, toe op de tijds-fractionele Fisher partiële differentiaalvergelijking. Het nut hiervan wordt duidelijk gemaakt door middel van verschillende numerieke experimenten.

Acknowledgements

I would like to thank some people who gave me help and continuous support.

First and foremost, I would like to express my sincerest gratitude to my daily supervisor Paul Zegeling. I feel myself lucky to work with him throughout my PhD project. He was very helpful and kind to me all the time. He has always put a lot of effort in guiding and educating me. Even in his intensive schedule, he could always manage to have time for me. He was always optimistic and tried to motivate me. I will never forget his long tutorials without any complaint and with much patience. I really enjoyed the discussions with Paul and I will always appreciate him.

I am also grateful to my promotor Rob Bisseling. He was one of the most important persons during this project with unlimited support and patience. His door was always open for me to discuss my PhD research and different other matters. It would not have been possible to write this thesis without his help and guidance.

I am indebted to the reading committee: Prof. Rob Stevenson, Prof. Arjen Doelman, Prof. Sorin Pop, Prof. Sjoerd Verduyn Lunel and Dr. Tristan van Leeuwen, for reading my thesis and giving helpful comments and feedback.

Many thanks to my colleague Hüseyin Şen at Utrecht University. We had many lunches together and shared interesting stories in our lives. All of these are precious memories and I greatly enjoyed them.

I am grateful to the Turkish Ministry of Education to support me financially and morally throughout my PhD. They also funded me every year for attending national and international conferences which played an important role to change my point of view on science. People in the ministry were very helpful and kind. They were sensitive to solve problems at any time. I should also thank to the people in the Turkish embassy in the Hague, especially people working in Lahey Education Consultancy. They have been always like a bridge between me and Turkey.

My parents Ali and Hüsniye and my brother Laşer deserve one of the greatest thanks for being there whenever I needed. They have unconditionally supported and encouraged me during my PhD. It was mentally really important to feel their assistance.

I want to also thank the Department of Mathematics of Utrecht University, and, especially, Prof. Gunther Cornelissen, Wilke Schram, Helga Hoiting, Cécile Lemette, Carin van de Weerd-Nijboer, Ria Bekkering-Bosboom, Jean Arthur and Sylvia Visser for their support and help during my PhD-project in Utrecht.

Curriculum Vitae

İnan Ateş was born in Antalya, Turkey on the 22^{th} of August 1984. In the period 1995-2002 he studied at the German-language high school Metin Nuran Çakallıklı Anatolian High School.

After obtaining his high school degree in October 2002 he moved to Izmir where he studied Applied Mathematics at Ege University. After one year language education at the university, between the period 2003-2004, he started to study mechanical engineering, but then he continued to study mathematics. He participated and made presentations in national conferences during his bachelor. He obtained his bachelor's degree in June 2008.

In July 2008, he was qualified to have a scholarship from the Turkish institution TUBITAK for his master degree. He started his master at Ege University and obtained his master degree in 2010.

In 2011, he was qualified to start an academical staff education program at Middle East Technical University in Ankara as a PhD candidate. After a few months, he obtained a scholarship from the Turkish Ministry of Education to continue his doctoral activities abroad. He started as a PhD candidate at the Mathematics Department, Utrecht University, in September 2011.

Between 2011 and 2017 he was a PhD student at Utrecht University under the guidance of Prof. Rob Bisseling and Associate Prof. Paul Zegeling.

He attended several conferences and workshops during his PhD study. He participated in the Woudschoten (2011-2015) conferences in Zeist, organized by the Werkgemeenschap Scientific Computing (WSC). In 2014, he presented a poster at the ICFDA (International Conference on Fractional Differentiation and its Applications) in Catania, Italy. Further, he attended the WSC Spring meetings at the CWI in Amsterdam. He also presented a poster at the NDNS+ workshop in Twente in June 2015. Finally, he gave a contributed talk at the SciCADE Conference in Potsdam in September 2015.